Investigations on the powder behaviour and the residence time distribution within a production scale rotary press with special focus on its geometric and parametric setups

Dissertation

with the aim of achieving a doctoral degree

at the Faculty of Mathematics, Informatics and Natural Sciences

Department of Chemistry

University of Hamburg

submitted by

Matthias Dülle

Hamburg 2019

The experimental studies and the preparation of this thesis were carried out between December 2015 and May 2019 in the Department of Chemistry at the University of Hamburg, Division of Pharmaceutical Technology, on the initiative and under supervision of Professor Dr. Claudia S. Leopold.

To do a common thing uncommonly well brings success.

- Henry J. Heinz -

Zusammenfassung

Im industriellen Maßstab werden Tabletten auf Rundläufer-Tablettenpressen hergestellt. Betrachtet man die einzelnen Bauteile dieser Tablettenpressen genauer, ist eines der zentralen Bauteile das Füllsystem, welches einen gleichmäßigen Pulverfluss vom Fülltrichter zur Matrize gewährleistet. In dieser Arbeit wurde das Augenmerk auf das Füllsystem einer Rundläufer-Tablettenpresse der Firma Fette Compacting gerichtet, sodass die Ergebnisse dieser Arbeit direkt auf die industrielle Herstellung von Tabletten übertragen werden können. Fragestellungen wie zum Beispiel die Abhängigkeit zwischen Drehzahl des Matrizentisches und der des Füllsystems sind bislang aufgrund ihrer Komplexität kaum untersucht worden. Dies hat zur Folge, dass im Produktionsalltag die parametrischen Einstellungen in Abhängigkeit vom Produkt individuell ermittelt werden müssen. Um ein besseres Verständnis des Pulververhaltens innerhalb der Füllsysteme zu erhalten, wurden unterschiedliche geometrische und parametrische Einstellungen untersucht.

In dieser Arbeit wurde das Pulververhalten eines Drei-Kammer-Füllsystems (Fill-O-Matic) der Rundläufer-Tablettenpresse Fette 102i und eines Ein-Kammer-Kegel-Füllsystems der Rundläufer-Tablettenpresse Fette FE55 charakterisiert. Hierbei lag ein besonderer Fokus auf der Verweilzeitverteilung von Pulverpartikeln in den Füllsystemen. Die Bestimmung der Verweilzeitverteilung der Pulver in den Füllsystemen und die daraus berechneten Werte für die Mittlere Verweilzeit und für die Varianz der Mittleren Verweilzeit wurden zur Auswertung der geometrischen und parametrischen Einstellungen herangezogen.

Im ersten Teil dieser Arbeit wurde der Einfluss der Geschwindigkeit der Matrizenscheibe und der Füllsystemräder sowie der Einfluss der Fülltiefe, der Füllkurve und des Abstreifers auf die Verweilzeitverteilung einer angefärbten Pulvermischung (Markermischung) im Füllsystem untersucht. Es konnte gezeigt werden, dass die Geschwindigkeit der Matrizenscheibe sowie die Änderung der Fülltiefe einen großen Einfluss auf die Verweilzeitverteilung ausüben. Die Verwendung unterschiedlicher Füllkurven bei gleichbleibender Fülltiefe zeigte keinen Einfluss auf die Verweilzeitverteilung. Ein interessantes Ergebnis zeigte die Untersuchung der Füllradgeschwindigkeit, die zu keiner Veränderung der Mittleren Verweilzeit führte, während die Durchmischung der Pulverpartikel, veranschaulicht durch die Varianz der Mittleren Verweilzeit, deutlich erhöht wurde.

Neben den geometrischen und parametrischen Einstellungen der Fill-O-Matic (FOM) wurde in einem zweiten Teil der Arbeit der Einfluss der Pulvereigenschaften auf das Pulververhalten in der FOM bei Verwendung einer Mischung aus mikrokristalline Cellulose als Modellpulver untersucht. Schwerpunkte dieser Studie lagen auf der Untersuchung des Einflusses unterschiedlicher Mengen an Markermischung und der Fließraten der Pulverpartikel durch das Füllsystem auf die Verweilzeitverteilung. Des Weiteren wurde der Einfluss der Restfeuchte der Pulverpartikel und die Partikelgröße auf das Pulververhalten sowie auf die Verweilzeitverteilung in der FOM untersucht. Es konnte gezeigt werden, dass insbesondere die Menge an Markermischung und die Fließrate der Pulverpartikel durch das Füllsystem einen großen Einfluss auf die Verweilzeitverteilung haben. Die unterschiedlichen Restfeuchten der Pulverpartikel und die Partikelgrößen der Markermischung zeigten keinen Einfluss auf die Verweilzeitverteilung. Ein interessantes Ergebnis der Untersuchung der Partikelverteilung in der Tablette war jedoch, dass die Partikelgröße einen

ausgeprägten Einfluss auf die Partikelverteilung innerhalb der Tablette zeigte. Große Markermischungspartikel kumulierten primär an der Tablettenoberseite, während kleinere Markermischungspartikel vermehrt an der Tablettenunterseite zu finden waren. Eine homogene Verteilung der Markermischungspartikel in der Tablette zeigte sich nur bei einer gleichmäßigen Partikelgröße der eingesetzten Pulver.

Diese Grundlagenkenntnisse aus dem ersten und zweiten Teil dieser Arbeit wurden herangezogen, um die einzelnen Bauteile der FOM im Hinblick auf eine mögliche Optimierung des Füllsystems bzw. eine Reduktion der Verweilzeit zu untersuchen. Zur Untersuchung der Reduktion der Verweilzeit und der Durchmischung der Pulverpartikel wurde eine Volumenreduktion der FOM durchgeführt, indem eine Plexiglasscheibe in die Dosierkammer eingelegt wurde. Weitere Schwerpunkte dieser Studie lagen auf dem Einfluss unterschiedlicher geometrischer Speichen des Füllrades, sowie der Spaltbreite eines Dichtungssegments zwischen FOM und Matrizenscheibe auf die Verweilzeitverteilung. Es konnte gezeigt werden, dass die Volumenreduktion durch die Plexiglasscheibe zu einer deutlichen Verkürzung der Verweilzeit und zu einer deutlichen Reduktion der Durchmischung der Pulverpartikel führte. Der Einbau der Plexiglasscheibe in die Dosierkammer führte leider dazu, dass kein Ausdosieren und somit auch kein exaktes Einstellen des Tablettengewichtes mehr möglich war. Der Einsatz der Plexiglasscheibe ist somit nur für den experimentellen Versuchsaufbau geeignet und kann nicht für den industriellen Einsatz verwendet werden. Die Untersuchung des Einflusses der Dichtungssegmente auf die Verweilzeit zeigte keinen signifikanten Effekt. Dennoch konnte gezeigt werden, dass eine Vergrößerung der Spaltgröße zu einer Verringerung der Tablettenmassen und zur Erhöhung der entsprechenden Standardabweichung führt. Die geometrische Speichenform des Füllrades hatte

einen großen Einfluss auf die Durchmischung der Pulverpartikel in der Füllkammer. Es konnte gezeigt werden, dass die runden Füllradspeichen zu einer Zunahme der Durchmischung führten, während die rechteckigen Füllradspeichen eine geringe Durchmischung bewirkten.

Im letzten Teil dieser Arbeit wurde die FE55 Rundläufer-Tablettenpressen, eine der neuesten und modernsten Tablettenpressen der Firma Fette Compacting, verwendet. Diese Tablettenpresse FE55 ermöglichte es, sowohl die Drei-Kammer-FOM als auch das Ein-Kammer-Kegel-Füllsystem zu verwenden. Dadurch war es möglich den Einfluss der FOM auf die Verweilzeitverteilung mit dem des Kegel-Füllsystems zu vergleichen. Beide Füllsysteme besitzen ein ähnliches Füllvolumen, sodass es möglich war den Einfluss des Pulverweges durch die unterschiedlichen Kammern der jeweiligen Füllsysteme auf die Verweilzeitverteilung zu untersuchen. Die Ergebnisse zeigten, dass die unterschiedlichen geometrischen Formen der Füllkammern einen ausgeprägten Einfluss auf den Pulverfluss durch die Füllsysteme und damit auf die Verweilzeitverteilung hatten. Des Weiteren wurde der Einfluss der Volumenreduktion der FOM durch speziell angefertigte Räder auf die Verweilzeitverteilung untersucht. Die Ergebnisse zeigten deutlich, dass die Verweilzeit der Pulverpartikel durch den Einsatz der volumenreduzierenden Räder verkürzt werden konnte und gleichzeitig die Funktion der drei Kammern nicht beeinträchtigt wurde, sodass die volumenreduzierenden Räder auch in der industriellen Herstellung von Tabletten eingesetzt werden können.

Grundsätzlich war es in der Arbeit von wissenschaftlichem Interesse, die Studien so nah wie möglich im industriellen Maßstab durchzuführen, sodass die erhaltenen Ergebnisse sowohl direkt auf die konventionelle Chargenherstellung als auch auf die kontinuierliche Herstellung von Tabletten übertragen werden können.

Summary

Tablets are the most manufactured oral pharmaceutical dosage form with a share of about 80 % on the market. For the industrial manufacturing of tablets usually rotary tablet presses are used. Looking more closely at the individual components of a rotary tablet press, one of the key components is its feed frame system. It ensures a uniform powder flow from the hopper to the dies. In the present thesis, the focus was on the feed frame system of a rotary tablet press developed by Fette Compacting, allowing a direct transfer to the industrial manufacturing of tablets. Issues such as the relationship between the speed of the die table and the feed frame system have not yet been investigated in detail because of their complexity. Thus, the parametric settings have to be determined individually depending on the respective product. To obtain a thorough understanding of the powder particle behaviour within the feed frame system, different geometric and parametric settings were investigated.

In this thesis, the powder behaviour within a three-chamber feed frame system (Fill-O-Matic) of the rotary tablet press Fette 102i as well as within a single-chamber filling cone feed frame system of the rotary tablet press Fette FE55 was investigated. Particular attention was paid to the residence time distribution of the powder particles in the feed frame. The determination of the residence time distribution of the filling material in the feed frame systems and the values of the mean residence time and the mean centered variance were used to evaluate the geometric and parametric settings.

In the first part of this thesis the influence of the die disc speed and of the feed frame speed, as well as the influence of the filling depth, filling cam and the scraper on the residence time distribution were investigated. It was shown that the die disc speed as well as a change of the filling depth have a pronounced influence on the residence

time distribution. The comparison of the results obtained from two filling cams with the same filling depth showed no influence on the residence time distribution. The investigation of the feed frame speed provided an interesting result: with increasing feed frame speed, the mean residence time remained constant, whereas the mixing of the powder particles, indicated by the mean centered variance, was significantly increased.

In addition to the geometric and parametric settings of the Fill-O-Matic (FOM), in a second part of the thesis the influence of the particle properties on the powder behaviour in the FOM was investigated using a microcrystalline cellulose (MCC) blend as model powder. The focus was to characterize the effect of the addition of different amounts of a tracer blend as well as the effect of the powder flow rate through the FOM on the residence time distribution. Furthermore, the powder properties, such as the residual moisture content of the powder particles and the particle size, were compared. It was shown that the amount of tracer blend and the flow rate of the powder particles through the FOM had an influence on the residence time distribution. The different residual moisture contents and the particle sizes of the tracer blend showed no influence on the residence time distribution. However, the different tracer blends with their different particle sizes had a pronounced effect on the particle distribution within the tablets. Large particles accumulated primarily on the top of the tablets, whereas the smaller the particles the more they were found on the bottom of the tablets. A homogeneous particle distribution within the tablet was observed with similar particle sizes of a tracer blend and the MCC blend.

This fundamental knowledge from the first and second part of this thesis was used to examine the effect of the individual FOM components with regard to an optimization of the feed frame system and a reduction of the residence time. To study the effect of

the reduction of the FOM volume on the residence time and on the intermixing of the powder particles, the dosing wheel of the FOM was replaced by a perspex disc. Furthermore, the influence of different geometric wheel rods as well as the influence of different gap sizes of the sealing segment between the FOM and the die disc was investigated. Interestingly, it was shown that the reduction of the feed frame volume with the perspex disc led to a remarkable decrease of the residence time and to a significant reduction of the powder particle intermixing. Unfortunately, with the application of the perspex disc in the dosing chamber, the dosing chamber was no longer available and the exact adjustment of the tablet weight was no longer possible. Thus, the use of a perspex disc is only intended for preliminary experiments and is unsuitable for industrial manufacturing of tablets. The investigation of the influence of the sealing segments on the residence time were non-significant. Nevertheless, it was shown that an increase of the gap size led to a reduction of the tablet weights and to an increase of their standard deviation. Moreover, the results of the filling wheel design showed that the rod shape of the filling wheels had a pronounced influence on the intermixing of the powder particles in the filling chamber, whereas the corresponding tablet weights and their relative standard deviation were not affected.

For the last part of this thesis the FE55 rotary tablet press was used, which is one of the most modern rotary tablet presses by Fette Compacting. The FE55 may be equipped with either the three-chamber FOM or with a single-chamber filling cone feed frame system. Thus, it was possible to compare the influence of the FOM on the residence time distribution with that of the filling cone feed frame system. Both feed frame systems have a similar filling volume, enabling to investigate the influence of the powder path through the different chambers of the respective feed frame system

on the residence time distribution. It was obvious, that the different geometric design of the feed frame systems had a significant influence on the powder flow and thus on the residence time distribution. Furthermore, the volume reduction of the FOM by specially constructed wheels and their influence on the residence time distribution was determined. With these volume-reducing wheels, the effect of the filling volume reduction of the FOM on the powder residence time distribution was investigated. It was shown that the volume reduction of the FOM with three modified large hub wheels led to a decrease of the powder residence time as well as a low intermixing of the powder particles. Remarkably, these results showed that the modified volume-reducing wheels might be a good option for the industrial manufacturing of tablets.

Generally, it has always been of scientific interest to carry out investigations under actual production conditions to obtained results which may be transferred directly to the conventional batch production as well as to the continuous production of tablets on a rotary tablet press.

Conference contributions and publications

In context with this work, the following contributions have been presented at conferences and published as journal articles:

Conference contributions - poster presentations

11th World Meeting on Pharmaceutics, Biopharmaceutics and Pharmaceutical Technology 2018, Granada, Spain; Investigation on the residence time distribution of a rotary tablet press with special focus on the feed frame system

---

Journal articles with authors contributions and reference chapters.

Title	Journal	Authors	Contribution to the work	Percentage	Reference chapters
Investigations on the residence time distribution of a three-chamber feed frame with special focus on its geometric and parametric setups	Powder Technology (accepted)	Dülle, M. Özcoban, H. Leopold.C.S.	Project plan, experiments, data analysis, publication Cooperation partner Supervisor	100 %	3.2.4. 3.2.9. 4.1.
Analysis of the powder behaviour and the residence time distribution within a production scale rotary tablet press	European Journal of Pharmaceutical Sciences (accepted)	Dülle, M. Özcoban, H. Leopold.C.S.	Project plan, experiments, data analysis, publication Cooperation partner Supervisor	100 %	3.2.5. 3.2.9. 3.2.10. 4.2.
The effect of different feed frame components on the powder behaviour and the residence time distribution with regard to the continuous manufacturing	International Journal of Pharmaceutics (accepted)	Dülle, M. Özcoban, H. Leopold. C.S.	Project plan, experiments, data analysis, publication Cooperation partner Supervisor	100 %	3.2.6. 3.2.8. 4.3.
Influence of the feed frame design on the powder behaviour and the residence time distribution	International Journal of Pharmaceutics (accepted)	Dülle, M. Özcoban, H. Leopold. C.S.	Project plan, experiments, data analysis, publication Cooperation partner Supervisor	100 %	3.2.7. 4.4.

Contents

List of Abbreviations

API	Active pharmaceutical ingredient
BM	Batch manufacturing
CM	Continuous manufacturing
CSTR	Continuous flow stirred tank reactor
DEM	Discrete element method
Eq.	Equation
E_t	Residence time distribution
E_θ	Normalized residence time distribution
FDA	Food and Drug Administration
Fig.	Figure
FOM	Fill-O-Matic
MCC	Microcrystalline cellulose
NIR	Near-infrared
PFR	Plug flow tube reactor
Ph. Eur.	European Pharmacopoeia
rpm	revolutions per minute
SD	Standard deviation
UV	Ultraviolet
Vis	Visible
θ	Normalized time
σ^2	Mean centered variance
τ	Mean residence time

1. Introduction

1.1. Tableting

1.1.1. General aspects

The development of the commercial manufacturing of tablets is based on William Brockedon and his invention of the first tablet press in 1843 [1]. An increased demand on this dosage form during the Civil War in the United States promoted their development and manufacturing [2]. In the following years, tablet presses were developed with great success. Nevertheless, the functionalities of the current tablet presses are still similar to the first developed tablet press [2]. Speculations that the tablet may only temporarily be up-to-date were not confirmed. Nowadays, tablets are the most commonly manufactured pharmaceutical dosage forms with a share of about 80 % [3], mainly because of the user-friendliness and the resulting improvement of the patient compliance [4]. In addition, because of their cost-effective manufacturing and a high output tablets are the dosage form of choice [5]. Other advantages are the rather good chemical and physical stability during manufacturing, packaging, and storage [6]. Therefore, tablets may protect unstable active pharmaceutical ingredients (APIs) [7]. In addition to the API, tablets are contained of excipients to improve their properties as well as their manufacturing process [8]. Examples of common excipients in a tablet formulation are fillers and binders (such as microcrystalline cellulose), lubricants (such as magnesium stearate), flow agents (such as colloidal silica) and disintegrants (such as croscarmellose sodium) [9,10].

A suitable composition of these excipients is important for the manufacturability and the resulting tablet quality [11]. Furthermore, it is important to know that many excipients are multi-functional, depending on their amount in the powder blend. For example, microcrystalline cellulose serves as an anti-adherent at a concentration

(w/w) of 5-20 %, as a disintegrant at a concentration (w/w) of 5-15 %, and as a diluent at a concentration (w/w) of 20-90 % [12].

1.1.2. *Preparation of tablet formulations*

The easiest way for preparation of tablet formulations is the direct compaction, i.e. powder compaction [13]. The direct compaction serves as the technique of choice for thermosensitive as well as moisture-sensitive APIs and excipients [14,15]. The most straightforward way of preparation is to weigh the APIs and the excipients and mix them in an appropriate blender. After addition of lubricants and flow agents, the powder blend is ready for tableting. Thus, the direct compaction requires the comparably least number of process steps, resulting in a short manufacturing time (Fig. 1).

In contrast to the direct compaction, the tableting process via granulation requires additional steps such as dry granulation or wet granulation. Granulation is necessary for APIs and excipients, which show an insufficient flow of the power blend as well as a poor compressibility. With an additional granulation step of the powder particles resulting in agglomerates, it is possible to optimise these poor powder properties to obtain an improved tablet formulation for tableting. Further advantages of granules for the manufacturing of tablets are the homogenous distribution of the APIs and excipients in the granules, the stability of the resulting tablets, and the reduction of electrostatic interactions between powder particles. An additional benefit with regard to tableting is the increase of the compressibility, because of the narrow particle size distribution and the hardness of the granules.

The dry granulation includes a roller compaction step, in which the powder particles flow into a slip between two rotating compaction rolls leading to scabs or briquettes of

the APIs and excipients. After the roller compaction step, the scabs or briquettes are reduced in size by an appropriate milling device to obtaine granules.

The wet granulation step can be classified into three different processes (low shear, high shear, and fluid bed granulation) through which the formation and the growth of the agglomerates is achieved by addition of a liquid or binder solution. In the case of water or aqueous binder solutions this step may result in an unwanted degradation of the APIs and excipients, such as hydrolysis [16–18]. Thus, an immediate removal of water by drying or the use of organic solvents is required for the stability of the agglomerates. After the drying step the final process steps are the particle size classification and a further blending step [13,19,20].
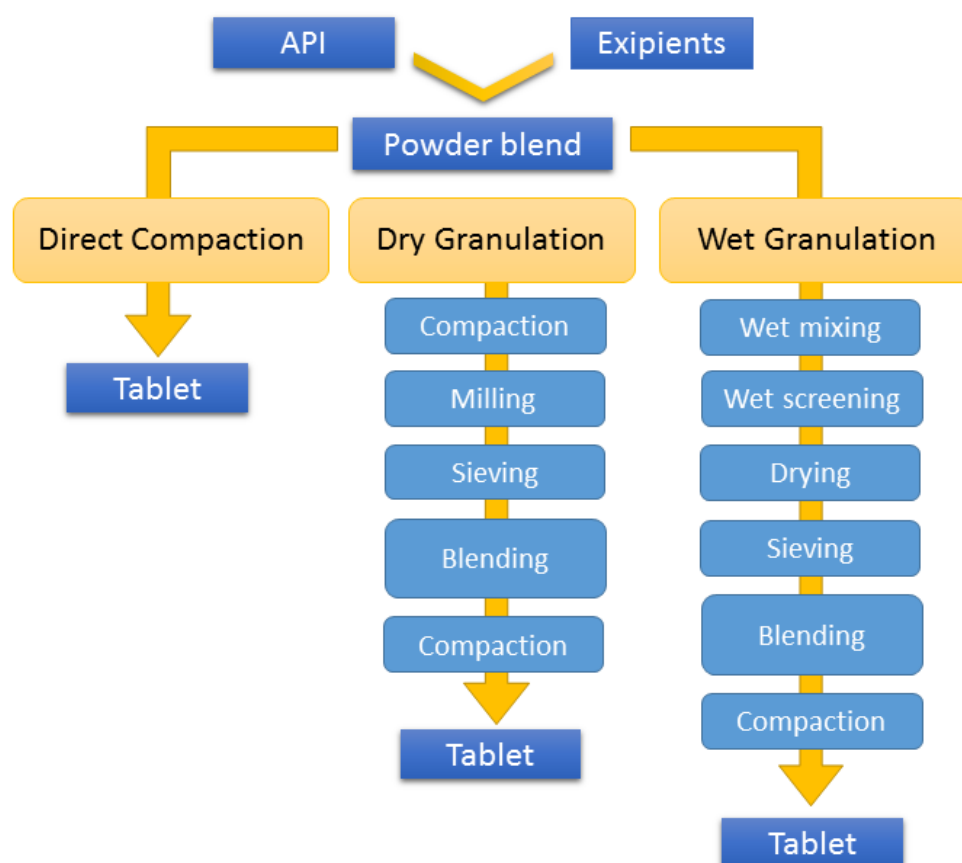

Fig. 1: Comparison of the involved process steps in the direct (powder) compaction as well as granule compaction, modified from [21].

1.1.3. Types of tablet presses

Tablet presses are mechanical devices that compact powders or granules into a single unit dosage form of equal shape, size, and similar content of ingredients (APIs and excipients). The most straightforward tablet press is the eccentric tablet press also known as the single punch tablet press. The eccentric press consists of a single set of tooling, a pair of an upper and lower punch as well as a die.

Therefore, the eccentric press is easy to operate and ideal for the development of tablet formulations as well as for a small tablet batch production. For example, the maximum tablet output of the Manestry F3 eccentric press is about 5,100 tablets/h. In the eccentric press, the lower punch is hold in place during compaction, whereas the upper punch is fixed to an eccentric rod that moves up and down above the die. The eccentric rod, which is driven by an eccentric sheave, moves in a vertical direction. The eccentric press is usually powered by an electric motor [22]. A movable funnel fills the tabletting mass into the die prior to the compaction step. During the compaction step, the die and the lower punch remain in a fixed position. The upper punch moves downwards and compacts the particles in the die. The reduction of the bulk volume and the successive particle deformation (preferably plastic or brittle) lead to a consolidation of the particles into a tablet. After compaction, the upper punch retracts and the lower punch moves upwards to eject the tablet. As the movable funnel returns to fill the die, it pushes the compacted tablet from the die to the ejection chute and scrapes all excess material away from the die surface. At the same time, the funnel fills the die with a new portion of particles and the compaction process begins again.

The manufacture of tablets with a rotary tablet press consists of several steps: the particle flow from the hopper to the feed frame [23,24] and through the feed frame

chambers [25,26], the filling of the dies [27–29], and the compaction of the particles [30,31]. The compaction properties of the tableting mass are defined by their ability to form strong mechanical compacts (called compactibility) as well as their ability to deform under pressure (called compressibility) [32,33]. It is important to have a well-balanced interplay between these individual steps. Each process step of the rotary tablet press is interdependent.

Modern rotary tablet presses are able to produce tablets with a current output of up to 1.6 million tablets/h [34]. This high production rate depends on the amount of punch stations of the die disc and the rotational die disc speed. For example, small lab-scale rotary tablet presses consist of about 6 punch stations, whereas high-performance rotary tablet presses for the industrial manufacturing of tablets consist of about 115 punch stations [34]. This configuration with different sizes of die discs makes it possible, to easily upscale the tablet manufacturing from lab-scale to industrial production-scale. Furthermore, rotary tablet presses can be modified to a double-sided tablet press, which offers the production of two tablets per die disc revolution.

In comparison to the single-punch eccentric press, the basic steps such as filling of the dies, dosing of the dies, compaction of the particles and ejection of the tablets are similar to those of the rotary tablet press, where these steps are performed simultaneously [35]. In Fig. 2, the respective steps of the tableting process on a rotary tablet press are illustrated. The main reason for the high productivity of rotary tablet presses is the use of numerous punch stations of the rotatable die disc [36]. The punch stations consist of a lower punch, an upper punch and a die, in which the particles are compacted. If the die disc rotates, these punch stations pass the following process steps during tablet manufacture [37]:

1. Filling of the dies: The dies of the die disc pass the feed frame chambers and the lower punch is pulled downwards by the filling cam. During the downward movement, the particles in the feed frame flow into the dies.

2. Dosing of the dies: The dosing of the dies and thus the mass adjustment of the tablets is set by a previously adjusted filling depth of the dosing cam. Therefore, a defined upward movement of the lower punch leads to a particle removal out of the dies and the excess particles are returned from the die disc to the feed frame chambers.

3. Compaction of the particles: After die filling and dosing of the die, the punch stations pass the pre- and the main-compaction rolls, where the upper and lower punch move into the die to exert a compaction force, which leads to the compaction of the particles. During pre-compaction step a preliminary compaction force is executed on the particles prior to the main-compaction step. Through pre-compaction the bed of the tableting mass is vented and the properties of the resulting tablets are improved [38]. The hardness of the tablets is controlled by the compaction force of the main-compaction roll.

4. Ejection of the tablets: After the compaction of the particles, the tablets are pushed out of the ejection cam by the upward movement of the lower punch. The ejection finger moves the tablets from the die disc surface to the ejection chute, and the produced tablets are collected.
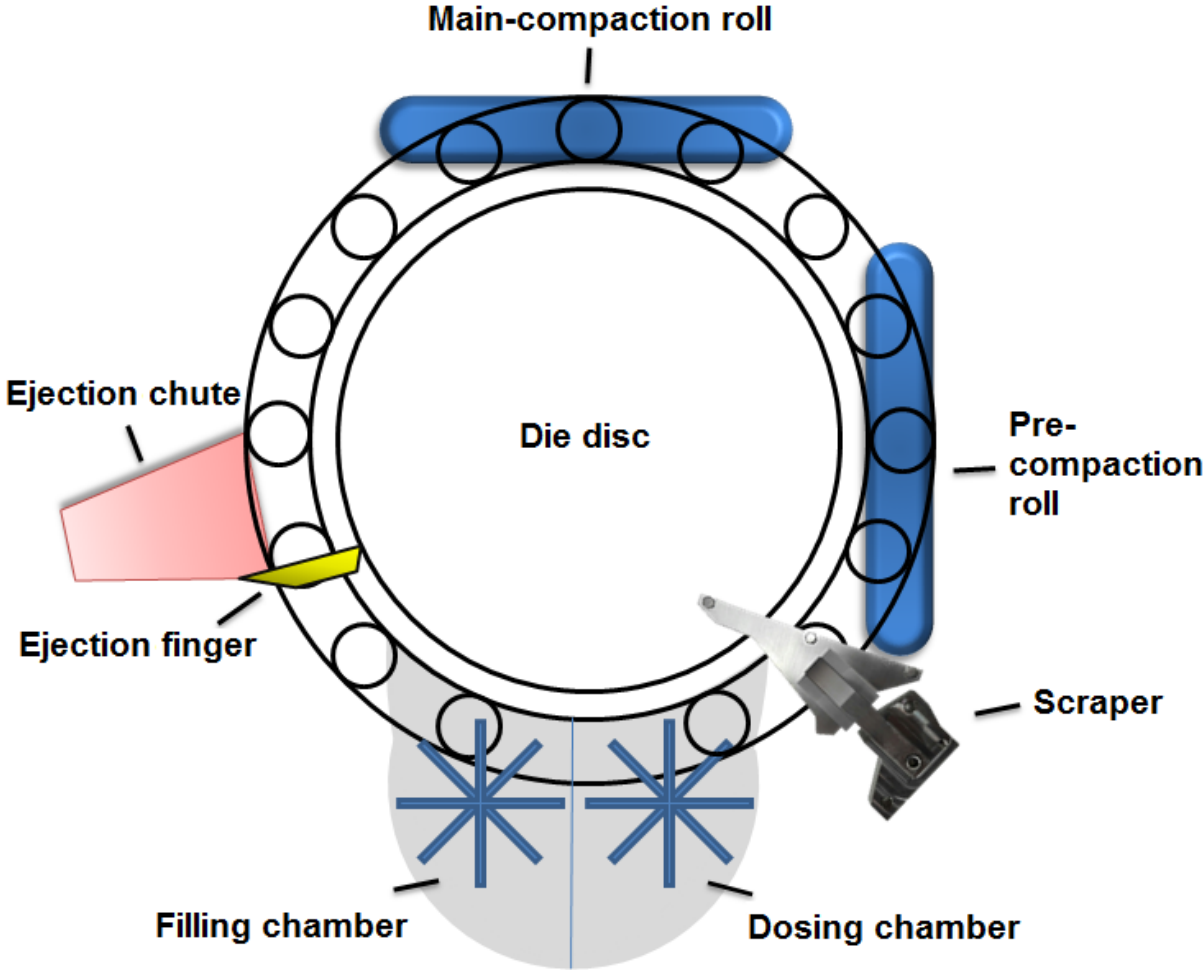
Fig. 2: Illustration of the compaction process on a rotary tablet press.

1.1.4. Feed frame systems

1.1.4.1. Three-chamber feed frame system

The manufacturer Fette Compacting equips their rotary tablet presses of the i-series with a three-chamber feed frame system (Fill-O-Matic). The Fill-O-Matic (FOM) consists of three chambers positioned at a high and a low level. The distribution wheel of the distributing chamber at the upper level (Fig. 3A) receives the particles from the feed pipe and distributes them to the filling and dosing chambers at the lower level (Fig. 3B). The FOM ensures a homogeneous particle flow from the hopper to the dies. Because of the three chambers, the FOM has a large volume, resulting in a high robustness against disturbances such as a brief interruption of the particle flow from the hopper to the feed frame. The wheel configuration of the FOM consists of a filling wheel with 12 flat rods, the last 20 mm of which are horizontally angled. The dosing wheel of the dosing chamber also consists of 12 flat rods arranged at a slight horizontal angle from the hub. The two levels of the FOM are separated by an intermediate plate, which contains perforations with different diameters. The orifice of the intermediate plate in the direction of the filling chamber is wider than that which leads to the dosing chamber. The wheels of the FOM are rotated by a drive shaft in a range between 10 and 120 rpm. The rotational speed of the FOM wheels are controlled individually by a control terminal. The filling wheel of the filling chamber fills the cavity of the dies, and the dosing wheel of the dosing chamber takes up the excess tableting mass of the dies as soon as the lower punches are pushed up by the filling cam. The dosing wheel returns the excess tableting mass back to the filling chamber. The tableting mass in the filling chamber is primarily used for the die filling process. However, a small amount of the tableting mass is needed in the dosing chamber for dosing of the dies. The intermixing of the particles in the feed frame may

be considered as an additional mixing process after the actual blending of the particles. However, a high intermixing as well as a long residence time of the particles in the feed frame may lead to an increase of the mechanical shear stress [25,39]. Considering the geometries of the feed frame system, the longer the particle exposition to the operation units, the more pronounced the particle attrition and powder overlubrication [25,39].
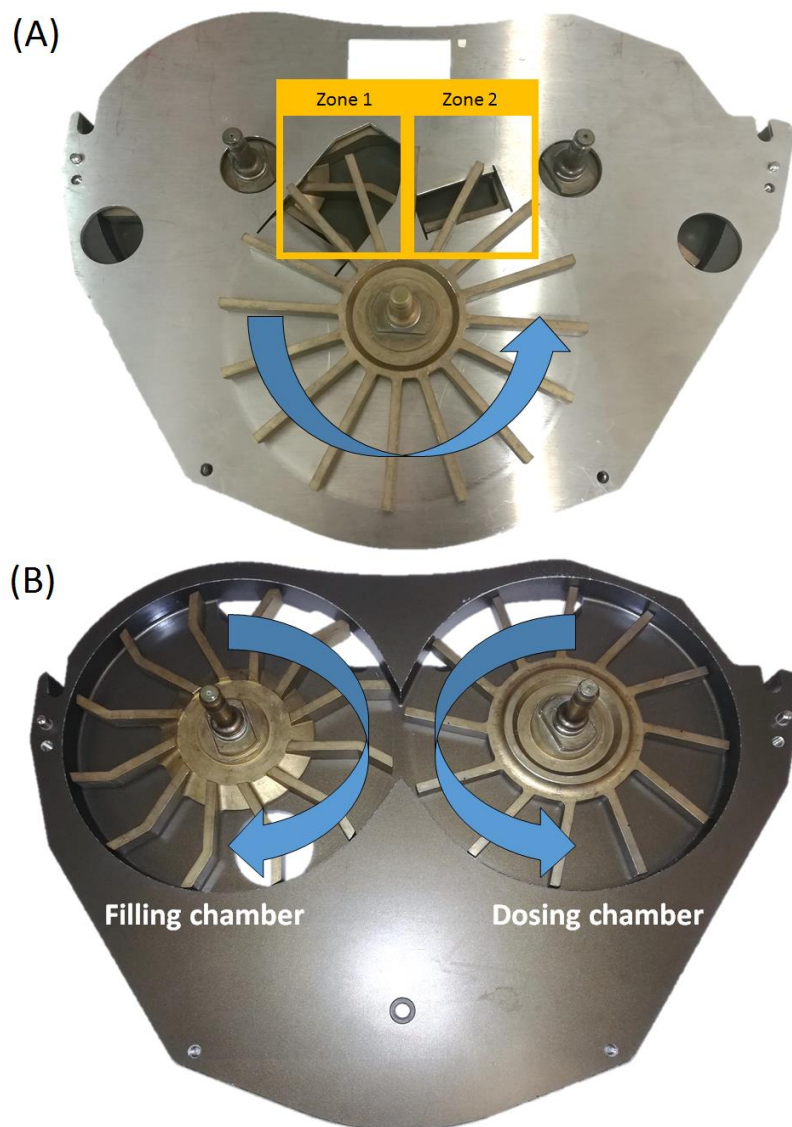

Fig. 3: Design of the Fill-O-Matic: (A) The distributing chamber with exit zones to the filling chamber (Zone 1) and dosing chamber (Zone 2) positioned at the high level and (B) the filling chamber (left) and dosing chamber (right) positioned at the low level.

1.1.4.2. Cone-shape feed frame system

The rotary tablet presses of the Fette FE-series are equipped with a cone shape feed frame system. In contrast to the FOM, the filling cone consists of a single chamber and one filling wheel (Fig. 4). Thus, the particle behaviour in the feed frame and the path of the particles through the feed frame are completely different. The cone-shape filling wheel receives the particles from the feed pipe and distributes them to the die disc and into the dies. Thus, the filling cone ensures a direct particle flow from the feed pipe into dies. If the filling volume of the FOM and that of the filling cone are compared, both feed frame systems have a similar filling volume of about 800 cm³. The filling cone consists of one filling wheel with a diameter of about 280 mm and a cone-shape hub comprising 12 flat rods, with a length of 40 mm each. The filling wheel rotates counterclockwise in a range between 10 and 240 rpm whereby this direction is important for the filling step of the dies. The rods of the wheel move the particles to the filling area and into the dies. The tableting mass in the filling area is primarily used for die filling. However, also a small amount of tableting mass is needed in the dosing area for dosing of the dies, as already described in chapter 1.1.4.1. Thus, the transfer of the particles from the filling area to the dosing area is fluent in contrast to the FOM with its filling and dosing chamber.
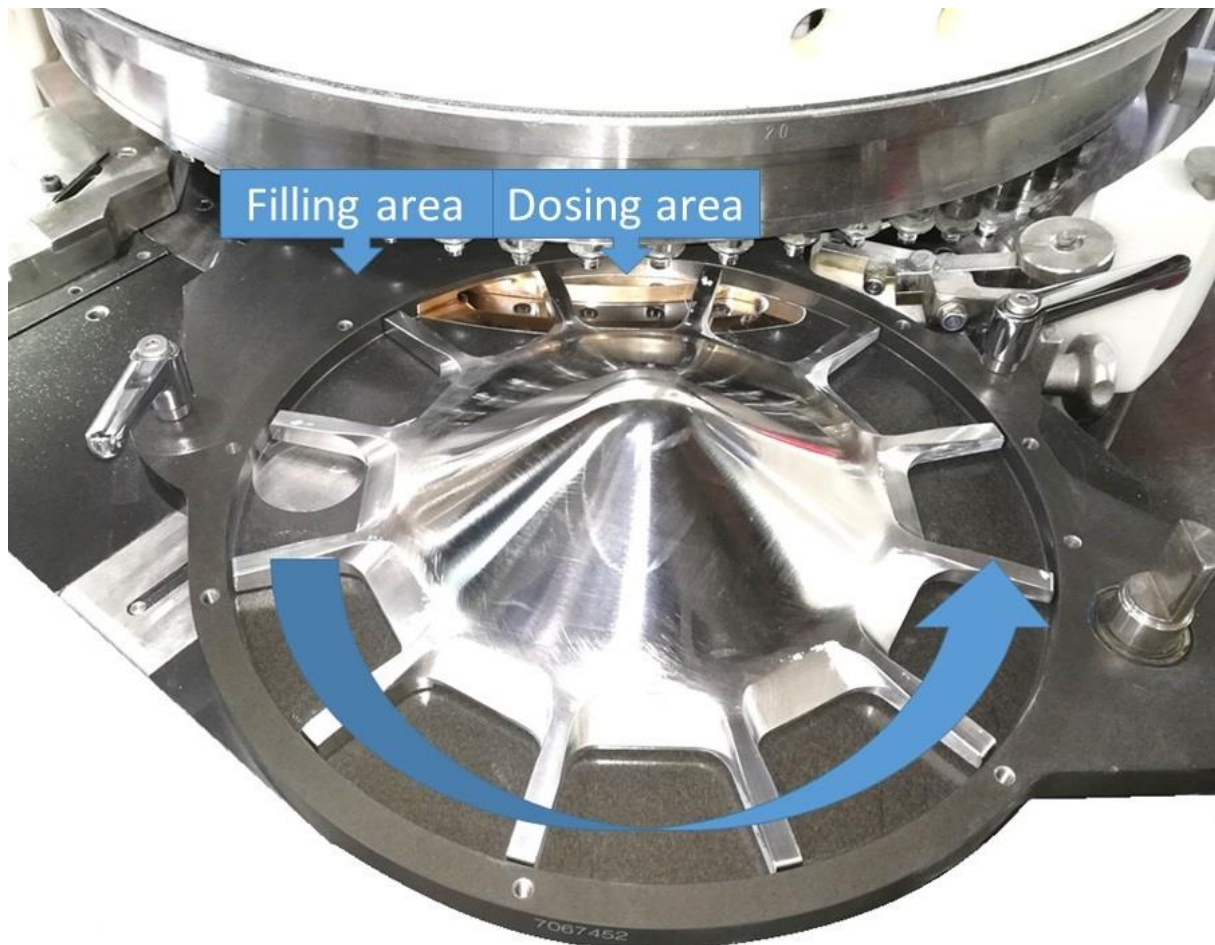
Fig. 4: Design of the filling cone feed frame system with its cone-shape filling wheel and the particle path through the feed frame (blue arrow) including the filling and dosing areas.

1.1.4.3. Filling and dosing of the dies

The filling and the dosing processes involve a complex interplay of several components. In addition to the feed frame system, a filling cam and a dosing cam are further fundamental elements needed for the filling and dosing of the dies. The uniformity of the tablet weight and the API content are determined by the consistency of the filling and dosing of the dies. Thus, it is also important to have a well-balanced interplay of the feed frame components, as not only the particle properties, such as particle size, density, and particle shape, affect the filling and dosing of the dies [40].

The feed frame parameters, such as the rotational wheel speed, the number of the wheels, and the geometry of the rods, also affect this process [41]. The filling cam guides the lower punches below the filling chamber to a maximum filling depth and the final filling depth of the dies is adjusted by a dosing cam (Fig. 5). At the position 1, the lower punch is pulled downwards by the filling cam resulting in a negative pressure, which ensures the flow of the particles into the die, until the die is completely filled. At the position 2, the lower punch is pushed upwards by the dosing cam up to the manually adjusted filling depth and the excess tableting mass will pushed out into the dosing chamber of the feed frame system.
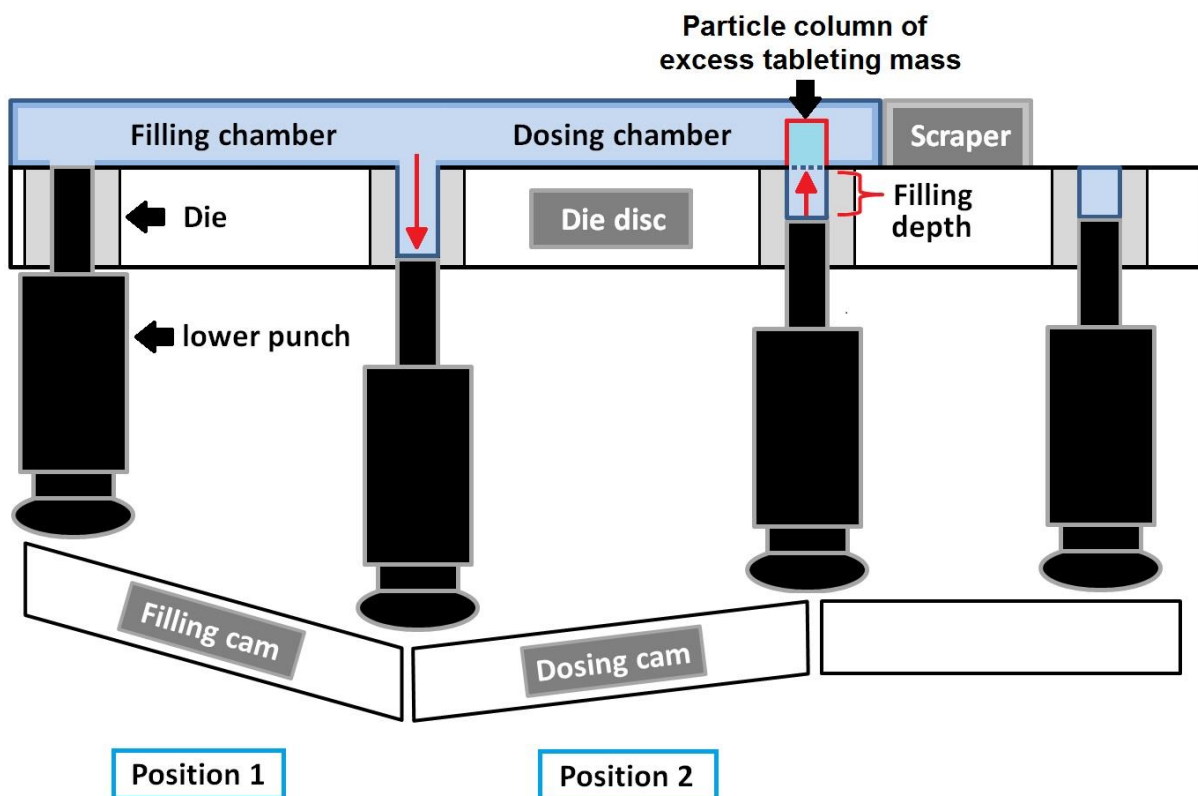
Fig. 5: Schematic overview of the die filling process in the Fill-O-Matic. Position 1: Filling of the dies. Position 2: Back-dosing of the dies.

The dosing wheel of the dosing chamber receives the excess tableting mass of the overfilled punches, as soon as they are pushed up by the filling cam. For example, with a filling cam of 12 mm and a filling depth of 7.5 mm the lower punch at the Position 1 is pulled 12 mm downwards and at Position 2 a powder column of 4.5 mm is pushed back from the die to the feed frame system (Fig. 5). The lower the filling depth the lower the tablet weight and the higher the amount of tableting mass which is dosed back [26]. The dosing wheel pushes the excess tableting mass back to the filling chamber (Fig. 6, red arrows).

Filling chamber   **Dosing chamber**

Fig. 6: Path of the excess tableting mass. The red arrows illustrate the movement of the particles from the dosing chamber to the filling chamber.

1.2. Continuous versus batch manufacturing

The pharmaceutical industry is one of the few industrial branches that still mainly applies in batch manufacturing (Fig. 7). An advantage of the tablet batch manufacturing is the exact control of the different production steps. After each production step, a quality check is carried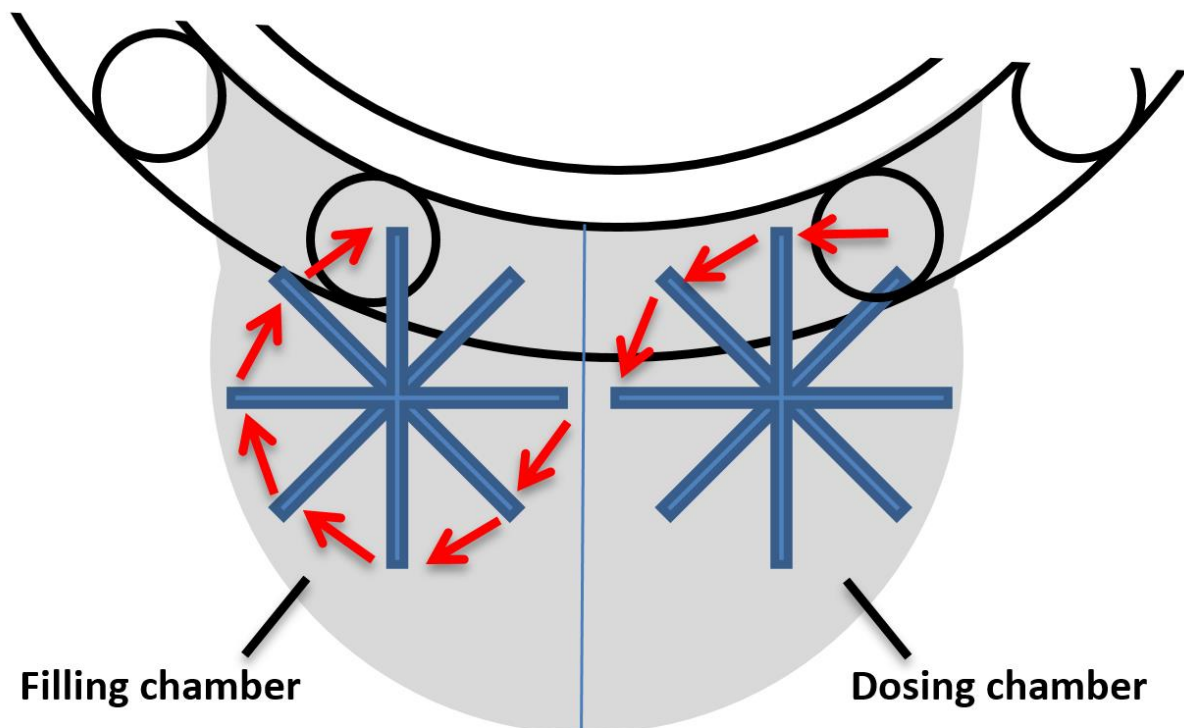 out with subsequent approval for the following production steps. If quality problems are detected, it is only possible to take countermeasures after the respective production step [42]. There are also further disadvantages of batch manufacturing. Withdrawal periods between the production steps as well as downtimes of the machines lead to an increase of the production costs [43,44]. Moreover, customers expect tight deadlines from the pharmaceutical manufacturing companies, as well as consistently high quality at all stages of manufacture, such as tablet production [45]. To reduce the costs, some of the raw materials are imported from low-wage countries [46]. The growing cost pressure resulting from the requirement for an high product quality needs a new approach for pharmaceutical manufacturing [47,48]. Schaber et al. published an analysis of integrated continuous manufacturing in which the authors concluded that the continuous manufacturing of pharmaceuticals is a realisable way for the pharmaceutical industry to achieve substantial cost savings. The comparative cost calculation of batch manufacturing (BM) and continuous manufacturing (CM) led to a cost saving of up to 44 % [49]. Furthermore, CM simulations showed an increase of the product output per time, an improvement of the robustness of the continuous processes, and the assurance of a consistent product quality [50,51].

The industrial manufacturing of pharmaceutical products is currently undergoing a change. Various pharmaceutical companies, research institutions as well as regulatory agencies are doing research on the CM of pharmaceutical products to

extend or replace the traditional BM [42,52,53]. The reduction of the production costs, a better flexibility manufacturing process, the robustness of the resulting products, and the safe manufacturing of the products are benefits of the CM [53,54]. Moreover, the waste which results from the production process is reduced, a smaller footprint is achieved, a faster product development is possible, and an easier scale-up are advantages of the CM [43,55,56]. Thus, the same equipment may be used for the product development as well as the industrial manufacturing [57]. Therefore, the implementation of CM in the pharmaceutical industry shortens the time for release of products to the market [58]. The basic principle of the CM is illustrated (Fig. 7).
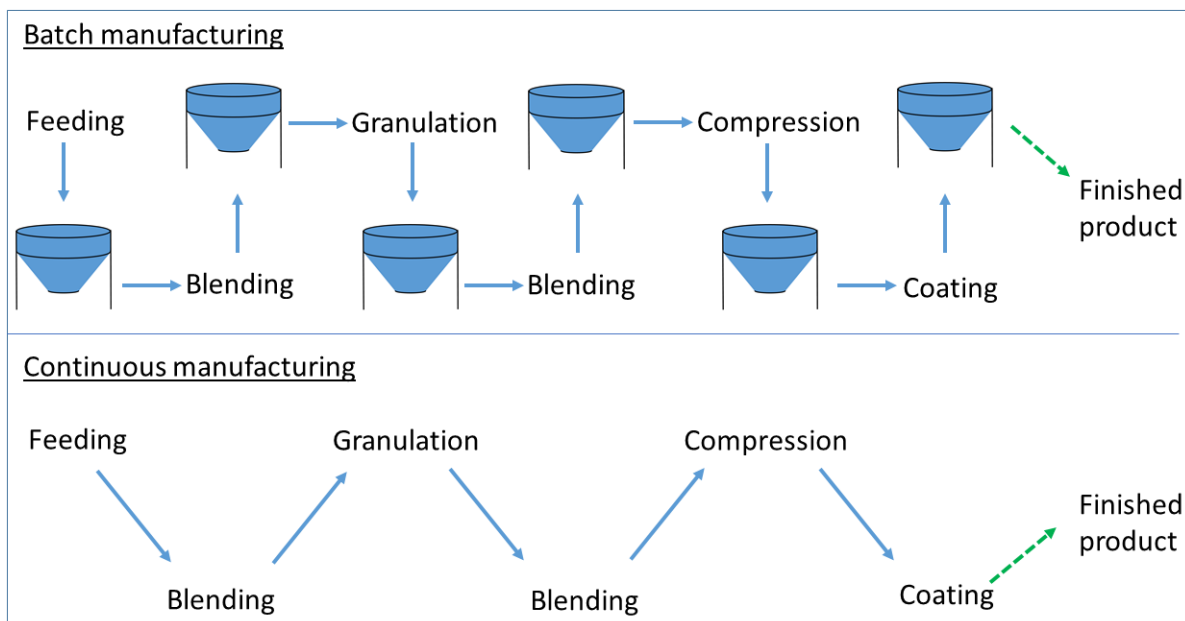

Fig. 7: Schematic illustration of the batch manufacturing and the continuous manufacturing.

The manufacturing steps of CM (e.g. powder feeding of the blender, blending, granulation, compression, and coating) are cascaded and are depended on each other [46]. These steps are monitored with specifically designed measurement tools for CM [59,60]. Therefore, CM allows a fast response to changes in production process. Moreover, CM needs less equipment compared to BM [48].

The raw materials which are added to the production system leave the operation unit continuously as end product [42,43,61]. Thus, with CM there is no longer the need to store the intermediate products between the respective process steps and human errors are ruled out with regard to the handling of the raw materials and the intermediate products [43,50].

Other industrial branches have changed their production to CM already years ago. These include the catalysts manufacture [62], mineral processing [63], and also the food processing [64,65]. The switch to CM in the pharmaceutical industry proceeds rather slow [66]. The reasons are the official requirements to ensure the high-quality standards of the pharmaceutical products. The manufacturing of pharmaceutical products is subject to a strict control with a variety of specifications and guidelines that have to be adhered to [67]. The quality controls of BM are performed after each manufacturing step. After these controls, the intermediate products are released for the next respective manufacturing step. In the case of an out-of-specification (OOS) event after the manufacturing step, countermeasures have to be initiated. This type of quality control leads to long downtimes between the production steps. The quality controls of the CM are performed simultaneously with the production process, e.g. with NIR spectroscopy [68,69]. This makes it possible to initiate countermeasures immediately [59,70].

It has been shown, that the implementation of CM particularly with its automated processes has the potential to improve the product quality [71]. This implementation of real-time quality control is one of the most important advantages of CM. For example, CM leads to less OOS products because of the implementation of real-time quality controls as well as the possibility of immediate countermeasures during the production process [72,73].

In the past, the regulatory agencies had the concern, that CM might be unsuitable if the product batch or its size changes daily and that CM is only suitable for large product batches. They claimed that the products manufactured by CM might be unable to meet the quality standards and thus may delay the approval of the products [74]. To confirm that this scepticism of the regulatory agencies is unsubstantiated, it is important to obtain a more comprehensive knowledge of the manufacturing process dynamics in relation to the operation units used during CM and of the design of the individual components installed in the operation units [53]. To facilitate the quality control, the Food and Drug Administration (FDA) introduced guidelines for the Process Analytical Technology (PAT) [75]. Furthermore, guidelines were released by the International Conference on Harmonization (ICH) to provide options for process monitoring of both the intermediate products and the end product [76,77]. It is important to guarantee a well-balanced interplay of all used operation units. A fundamental understanding of the relationship between the process conditions and the behaviour of the intermediate products in the continuous system is necessary. To obtain such a fundamental understanding of this relationship, the residence time distribution (E_t) may be used [78,79]. E_t describes the distribution of the residence time of elements, such as powder particles, inside the operation unit. Thus, differences in the resulting E_t versus time profiles may describe the influence of the

equipment on the particle behaviour [66,80]. The residence time of the particles depends on the operation conditions [81], the geometric design of the operation unit [25], and on the properties of the particles [66].

1.3. Residence time distribution in operation units

The residence time distribution E_t has become an important parameter for the measurement and analysis of the behaviour in chemical reactors and continuous flow systems. The theoretical analysis is usually based on the ideal assumption of a plug flow tube reactor (PFR) or continuous flow stirred tank reactor (CSTR). The PFR and the CSTR are two models that describe different mixing conditions and different E_t versus time profiles of a tracer in a chemical reactor [78]. The ideal model of a PFR is based on the assumption that all particles in the PFR move in axial direction. Whereas in axial direction no mixing occurs, in radial direction the particles are homogeneously mixed. Thus, tracer particles which enter the PFR at time point 0 will exit the reactor at time point t > 0, because of the same velocity of the tracer and the plain particles. The E_t of the tracer particles correspond to the mean residence time τ (Fig. 8A).

In contrast, the ideal model of the CSTR describes a homogenous mixing condition of all particles in the reactor [82]. However, the ideal CSTR leads to a long residence time of the tracers particles because they are mixed with the plain particles in the CSTR (Fig. 8B). Referring to the continuous manufacturing of tablets it is desirable to have an E_t which is very close to the ideal PFR model with minimum mixing and a rapid discharge of the particles.
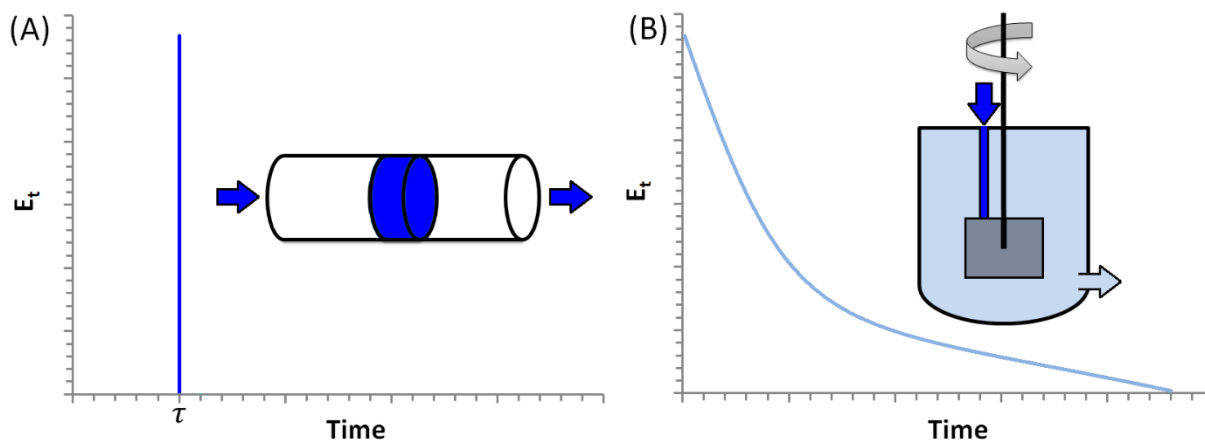
Fig. 8: Ideal models of (A) the plug flow tube reactor and (B) the continuous flow stirred tank reactor with their E_t versus time profile.

The true flow conditions in chemical reactors and continuous flow systems show significant deviations from the ideal theoretical models [83]. In praxis, differences in the temperature or concentration within a chemical reactor may lead to macroscopic effects such as an uneven flow behaviour. In this case, some regions of the system contain less particles or are not optimally flowed through with particles. In this context, E_t provides an accurate information on the actual behaviour of the particles within the system. Thus, investigations of the actual behaviour of the particles in the system are necessary for the optimization and the development of the reactors and flow systems. Assuming that the particles, which enter the system at the same time point show a non-uniform residence time because the aforementioned macroscopic effects, the E_t versus time profiles are broad.

The residence time distribution E_t has already been introduced in the chemical and food industry to develop models, characterize mixing effects, and design new equipment [84]. It has turned out to be a major tool for development and control strategies [85]. Lately, E_t has also been introduced in the pharmaceutical industry. Efforts have been made to use E_t for the description of manufacturing processes

involving solid materials such as continuous powder feeding of blenders [86,87], powder blending [80,88], powder extrusion [89,90], twin screw granulation [81,91], and fluid bed granulation [92,93]. The main parameters used to investigate the influence of the respective process on the powder behaviour in the operation units are the E_t with its mean residence time and its mean centered variance. Sisay et al. reported that the residence time of a solid material in a continuous flow system has a direct influence on the product quality [79]. Thus, a long residence time of the powder particles in the feed frame of a rotary tablet press may lead to a reduction of the quality, particularly for those powder particles the properties of which are highly sensitive to mechanical shear stress. Furthermore, numerous modelling techniques have been applied to calculate the behaviour of powder particles and the powder flow within operation units such as a powder blender with the discrete element method (DEM) [94,95]. The E_t is critical for the batch manufacturing as well as the continuous manufacturing of pharmaceutical tablets. However, the E_t of the powder particles in a rotary tablet press is subject of interest in continuous manufacturing for the traceability of powder blends, development of predictive models, and for a better understanding of the influence of the feed frame design on the powder flow rates. Furthermore, the E_t versus time profile shows a better understanding of the influence of the geometric and parametric setups of the rotary tablet press. In addition, the feed frame has been subject of research with regard to the E_t. Mateo-Ortiz et al. described the relationship between E_t and the force applied by the paddle wheel [84] and computationally simulated the powder movement in the feed frame by means of DEM [25]. Considering the different geometries of the feed frame, there is a wide variety of possible setups resulting in numerous influencing factors on the residence time. For further development of feed frames, it is important to understand the relationships

between the geometric as well as parametric setup and the resulting residence time of the powder, to ensure a high tablet quality. Potapov et al. simulated the particle attrition in a two-dimensional shear cell containing composite, non-spherical particles by DEM [39]. It was shown that the attrition is directly related to the overall shear stress in the system. Furthermore, a too high concentration of lubricant as well as an a high shear stress on the lubricant lead to an overlubricated state, which has a negative influence on the tablet quality [96–99]. The lubricants present in the tableting mixture reduce the friction between the metal components of the feed frame and the powder particles. For these reasons, it is important to optimize the geometric and parametric setup of the tablet press to reduce the residence time and to minimize the applied shear stress on the powder in the feed frame. Engisch et al. defined the CM as a series of single batches with an interface region [42]. This interface region describes the intermixing effect between the batches.

1.4.   UV-Vis spectrophotometry

1.4.1.   General aspects

Ultraviolet and visible (UV-Vis) light are electromagnetic radiations within a certain range of the electromagnetic spectrum. The UV radiation represents a range of the electromagnetic spectrum with wavelengths between 100 to 400 nm [100] whereas the visible radiation represents a spectrum from 400 to 800 nm [101]. Furthermore, the radiation of the Vis spectrum comprises photon energies of 36 to 72 kcal/mol and the radiations of the UV spectrum extend this energy range to 143 kcal/mol [102].

If sample molecules are exposed to light with a radiation energy that corresponds to a possible electronic transition within the molecule, a part of the light energy is absorbed if the electron is transported onto a higher energy level. Therefore, if a sample solution is irradiated by monochromatic light (I_0), the intensity of the transmitted light (I) is reduced. The Beer-Lambert law of absorption is defined as the decimal logarithm of the quotient of the intensity of the incident light and the intensity of the transmitted light (1) [103].

$$A = \log \left[\frac{I_0}{I} \right] = \varepsilon \cdot c \cdot d \tag{1}$$

A = Absorbance

I_0 = Intensity of the incident light

I = Intensity of the transmitted light

ε = Molar absorption coefficient [$\frac{1}{mol \cdot l}$]

c = concentration [$\frac{mol}{l}$]

d = length of the light path [cm]

Furthermore, the absorption is dependent on the molar absorption coefficient, the concentration of the sample solution, and the length of the light path. At a certain wavelength λ, the molar absorption coefficient ε indicates the absorption of a 1 molar solution and a length of the light path of 1 cm. Therefore, the molar absorption coefficient ε is a material constant and with a known ε, wavelength, and absorption it is possible to calculate the concentration of a solution.

1.4.2.   Construction of a UV-Vis spectrophotometer

The wavelengths at which absorption occurs as well as the intensity of the absorption at each wavelength may be recorded by a spectrophotometer (Fig. 9), which is equipped with a xenon light source, emitting a spectrum similar to daylight. The monochromator selects a narrow band of wavelength from the daylight spectrum, which allows measurements at either one wavelength or within a defined band of wavelength. A beam splitter is used, to split the light into two beams with equal intensity, one beam is directed to the reference cell, because a part of the light is lost through reflection and absorption at the cell surface and the solvent [103]. The other beam is directed to the sample cell for the measurement of the sample concentration. Some detectors have two silicon photodiodes, which measure the light pass through the reference cell and the sample cell at the same time whereas in other detectors the beams from the reference cell and the sample cell pass through a beam chopper, which alternately blocks one beam. The spectrophotometric data as percentage transmittance or absorbance are converted and forwarded to an evaluation unit. The advantage of the sample measurement with a UV-Vis spectrophotometer is a fast procedure, which makes it possible to measure a large numbers of samples within a short time.
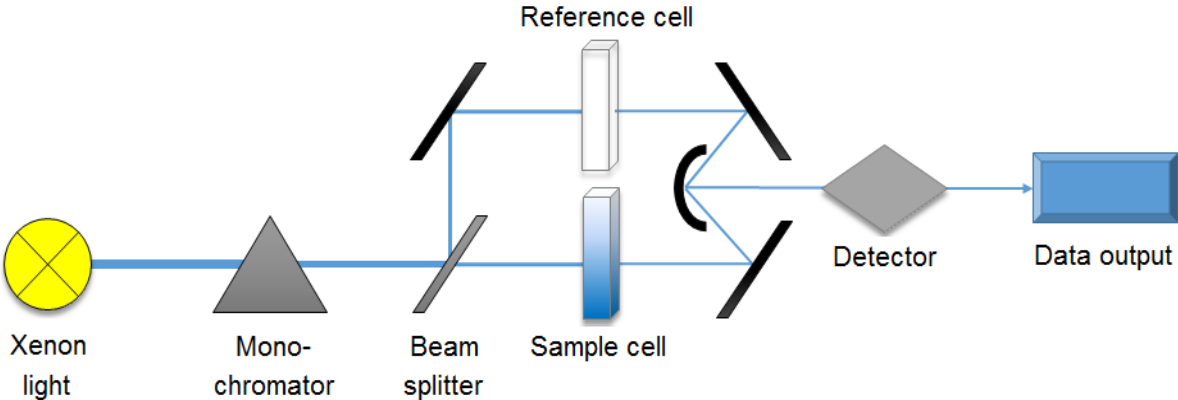
Fig. 9: Schematic illustration of a dual-beam spectrophotometer.

2. Aim of this work

The aim of the present work was to offer a more comprehensive knowledge of the powder particle behaviour in the feed frame systems developed by Fette Compacting. The main focus was the investigation of the powder particle behaviour and the residence time distribution of a Fill-O-Matic (three-chamber feed frame system, composed of three wheels positioned at two different height levels) and a filling cone feed frame system (single chamber with only one cone-shape wheel). Previous studies showed that the powder behaviour in the feed frame could not be analysed because of their complexity. In view of the current trend towards the implementation of continuous manufacturing in the pharmaceutical industry, it is of particular importance to know the influence of the operating conditions and the system geometry on the powder flow through the feed frame. A method to investigate the influence of these variables factor on the powder flow is the residence time distribution. To obtain an advanced knowledge on the continuous manufacturing of tablets the experiments were carried out on a production scale rotary tablet press. Furthermore, the present work deals with microcrystalline cellulose as model excipient, which is a widely used pharmaceutical filling material for tablets. The obtained results are important for the scaling up and optimization of the corresponding tablet manufacture equipment. With this knowledge of the powder behaviour, it is possible to reduce the residence time as well as to minimize the powder shear stress in the feed frame and thus to increase the quality of the resulting tablets in the batch and the continuous manufacturing.

Specifically, the four aims of this work may be summarised as follows:

The first aim was to understand the effect of the feed frame system setup on the powder behaviour. Therefore, the influence of a geometric setup (filling cam and inner/outer scraper) and a parametric setup (die disc speed, feed frame speed, and filling depth) on the residence time distribution was determined.

The second aim was to understand the influence of the powder properties on the powder behaviour in the feed frame system. Therefore, the effect of various amounts of a tracer blend, the particle size, the residual moisture, and different flow rates on the residence time distribution and the powder behaviour were investigated.

With the obtained knowledge of aim I and aim II, the components of the Fill-O-Matic were developed to optimize the residence time distribution of the powder particles of the feed frame system. Thus, the effect of a sealing segment between the feed frame and the die disc, the spoke shape design of the filling wheel, and the reduction of the feed frame volume with a perspex disc for scientific purposes were investigated.

The fourth aim was to compare the powder behaviour and the residence time distribution within a single-chamber feed frame with that within a three-chamber feed frame system. Furthermore, specially developed volume-reducing wheels were used to investigate the effect of the different feed frame volumes on the powder behaviour and the residence time distribution.

3.   Materials and Methods

3.1. General materials

3.1.1. Microcrystalline cellulose

Microcrystalline cellulose (MCC) is optically a white, crystalline powder of porous particles [12]. MCC consists of purified α-cellulose, obtained by hydrolysis of wood and cotton cellulose using dilute mineral acid. Other source materials for the production of MCC are coconut shell [104], sugar cane bagasse [105,106], wheat straws [107], and flax straws [108]. During the production of MCC the amorphous structures of the cellulose are hydrolysed to a bundle of needle-like microcrystals [3,109]. Various degrees of fineness for different fields of application are obtained by a subsequent spray-drying process or by a sieving process.

MCC is a commonly used excipient in the food, cosmetic, and pharmaceutical industry [110]. In the pharmaceutical industry, MCC types with large particles are used as fillers and as dry binders for the direct compaction of tablets [111,112], whereas the MCC types with small particles are used as excipients during dry granulation to increase the hardness of the granules [113]. The properties of MCC such as being chemically inert and compatible with most of the active pharmaceutical ingredients are ideal for the application in the pharmaceutical industry [3]. A further advantage of MCC for the manufacturing of tablets is its good compactibility at low pressures, which results from the formation of hydrogen bonds between the cellulose chains of the adjacent cellulose chains [114]. Thus, tablets with a high hardness are obtained, which show a fast disintegration in contact with water. Because of the porosity of MCC, water quickly penetrates into the tablet (wicking effect). This effect results in a fast moisture expansion of the amorphous structures. The breakage of the hydrogen bonds leads to a rapid disintegration of the tablets [115]. These properties such as the excellent compactibility at low pressures, the fast

disintegration in water, and the wicking effect are reasons for the application of MCC in the pharmaceutical manufacturing of tablets. In the present thesis, two types of microcrystalline cellulose were used: Vivapur® 102 and Vivapur® 200 (JRS Pharma, Germany).

3.1.2.   Colloidal silica

Colloidal silica is manufactured by pyrolysis from silicon tetrachloride and hydrogen. During the pyrolysis of colloidal silica, loose and flake-like aggregates of colloidal particles with a mean diameter of 7-12 nm are obtained. In the present thesis, the common type of colloidal silica Aerosil® 200 (Evonik Industries, Germany) was used. The number 200 after Aerosil® refers to the high specific surface area of 200 m²/g. Furthermore, Aerosil® 200 has a low tapped density of about 0.05 g/ml [116].

Colloidal silica is widely used as a free flowing and anti-caking agent to improve the flow properties of powders and as a viscosity-increasing agent to thicken liquids in the pharmaceutical industry as well as in the food industry for more than 50 years [116]. The colloidal silica particles accumulate around powder particles and may serve as a spacer. Because of the increased distance and the decreased cohesiveness of the powder particles, the flowability of the powder particles is improved. Furthermore, colloidal silica shows a pronounced gliding and rolling effect, which also improves the flowability of the powder particles. Colloidal silica absorbs water up to 40 % of its own weight without losing its powder properties [6]. This effect is based on the adsorption of water molecules to the hydrophilic silanol groups of the colloidal silica molecules [117].

3.1.3. Indigo carmine

Indigo carmine has been used in the past for various cosmetic applications and nowadays for industrial applications such as colouring agent in the cotton and textile industry [118]. Indigo carmine is an organic salt, which is derived from sulfonation of natural indigo [119]. In the pharmaceutical industry indigo carmine is used as a colorant [120], because the molecule has a high adsorption capacity. Indigo carmine has a blue colour, because it absorbs primarily the wavelengths of the light in the range between 585 and 620 nm with an absorption maximum of 608 nm [121]. In Fig. 10 the chemical structure of Indigo carmine is displayed. In the present thesis, indigo carmine (Carl Roth, Germany) was used for the spray colouring of MCC to obtain a tracer blend.
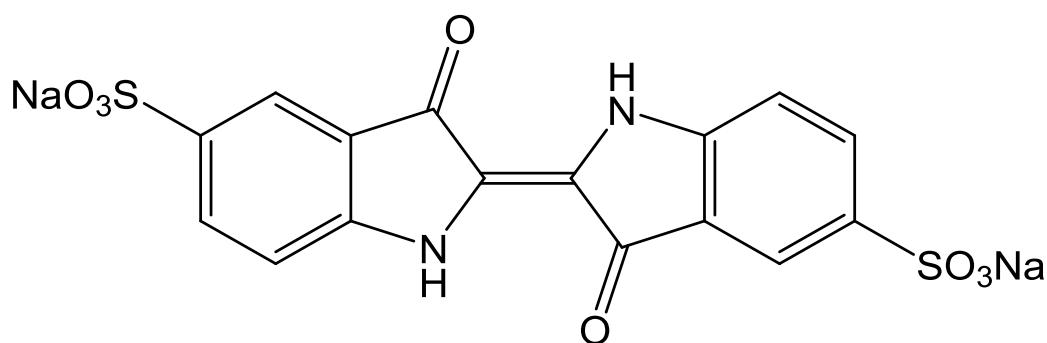
Fig. 10: Molecular structure of indigo carmine

3.2.   Methods

3.2.1.   *Preparation of the powder blends*

3.2.1.1. Preparation of a tracer blend and an MCC blend

For the present thesis, two powder blends based on MCC were prepared. The MCC blend consisted of 99.5 % [w/w] MCC as a widely used excipient for direct compression and 0.5 % [w/w] colloidal silica as a glidant. To determine the residence time distribution (E_t), a tracer blend consisting of 0.1 % [w/w] of the blue dye indigo carmine and 99.9 % [w/w] MCC blend was prepared. Indigo carmine is only slightly soluble in water (10.0 g/l) [122]. However, in the present study the concentration of the indigo carmine solution used for the fluidized bed spray granulation (2.5 g/l) was below the solubility limit. Therefore, it was possible to use indigo carmine for the spray colouring of the MCC particles.

To prevent powder segregation [123,124] and powder attrition [25,125] within the tracer blend, 900 g of MCC were spray-coloured with 360 ml of a 0.25 % [w/w] aqueous solution of indigo carmine by fluidized bed spray granulation (Solidlab 1, Bosch, Germany). During the spray-colouring process, indigo carmine was adsorbed to the surface of the MCC particles in the Solidlab chamber. After the drying step the powder properties of the tracer blend and the MCC blend were identical. According to Mateo et al. it is important to ensure identical powder properties of the tracer blend and the MCC blend [124]. However, interactions between the powder particles of the powder blends such as attraction or repulsion, segregation, and lubrication may affect the powder behaviour and E_t in the feed frame system.

3.2.1.2. Characterization of the powder blends

To confirm the uniformity of tracer and the MCC blend, several in-process controls were performed. The stereomicroscope SteREO Discovery.V8 (Carl Zeiss, Germany) was used to analyse the particle size of the two powder blends (Fig. 11) and the particle size distribution was measured by laser diffraction (Helos, Sympatec, Germany) according to the Ph. Eur. monograph 2.9.31. "Particle size analysis by laser light diffraction" (Fig. 12). It is obvious that both, the visual analysis of the powder particles as well as the characterization of the particle size distribution (tracer blend: d_{50} = 111.3 μm ± 0.2 μm, MCC blend: d_{50} = 117.0 μm ± 0.5 μm) show no difference between the tracer blend and the MCC blend.
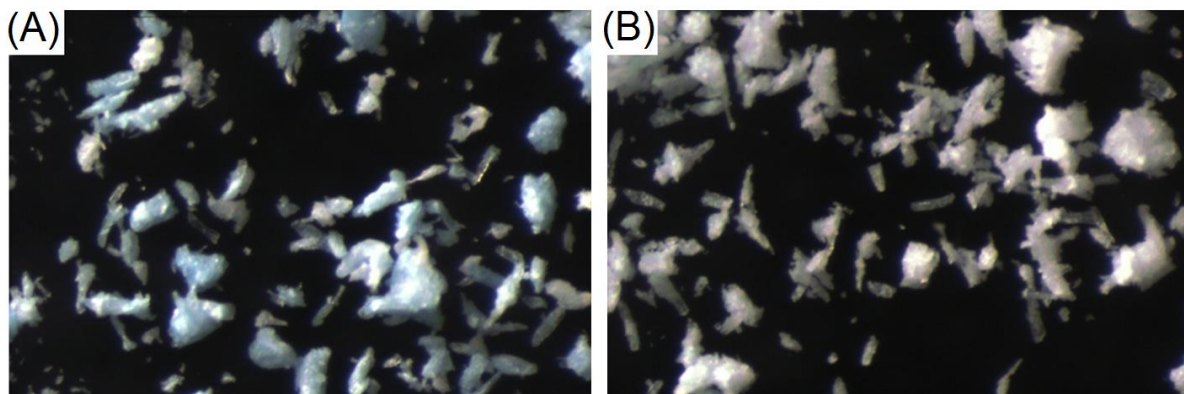

Fig. 11: Comparison of the prepared power blends: (A) tracer blend and (B) MCC blend.

Further in-process controls were the determination of the angle of repose (tracer blend: 26.24° ± 1.50°, MCC blend: 26.34° ± 2.14°,), the bulk density (tracer blend: ρ_{bulk} = 0.368 g/ml ± 0.001 g/ml, MCC blend: ρ_{bulk} = 0.348 g/ml ± 0.004 g/ml), and the tapped density (tracer blend: ρ_{tapped} = 0.478 g/ml ± 0.011 g/ml, MCC blend: ρ_{tapped} = 0.472 g/ml ± 0.011 g/ml). All experiments were performed in triplicate according to the Ph. Eur. monograph 2.9.34. "Bulk density and tapped density of powders", and monograph 2.9.36. "Powder flow".
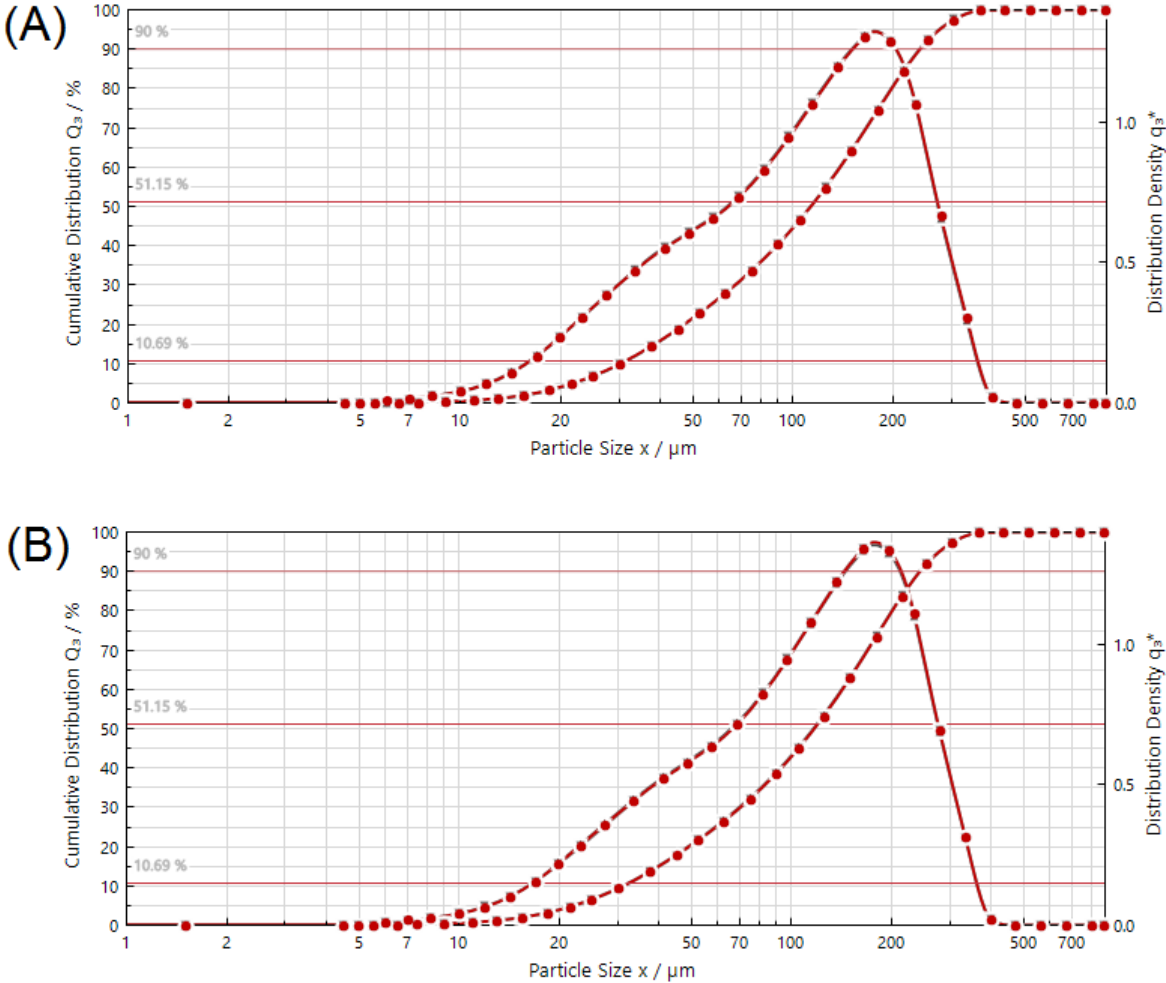
Fig. 12: Particle size distributions of the prepared powder blends: (A) tracer blend and (B) MCC blend.

3.2.2. Rotary tablet press and feed frame

A lab-scale rotary tablet press (102i, Fette Compacting, Germany) was upgraded with a die disc (30 pairs of 8 mm diameter flat-faced punches) to a production-scale rotary tablet press. This allows the transfer of the obtained results directly to the pharmaceutical production of tablets.

Lately, the influence of different funnel shapes on the flow behaviour was investigated [23,24,126]. It was shown, that the funnel shape had a pronounced influence on the powder flow, which manifested itself in an inhomogeneous flow of the powder particles. To avoid this influence of the funnel shape on the powder flow and to ensure a homogeneous powder flow from the funnel to the feed frame system, the standard funnel unit was replaced by a feed pipe unit (Fig. 13).
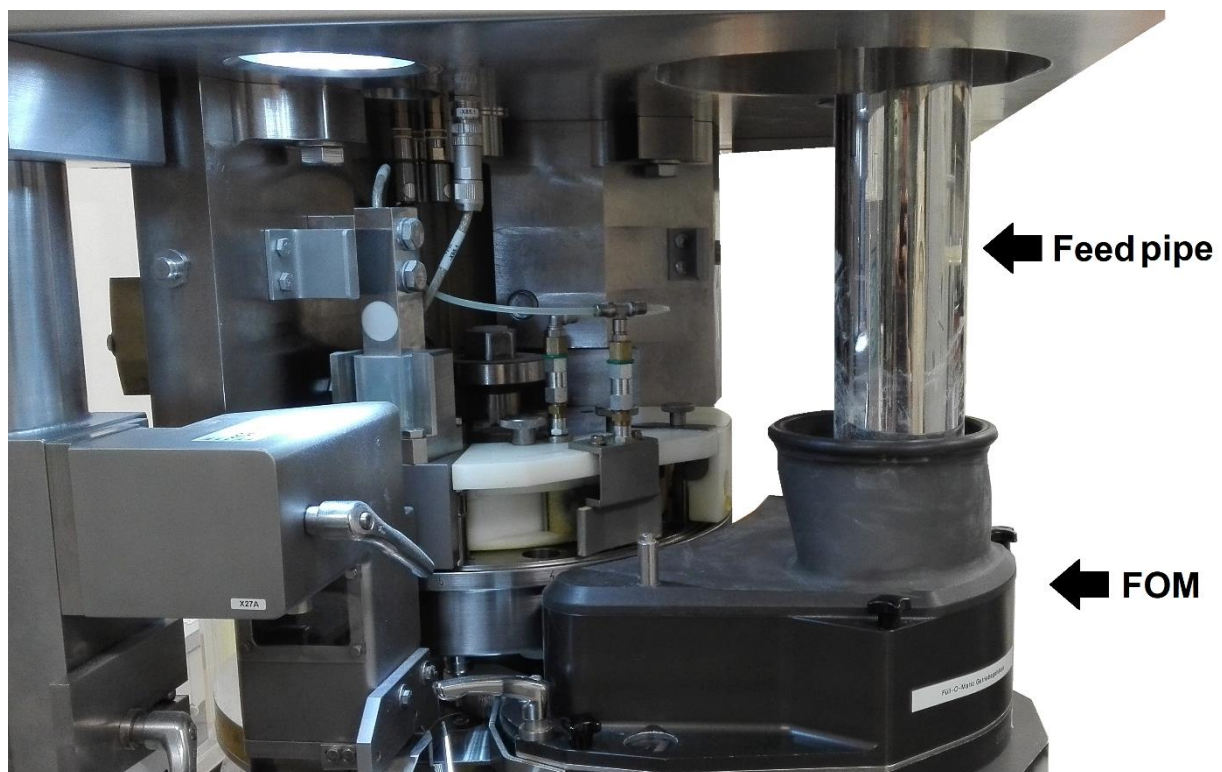

Fig. 13: Fette 102i tablet press mounted with a feed pipe and a Fill-O-Matic.

The second tablet press, which was used in this thesis, was the FE55 rotary tablet press (FE55, Fette Compacting, Germany), equipped with 60 pairs of 8 mm diameter flat-faced punches (Fig. 14). Thus, the obtained results of this study may be transferred directly to the industrial manufacturing of tablets. The FE55 was used for the investigation of different feed frame designs, because it is the first new generation of tablet presses that includes a new filling system (single-chamber filling cone) [127]. Furthermore, it is possible to equip this tablet press both with the three-chamber Fill-O-Matic (FOM) as well as with a single-chamber filling cone, respectively. To ensure a continuous powder flow from the funnel into the FOM without any influence of the funnel shape [24,128] and without intermixing effects in front of the FOM, the standard funnel unit was also replaced by a feed pipe unit on the FE55.
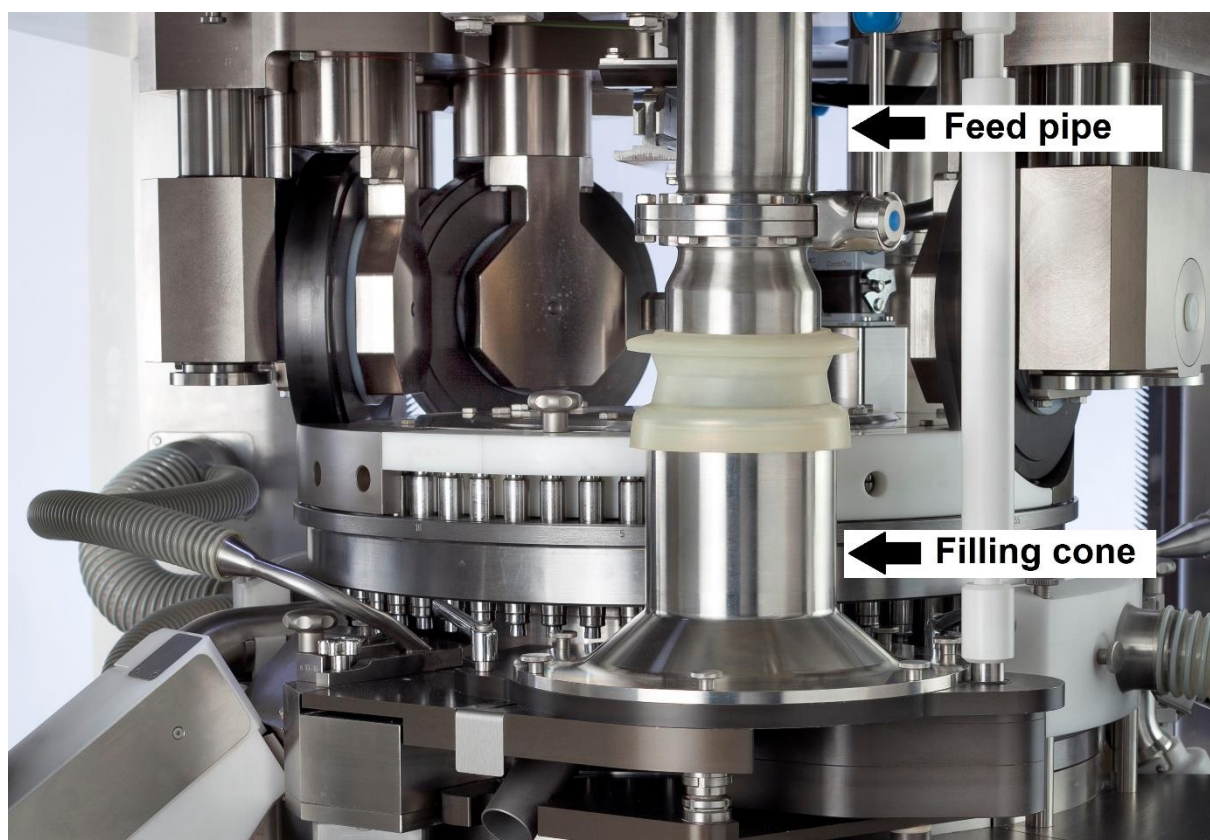

Fig. 14: Fette FE55 rotary tablet press mounted with a feed pipe and a filling cone.

3.2.3. Preparations of the tableting runs

To compare the geometric and parametric setups in the following chapters and their effects on E_t, the tableting runs of each feed frame configuration had to be identical. Therefore, for one tableting run, the feed pipe was initially filled with 900 g of the MCC blend. To distribute the MCC blend within the feed frame and to fill the feed frame completely, the FOM wheels were rotated thirty times, which was shown in preliminary experiments to be sufficient to reach a constant filling level. Subsequently, a defined amount of tracer blend was layered onto the MCC blend. For the most investigations of the geometric and parametric setup on the powder behaviour and E_t, an amount of tracer blend of 160 g was layered onto the MCC blend. Deviating from the amount of tracer blend of 160 g, for the investigation of the influence of different amounts of tracer blend on E_t in chapter 4.2.1 and chapter 4.4, different amounts of tracer blend in a range of 20 and 2,700 g were used. Finally, 2,400 g of the MCC blend were placed on top of the tracer blend to push the tracer blend completely out of the feed frame as well as to guarantee a continuous powder flow through the feed frame. The respective tableting runs were stopped 3 min after the tracer blend was not observed any longer on the tablet surface.

3.2.4.   Variation of the geometric and parametric setup

3.2.4.1. Variation of the scraper and the filling cam configurations

Two configurations of the powder scraper system were used to determine its influence on E_t. Usually, the inner scraper is attached behind the feed frame, thus removing excess powder particles from the die disc (Fig. 15A, 1). The standard equipment consists of an inner scraper (Fig. 15B) which removes the excess powder from the dies and directs it into an inner collecting channel. After one rotation of die disc the powder particles are led back into the FOM by a retractor placed directly in front of the FOM (Fig. 15A, 2), thus allowing to recycle the powder particles.
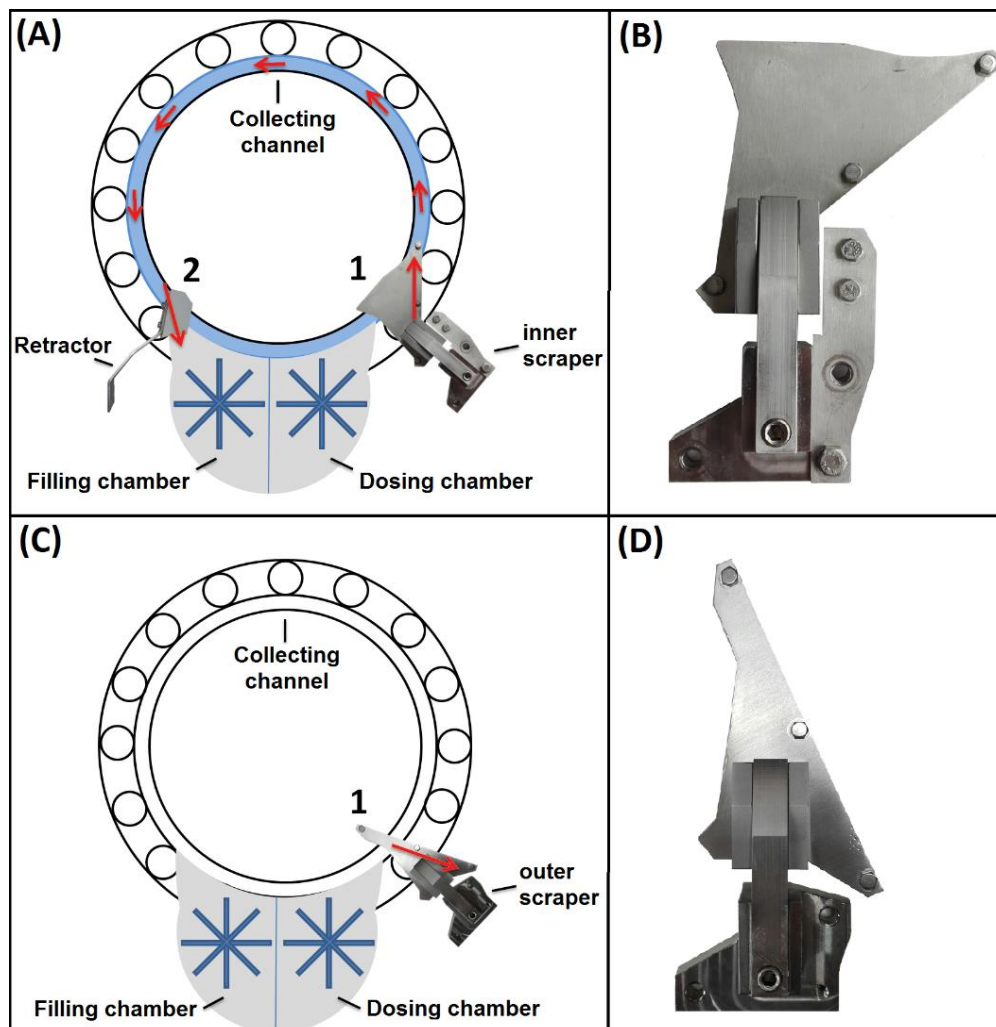

Fig. 15: Configurations of the scrapers. Arrows depict the movement of the powder particles.

To avoid the effect of recirculation of the scraped powder particles the inner scraper was replaced by an outer scraper (Fig. 15D). In contrast to the inner scraper, the outer scraper removes the excess powder particles from the dies and directs it out from the system (Fig. 15C, 1). This scraper might decrease E_t of the powder particles, by its removal out of the system. A further component of the rotary tablet press is the filling cam, which guides the lower punches below the filling chamber to a maximum filling depth of the respective filling cam. The actual filling depth of the dies is adjusted by a dosing cam, which pushes up the lower punch to the manually adjusted filling depth. Thus, the excess powder particles will be pushed out into the dosing chamber of the FOM. This excess powder is recirculated during its transport back from the dosing chamber to the filling chamber. For the investigation of the influence of the filling cams and filling depths on E_t, a 12 mm filling cam and an 8 mm filling cam as well as two different filling depths (11.5 mm and 7.5 mm) were used. Thereby, at a filling depth of 11.5 mm a tablet weight of about 200 mg and at a filling depth of 7.5 mm a tablet weight of about 150 mg was obtained.

3.2.4.2. Variation of the die disc and the feed frame speeds

Two die disc speeds (20 rpm and 36 rpm) as well as four feed frame speeds (40, 70, 100, and 120 rpm) were selected to investigate their influence on E_t. The feed frame speed, i.e. the speeds of the feed frame wheels, might have an influence on the quality of the produced tablet. Powder attrition and powder lubrication are influencing factors that may affect powder quality [25]. The faster the feed frame wheels the higher the stress on the powder particles. It is important to find the optimum setting for a short residence time to minimize the powder attrition and lubrication and thus to ensure a high quality of the powder as well as of the tablet.

3.2.5.   Variation of the powder properties

3.2.5.1. Variation of the amount of tracer blend

For the investigation of the effect of the amount of tracer blend on E_t in the three-chamber Fill-O-Matic (FOM) eight different amounts of tracer blend were used (20 g, 40 g, 80 g, 160 g, 320 g, 640 g, 1,600 g, and 2,700 g). For every tableting run a basic setting (rotational die disc speed: 20 rpm, rotational feed frame speed: 40 rpm, filling cam: 12.0 mm, and filling depth: 11.5 mm) was adjusted. For a rotational die disc speed of 20 rpm (36,000 tablet/h) and a mean tablet weight of 208.45 mg with an SD of 0.68 mg, the flow rate was approximately 7.5 kg/h.

3.2.5.2. Variation of the flow rate

To obtain a better understanding of the effect of the flow rate of the powder particles through the feed frame on E_t, five different rotational die disc speeds (10, 20, 36, 52, and 62 rpm) were used. Furthermore, for each tableting run the same amount of tracer blend (160 g) was used. Based on the tablet mass, the rotational die disc speed, and the number of the dies, the powder flow rates through the FOM were 3.8, 7.5, 13.4, 19.3, or 22.7 kg/h, respectively. To meet the same velocity of the feed frame and the die disc at the position of the dies during the filling step, the circumference of the die disc and the feed frame wheel were measured to determine the five rotational die disc speeds. The results of the experiments performed under these conditions may be interesting for the scale-up of the manufacturing from the laboratory scale to the production scale.

3.2.5.3. Variation of the residual moisture content

Sisay et al. showed that the moisture content had a significant influence on E_t in a twin-screw extruder [79]. Differences in the residual moisture content (RMC) led to a variation of the particles mass because of the different amount of water in the particles. If increasing the RMC and thereby increasing the particles mass, τ is decreased [79]. This result might be interesting for the continuous manufacturing of tablets, because the particles from the granulation process flow to the tableting process, directly. It is important, that the RMC comply with the regulatory requirements to ensure a continuous quality of the produced tablets. In this study, three different RMCs of the tracer blend were used, respectively, to investigate the effect on the powder behaviour and E_t versus time profile. Therefore, a laboratory fluid bed system (Solidlab 1, Bosch, Germany) was used to spray-colour and dry the Vivapur® 102 (=tracer blend) to three defined residual moisture contents (wet: 7.37 %, medium: 3.88 %, dry: 1.39 %). To obtain the wet tracer blend, the drying step was stopped directly after the application of the dye solution and for the medium tracer blend the drying step was stopped at a moisture content of 7 g/kg in the Solidlab chamber. For the dry tracer blend, the time period of the drying step was doubled. These residual moisture contents were measured with a moisture analyser (MA30, Sartorius, Germany).

3.2.5.4. Variation of the particle sizes of the tracer blend particles

Previous studies have shown that particles of different size behave differently in the feed frame [84,124]. Mateo et al. was able to simulate the particle segregation in the feed frame by means of the discrete element method. They showed that large particles were found predominantly in the upper region of the feed frame and the

dies, whereas small particles were found in the lower region of the feed frame and the dies.

It was examined whether the influence of the particle size on the segregation in the feed frame leads to an inhomogeneous distribution of the differently sized particles within the manufactured tablet and whether it affects E_t of the tracer blend particles in the FOM. Therefore, a tracer blend based of Vivapur® 200 was sieved with metal sieves of different meshes to obtain three tracer blend fractions of different particle sizes: 400-315 µm, 180-125 µm, and <50 µm. The certificate of analysis specifies the particle size distribution of Vivapur® 102 by a d_{50} of 131 µm. Thus, the particles of this MCC type had similar particle sizes as the tracer blend particles from the fraction 180-125 µm.

3.2.6. Variation of the feed frame components

3.2.6.1. Reduction of the FOM volume with a perspex disc

As an approach to reduce the volume of the FOM as well as the intermixing of the powder particles, a perspex disc was used instead of the dosing wheel (Fig. 16). Thus, the perspex disc was placed into the dosing chamber and thereby this chamber was no longer available. As a result, the dosing out of the dies was no longer possible while the lower punch still attempted to push up the powder. Therefore, instead of the standard filling depth (11.5 mm) a filling depth of 12.0 mm was selected, causing the lower punch to not move up and down any longer and to remain in the position of the dosing chamber. This filling depth was set for both tableting configurations: the perspex disc configurations and the standard configuration. It has to be mentioned that the FOM configuration with the perspex disc was only investigated for scientific purposes because the dosing chamber with its dosing wheel is an essential component of the FOM and is of particular importance for the manufacturing of tablets.
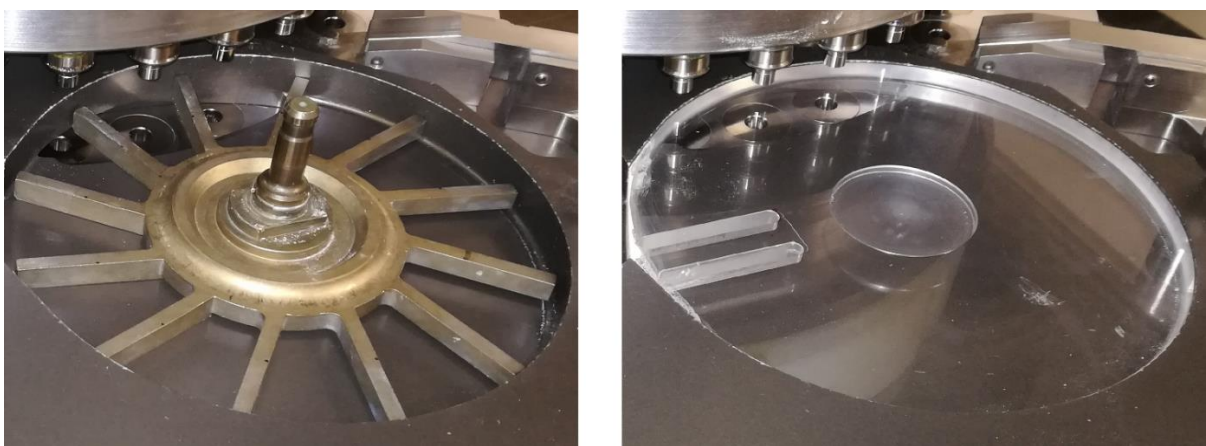

Fig. 16: Dosing chamber of the FOM with the standard configuration (left) and a FOM configuration, volume-reduced with a perspex disc (right).

3.2.6.2. Variation of the filling wheel design

The filling wheel of the filling chamber is one of the three wheels of the FOM. According to the geometric design of the FOM, the filling wheel has several tasks. The main task of the filling wheel is the constant filling of the dies. Further tasks are the uptake of the powder from both the dosing chamber and the distributing chamber. The standard filling wheel with a diameter of 170 mm contains 12 flat rods, which are horizontally angled over the last 20 mm (Fig. 17, left). Thus, the rods are able to transport the powder into the dies. The round rod filling wheel consists of 16 alternately positioned vertically angled rods (Fig. 17, right). In this study, the effect of the flat rods and that of the round rods of the filling wheel on E_t in the FOM was compared.
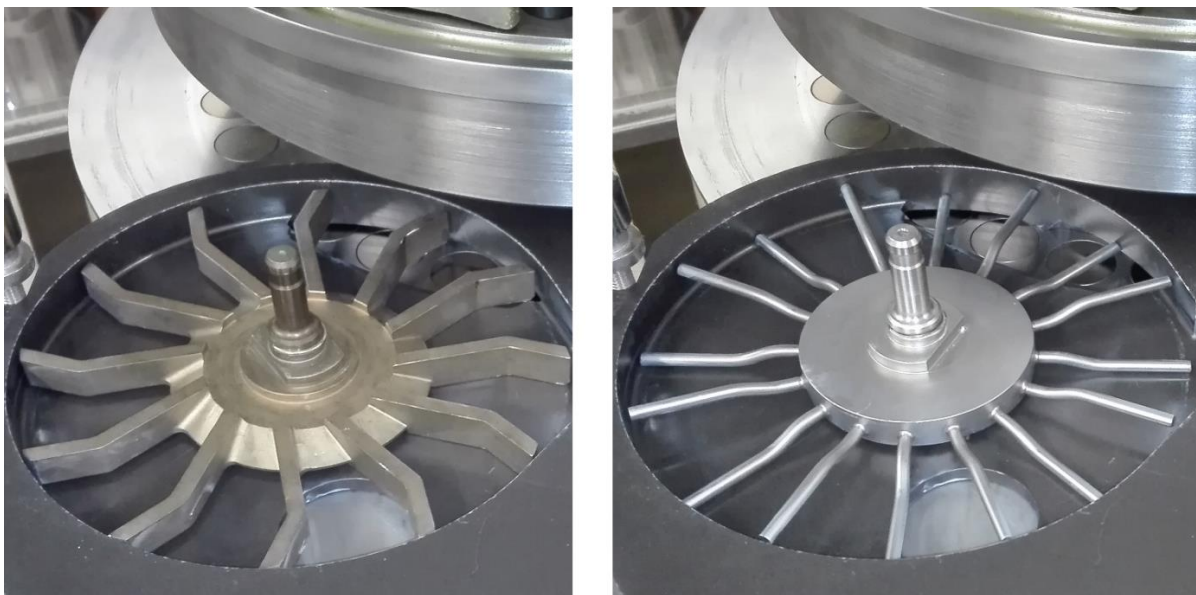

Fig. 17: Filling chamber of the FOM with the standard flat rods (left) and with the round rods (right).

3.2.6.3. Variation of the gap size between FOM and die disc

In this study, the effect of different gap sizes between the FOM and the die disc on E_t of the tracer blend in the FOM were investigated. Therefore, two different bottom plates were used for the investigation. One configuration of the FOM consisted of a bottom plate with a gap size of 25 mm between the FOM and the die disc (Fig. 18A). A further FOM configuration consisted of a bottom plate with a sealing segment of a gap size of 11 mm (Fig. 18B). The sealing segment is a component, which is attached to the outlet of the FOM.
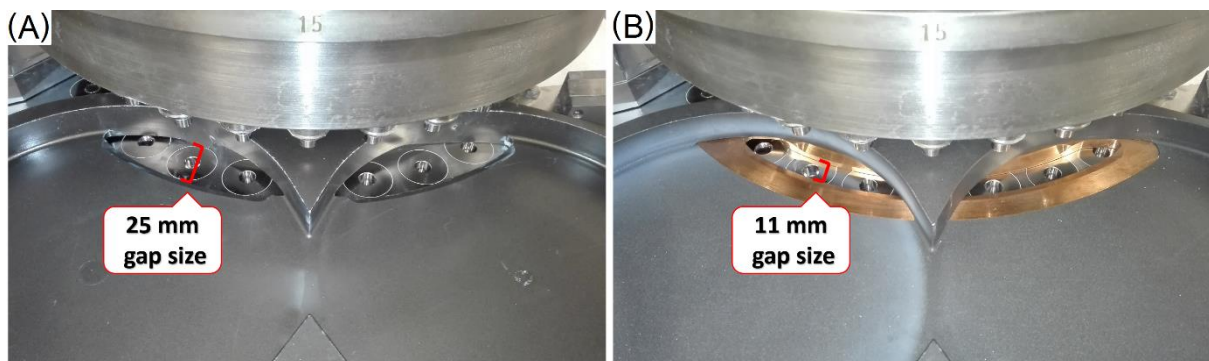

Fig. 18: Bottom plate of the FOM with (A) a 25 mm gap size configuration and (B) with an 11 mm gap size configuration.

3.2.7.   Variation of different feed frame designs on a FE55 tablet

3.2.7.1. Variation of the feed frame geometries

Two different feed frame designs were investigated. The first feed frame system was a three-chamber Fill-O-Matic (FOM). The three chambers of the FOM are positioned at two different levels (Fig. 19A). The distributing chamber receives the powder from the feed pipe and distribute it into the filling and dosing chamber. The second feed frame system was the cone-shape feed frame, following named as filling cone (Fig. 19B). In contrast to the FOM, the filling cone has only a single chamber with one feed frame wheel. The powder particles from the feed pipe flows directly on the centre of the cone-shaped wheel and the 12 rods of the feed frame wheel transported the powder particles to the edge of the chamber into the dies.
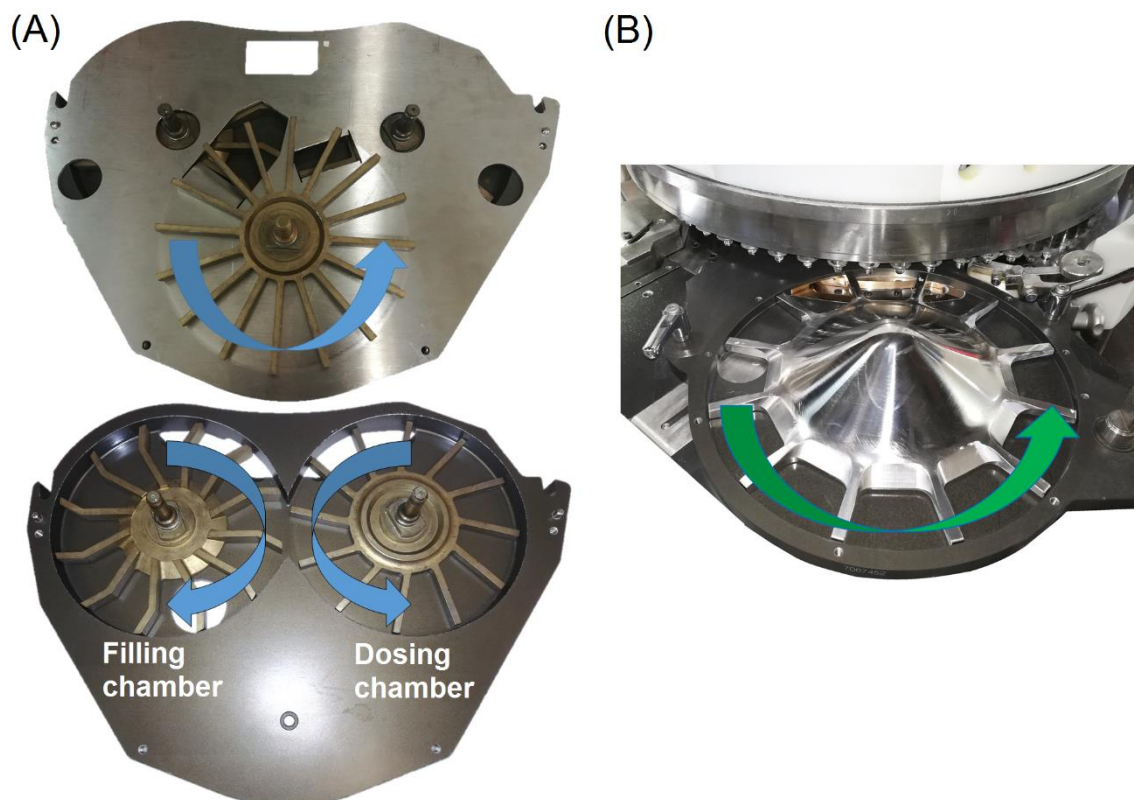

Fig. 19: (A) The design of the FOM with its three chambers and the powder path through the FOM (blue arrows) and (B) the design of the filling cone feed frame with its single chamber and the powder path through the feed frame (green arrow).

The focus of the feed frame design experiments was on the rotational feed frame speed, the tablet output/h, and the amount of tracer blend. Three different feed frame speeds of the respective feed frame system were adjusted to evaluate the effect of the wheel speed at a low, a medium, and a high wheel speed on E_t. For this investigation, a tablet output of 65,000 tablets/h was adjusted to ensure the identical powder flow through the feed frames. Furthermore, a 12 mm filling cam was used for the tableting runs as well as the filling depth was adjusted to obtain a tablet weight of about 200 mg. Thus, the filling depth of the FOM configuration was set to 11.5 mm and for the filling cone configuration, a filling depth of 9.3 mm was used. The rotational feed frame speeds of the FOM were 40 rpm (low), 70 rpm (medium), and 100 rpm (high) and the rotational feed frame speed of the filling cone were 45 rpm (low), 100 rpm (medium), and 150 rpm (high). Furthermore, three tablet output/h (65,000, 95,000, and 125,000 tablets/h) and three different amount of tracer blends (40 g, 160 g, and 640 g) were subject on the investigation of the two feed frame designs.

3.2.7.2. Reduction of the FOM volume with different feed frame wheels

The influence of the inner volume of the three-chamber FOM on the residence time of the powder particles through the FOM with modified feed frame wheels was investigated. A reduction of the inner volume of the FOM with a perspex disc, which was placed into the dosing chamber is examined in chapter (see chapter 4.3.1). Thus, the dosing chamber was completely filled with the perspex disc and the powder particles from the feed pipe flew only through the distribution chamber and filling chamber to the dies. Unfortunately, with this configuration of the perspex disc, the dosing chamber was no longer available and the function of the exact dosing of the

dies was not possible. It has to be noticed, that the volume reduction with a perspex disc would not be suitable for the use in the pharmaceutical manufacturing of tablets. Moreover, a new approach of the volume reduction was examined. Therefore, the design of the standard FOM wheels were modified to both reducing the inner volume of the FOM as well as ensuring the function of the dosing chamber (Fig. 20).
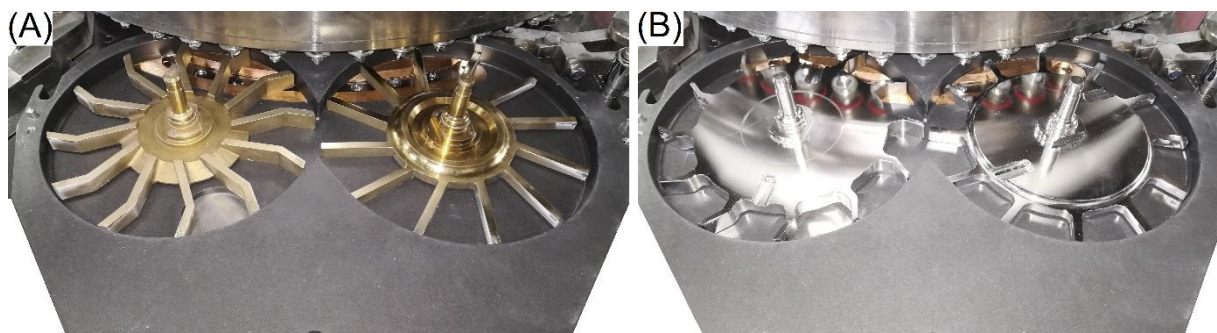

Fig. 20: Filling and dosing chamber of (A) the standard FOM and (B) the volume reduced FOM.

The standard configuration of the FOM with its three standard wheels has a filling volume of about 800 cm³ and the volume reduced FOM with its three large hub wheels has a filling volume of about 600 cm³. Thus, the FOM configuration with the modified feed frame wheels resulted in a volume reduction of about 25 %. The focus of the filling volume experiments was on the rotational feed frame speed, the tablet output/h, and the amount of tracer blend. Therefore, three different rotational feed frame speeds (40, 70, and 100 rpm), three different tablet output/h (65,000, 95,000, and 125,000 tablets/h), and three different amount of tracer blends (40 g, 160 g, and 640 g) were used.

3.2.8.   UV-Vis spectrophotometry

Tablet samples were collected during the tableting process at predefined time points and also after compression at the same position of the ejection chute. A GENESYSTM 10S UV-Vis spectrophotometer was used to determine the concertation of indigo carmine in the investigated samples at a wavelength of 608 nm after tablet disintegration in demineralized water. By measurement of the indigo carmine concentration, a calibration curve was created by mixing the tracer blend and the MCC blend at different ratios. With this calibration curve, the percentage of the tracer blend in the tablet samples could be determined. To meet the requirements of this method, a method validation (linearity, recovery, and precision) was established and only values within the calibration range between A 0.05 and A 1.00 were used.

3.2.9.   Residence time distribution in the feed frame

The residence time distribution E_t served to describe the powder behaviour in the FOM. The concentration versus time profile of each tableting run was used to calculate E_t, which is a mathematical function to describe the time distribution of particles in the operation unit e.g. feed frame. A long residence time may lead to a high strain applied to the powder particles, resulting in a decline of quality [79]. Referring to the continuous manufacturing of tablets it is desirable to have an E_t which is very close to the ideal PFR model with minimum mixing and a rapid discharge of the powder. In this study, E_t was used to describe the distribution with which a tracer particle enters the feed frame at the time point t_{Start} and leaves the feed frame after a time point $t > t_{Start}$ (Fig. 21).
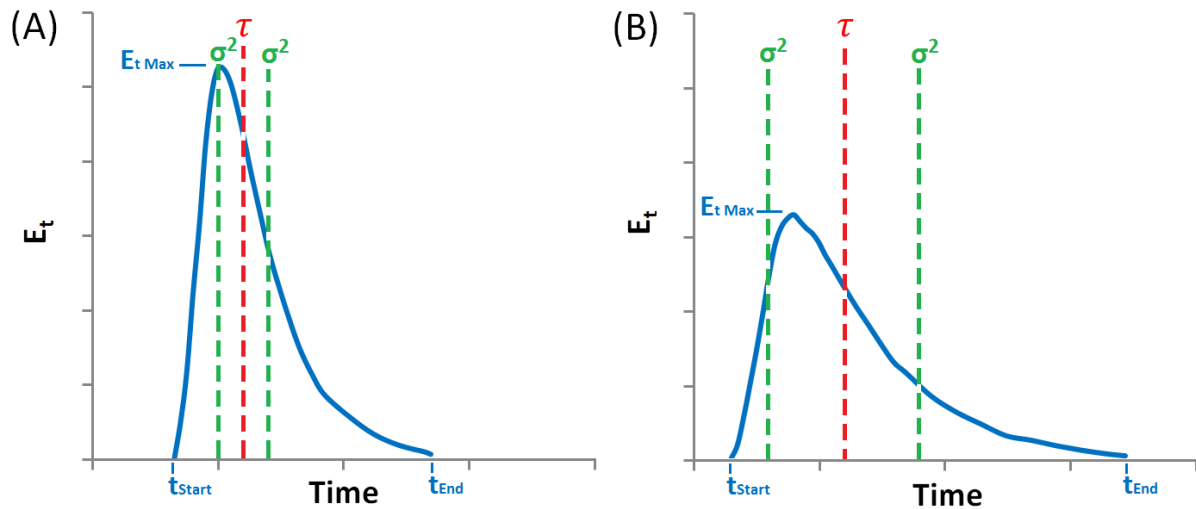
Fig. 21: Examples of two different E_t versus time profiles with (A) the same τ and (B) a different σ².

It is assumed that all powder particles have left the feed frame to infinity resulting in an area under the E_t versus time profile equal to unity (2).

$$\int_0^\infty E_t \, dt = 1 \tag{2}$$

This assumption allows a comparison of the different E_t versus time profiles of each tableting run and the effect of the respective experimental setup.

The E_t is given by the following equation (3) [66,129]:

$$E_t = \frac{c}{\int_0^\infty c \, dt} \tag{3}$$

where c is the concentration (w/w) of tracer blend in the tablet at the time point t and $\int_0^\infty c \, dt$ is the area under the concentration versus time profile. The E_t values are plotted against the time of the tableting run to get an E_t versus time profile. Therefore, E_t versus time profile is a normalized concentration versus time profile by the total amount of tracer blend [130]. For this, it is assumed that after a time of infinity all tracer blend particles have left the FOM. If a part of the tracer blend flows through the

FOM quickly and a part of the tracer blend circulates longer in the FOM, the E_t versus time profile is very broad. With regard to the continuous manufacturing, a broad E_t versus time profile may lead to problems in well-defined batches, caused by the intermixing between the powder particles of different batches. Thus, a narrow E_t versus time profile display a lower intermixing of powder particles in the FOM. The E_t measurement is based on the assumption that the transport of all powder particles through the FOM is continuous.

The mean residence time (т) (4) and the mean centered variance (σ^2) (5) are two parameters characterize the shape of the E_t versus time profile. They were used to describe the behaviour of the powder in the feed frame.

The т and σ^2 are given by the following equations [42,78]:

Mean residence time (т):

$$\tau = \int_0^\infty t \cdot E_t \, dt \qquad (4)$$

Mean centered variance (σ^2):

$$\sigma^2 = \int_0^\infty (t - \tau)^2 \cdot E_t \, dt \qquad (5)$$

т describes the mean of the residence time distribution of the powder particles in the feed frame and σ^2 describes the variance of the mean residence time [78] and thus, the σ^2 describes the intermixing effect of the powder in the feed frame [80]. The smaller the σ^2 values the lower the applied shear strain exerted by the feed frame wheels on the powder particles.

Two different E_t versus time profiles (blue lines) are shown in Fig. 21. To describe the differences between the two different profiles, the т and σ^2 values were used. It may be observed that both E_t versus time profiles have the same т value (red). As an

exemplary illustration, in Fig. 21A a narrow profile shape with a high $E_{t\,Max}$ and in Fig. 21B a broad profile shape with a low $E_{t\,Max}$ are displayed. The width of the profile shape and thereby the intermixing effect of the feed frame is indicated by the σ^2 (green). In general, a high intermixing should be avoided, as it is accompanied by decline of the product quality [79].

A variation of the filling depth leads to a change of the die volume and therefore the flow rate of the powder the tablet press. Furthermore, a variation of the die disc speed leads to a change of the tablet produced rate. To compare the suitability of the two setups, the E_θ was used, where θ is the normalized time. From a mathematical point of view, the equation of E_t and τ were used to obtain E_θ (6):

$$E_\theta = E_t \cdot \tau \; ; \; \text{with } \theta = \frac{t}{\tau} \tag{6}$$

To state the experimental error and to evaluate the robustness of the results. For one experimental condition (die disc speed of 20 rpm and a feed frame speed of 40 rpm using a 12 mm filling cam with a filling depth of 11.5 mm and an outer scraper) the tableting runs were performed in triplicate and the experimental error was determined. The E_t versus time profiles of the three tableting runs are identical. The mean residence times of the three tableting runs were 6.50 min, 6.48 min, and 6.51 min, respectively, with an arithmetic mean of 6.50 min and a standard deviation SD of 0.01 min. The mean centered variances of the three runs were 3.70 min², 3.92 min², and 3.63 min², respectively, with an arithmetic mean of 3.75 min² and a standard deviation SD of 0.12 min². These results confirm the reproducibility of the experimental investigation and the robustness of the conclusions.

3.2.10. Measurement of the number of paddle passes

During the tableting process, the powder was strained by the feed frame wheels of the FOM. It was impossible to measure the force of the paddles exerted onto the powder particles directly. Therefore, an approximation function was used to calculate the applied strain. An estimation to illustrate the applied strain by the feed frame wheels is the number of paddle passes (7) [26].

The paddle passes were calculated as a function of τ, the feed frame speed, and the number of paddles. In the present study, the number of paddles (12) of the filling wheel was used. The larger the number of paddle passes the higher the probability that powder attrition and powder overlubrication will occur [84].

With the following equation, the number of paddle passes is calculated [26]:

$$N_{pp} = N_p \cdot FF_{rpm} \cdot τ \tag{7}$$

where N_{pp} is the number of paddle passes of the filling wheel, N_p is the number of paddles of the filling wheel, FF_{rpm} is the feed frame speed in revolutions per min, and τ is the mean residence time in min. With focus on the continuous manufacturing, τ is desired to be low. Thus, the reduction of the factor τ in the function leads to a decrease of the N_{pp} and the applied strain, respectively.

4. Results and Discussion

4.1.   Variation of the geometric and parametric setup

4.1.1.   Variation of the scraper and the feed frame speed

The influence of two powder scraper systems and the influence of the feed frame speed on the residence time of the tracer blend in the FOM was examined. For determination of residence time the experimental conditions have to be completely free of interfering factors. For this reason, a 12 mm filling cam with an 11.5 mm filling depth was selected to minimize the effect of back-dosing on the residence time. In Fig. 22, the residence time distribution (E_t) profile of the outer scraper and the inner scraper at four feed frame speeds (40, 70, 100, and 120 rpm) and at a die disc speed of 20 rpm (36,000 tablets/h) are shown. At a tablet weight of approximately 200 mg the powder flow rate through the FOM is about 7,200 g/h.

The E_t versus time profiles of the two powder scraper system have similar curve shapes. If the E_t versus time profile of the outer scraper is compared with that of the inner scraper at the feed frame speed of 40, 70, and 100 rpm, a shift along the x-axis may be observed. The curve of the outer scraper begins earlier than that of the inner scraper and the E_t curve of the outer scraper ends earlier than the E_t curve of the inner scraper. At the feed frame speed of 120 rpm this effect diminishes and the E_t versus time profile of the outer scraper do not show a shift along the x-axis.
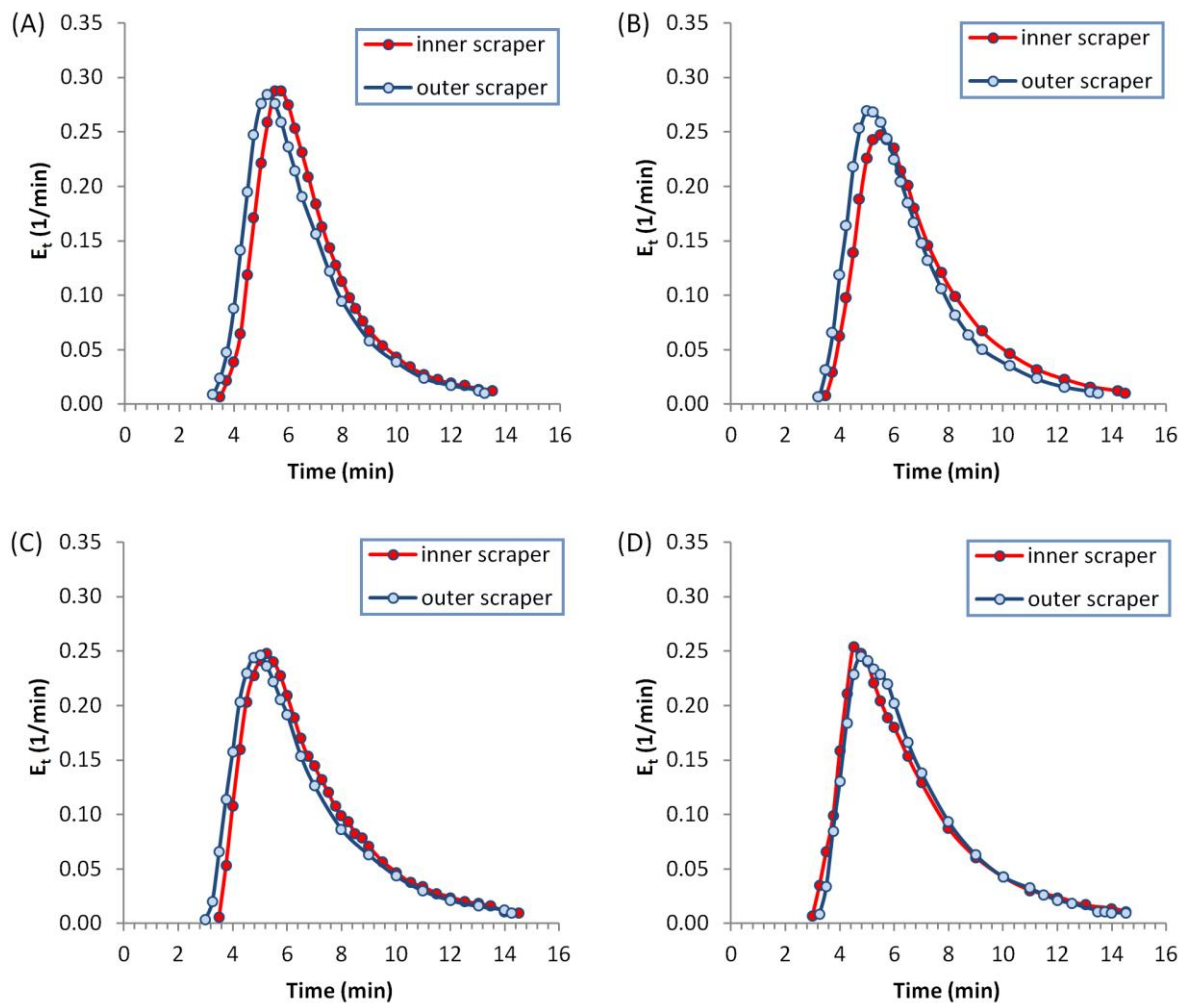
Fig. 22: E_t versus time profiles of the inner and the outer scraper at four feed frame speeds: (A) 40 rpm; (B) 70 rpm; (C) 100 rpm; (D) 120 rpm.

In Fig. 23 the τ and σ² values of two configurations of scrapers at feed frame speeds 40, 70, 100, and 120 rpm are shown. It is evident that the τ is not affected by the feed frame speed. In both settings the same die disc speed of 20 rpm was used, which ensured a constant powder flow of 7,200 g/h through the FOM. The feed frame speed had no influence on the powder flow of the tracer blend through the FOM. Thus, the mean residence time of the tracer blend in the FOM is independent of the feed frame speed.
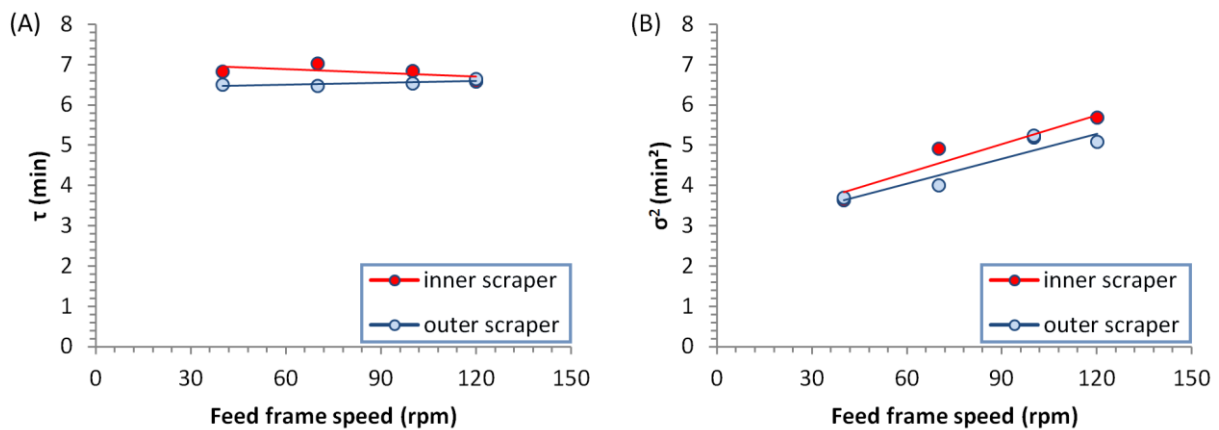
Fig. 23: Influence of the outer and inner scraper on (A) τ and on (B) σ^2 at four feed frame speeds.

From the results of the σ^2 values at different feed frame speeds, it can be observed that the σ^2 increase significantly by increasing the feed frame speed. However, the intermixing effect between the tracer blend in the FOM and the powder particles from the filling tube increases with increasing feed frame speed. A constant τ in combination with an increasing σ^2 leads to a high mechanical stress of the powder particles, such as particle attrition and powder overlubrication [25].

The results in (Fig. 22) and (Fig. 23) show that the outer scraper has an influence on the residence time of the powder particles in the feed frame. The influence may be explained by the path of the powder particles as shown in Fig. 15. In the case of the inner scraper (Fig. 15B), the excess powder on die disc surface is scraped into the inner collecting channel (Fig. 15A, 1) and returns to the FOM by a retractor after one rotation of the die disc (Fig. 15A, 2). The empty dies in the filling chamber are simultaneously filled with the powder particles from the inner collecting channel and the powder particles from the filling chamber. This fact results in a competitive filling of MCC with the lower concentration of indigo carmine from the collecting channel

and MCC with the high concentration of indigo carmine from the filling chamber. Comparing the path of the powder particles (Fig. 15A, red arrows), the outer scraper removes the powder from die disc surface and it is therefore no longer available. If removing the powder particles from the system by the outer scraper, no competitive filling occurs in the filling chamber, which allows more tracer blend to reach the dies, thus enabling an earlier increase in tracer blend concentration. This earlier increase in concentration leads to a shorter residence time of the tracer blend and a curve shift along the time axis. Furthermore, this may explain that using the outer scraper may result a less mean residence time (τ) and mean centered variance σ^2.

4.1.2.   Variation of the die disc speed

In addition to the configuration of the scraper, the die disc speed is another parameter that might affect the E_t. Previous studies demonstrated that an increasing flow rate leads to an alteration of the residence time [26,124]. For example, Kumar et al. showed that an increase of the flow rate in a twin screw granulator leads to an alteration of the residence time [81]. Vanarase et al. found the same effect by increasing the flow rate in a continuous powder mixer [66]. For this reason, it should be investigated, to what extent the die disc speed has an effect on the E_t of a rotary tablet press.

In this part of the study, only the outer scraper was used. Furthermore, a 12 mm filling cam with a filling depth of 11.5 mm was applied for this experimental setup. In Fig. 24A the E_t versus time profiles at the die disc speeds of 20 rpm (36,000 tablets/h ≙ 7.5 k/h) and 36 rpm (64,800 tablets/h ≙ 13 kg/h) as well as at a feed frame speed of 100 rpm, representative for all four feed frame speeds, are shown. It is evident that the shape of the E_t versus time profile at the die disc speed of 36 rpm is narrower

and smaller than at the die disc speed of 20 rpm. Increasing the die disc speed leads to a decrease of the powder residence time. This result might be explained by the two different flow rates. As a result, the distribution of the powder residence time was reduced, indicated by a narrower E_t.

To compare the suitability of the parametric setup the values of E_t and t have been normalized (E_θ; θ). This makes it possible to compare both setups and to identify negative influences which may lead to an alteration of the residence time. These considerations are important for the industrial scale up of the die disc speed. In Fig. 24B the E_θ versus θ profiles at the die disc speeds of 20 rpm and 36 rpm, respectively, as well as the feed frame speed of 100 rpm, representative for all four feed frame speeds, are displayed. Both E_θ have an identical curve shape. This result indicates that the suitability of FOM is independent of a change in the die disc speed.
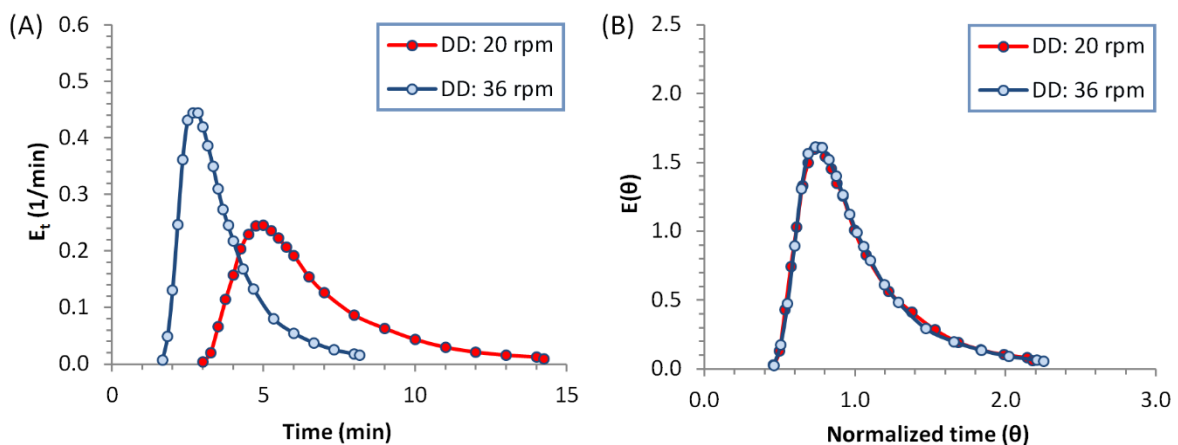

Fig. 24: E_t versus time profiles of the die disc speeds at 20 rpm and at 36 rpm at a feed frame speed of 100 rpm (representative for all four feed frame speeds) of (A) E_t and on (B) E_θ.

The data from the τ (Fig. 25A) and σ^2 (Fig. 25B) reveal that increasing the die disc speed leads to a decrease of the τ values and the σ^2 values. According to chapter 4.1.1, the data in Fig. 25A illustrate that all τ values at the different feed frame speeds remain constant and all σ^2 values displayed in Fig. 25B increase with increasing the feed frame speed. If the σ^2 values at the die disc speed of 20 rpm and the σ^2 values at 36 rpm are compared, it is noticeable that the corresponding regression lines have the same slope. The results of this investigation show that the influence of the feed frame speed and the influence of the die disc speed on τ and σ^2 do not interact. Thus, the intermixing of the powder particles in the FOM increases proportionally to the feed frame speed.
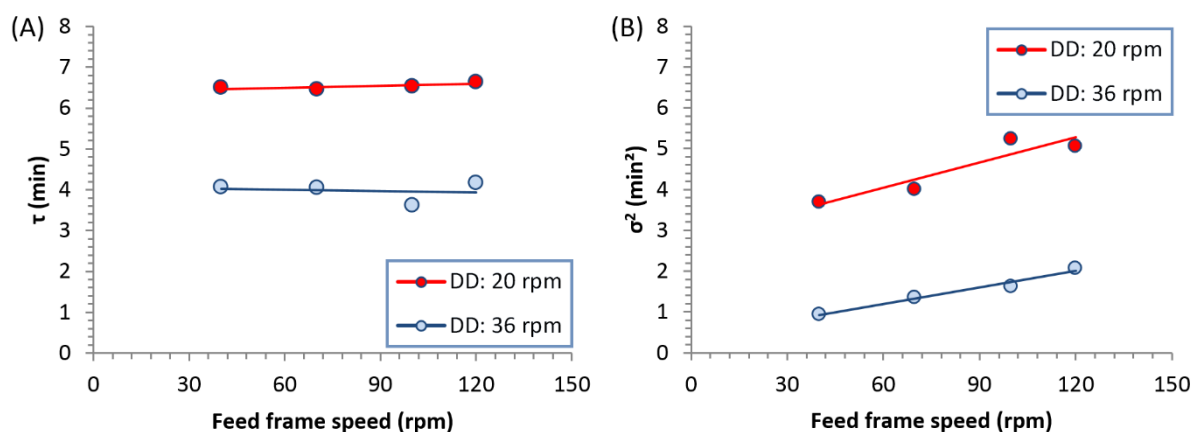

Fig. 25: Influence of the die disc speeds at 20 rpm and at 36 rpm on (A) τ and on (B) σ^2 at four feed frame speeds.

4.1.3.   Variation of the filling cam and the filling depth

4.1.3.1. Variation of the filling cam

In this part of the study, an 8 mm and a 12 mm filling cam with a filling depth of 7.5 mm each were used to determine the influence of the filling cams and the effect of powder recirculation, respectively, on the E_t. Furthermore, a constant die disc speed of 20 rpm each was applied. If the 12 mm filling cam was used (initial volume

of the dies about 603 mm³), a powder column with a height of 4.5 mm (column volume 226 mm³) is dosed back into dosing chamber. If the 8 mm filling cam was used (initial volume of the dies about 402 mm³), a powder column of 0.5 mm (column volume 25 mm³) height resulted. These powder columns were recirculated from the dosing chamber through the filling chamber back to the dies. This powder recirculation of the back-dosed powder may lead to a longer residence time. In Fig. 26 the E_t versus time profiles of the two filling cams at the four feed frame speeds are displayed. It is evident that with each feed frame speed the respective E_t profiles are almost identical.
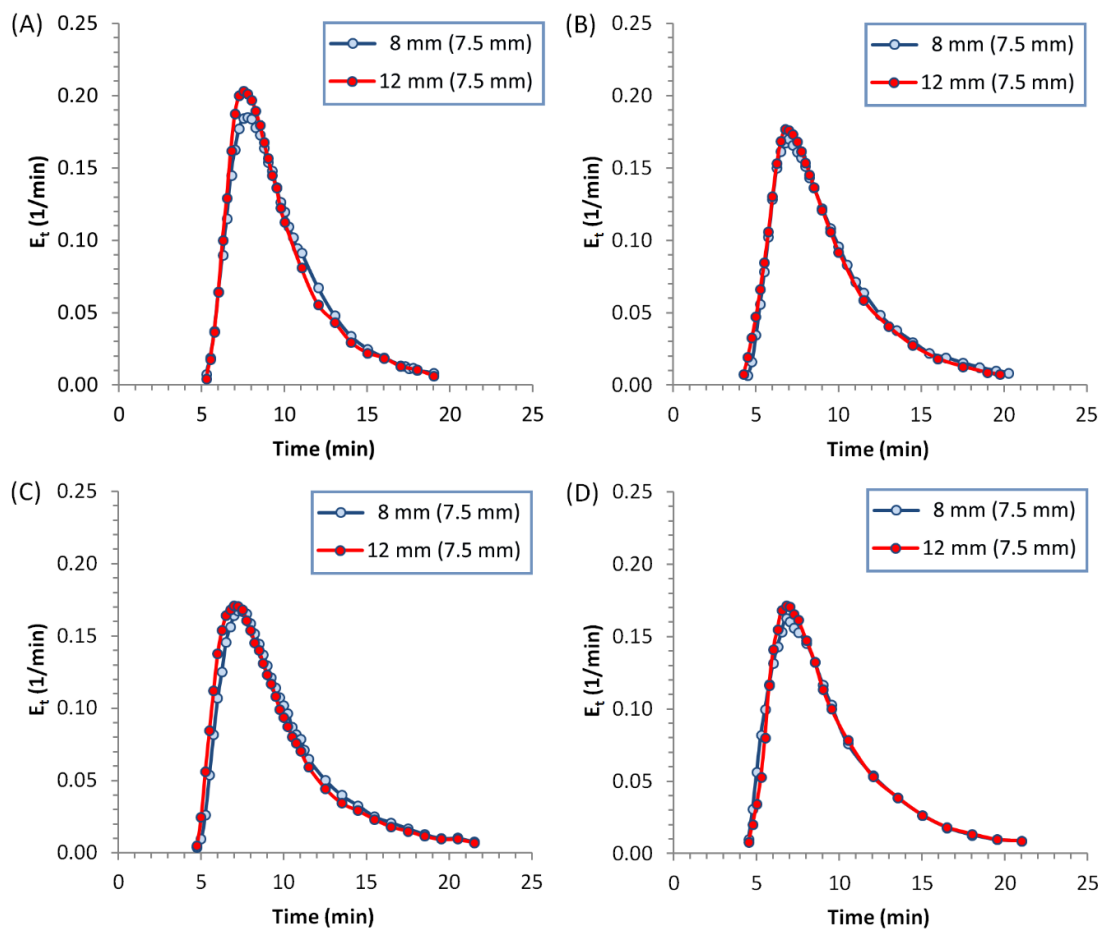

Fig. 26: E_t versus time profiles of the two different filling cams (8 mm, 12 mm) and a filling depth (7.5 mm) each at the four feed frame speeds: (A) 40 rpm; (B) 70 rpm; (C) 100 rpm; (D) 120 rpm.

The τ values determined from the E_t profiles of the two filling cams at the different feed frame speeds are shown in Fig. 27A. It is evident that τ is unaffected by both the filling cam as well as the feed frame speed. The intermixing effect is depicted in Fig. 27B. The σ^2 increases with increasing feed frame speed. It can also be notice that the σ^2 values of the two filling cams are almost identical. To summarize, there is no significant difference between τ and σ^2 at the different feed frame speeds and the different filling cams. The selection of a filling cam with constant filling depth as well as the effect of recirculation do not influence the residence time.
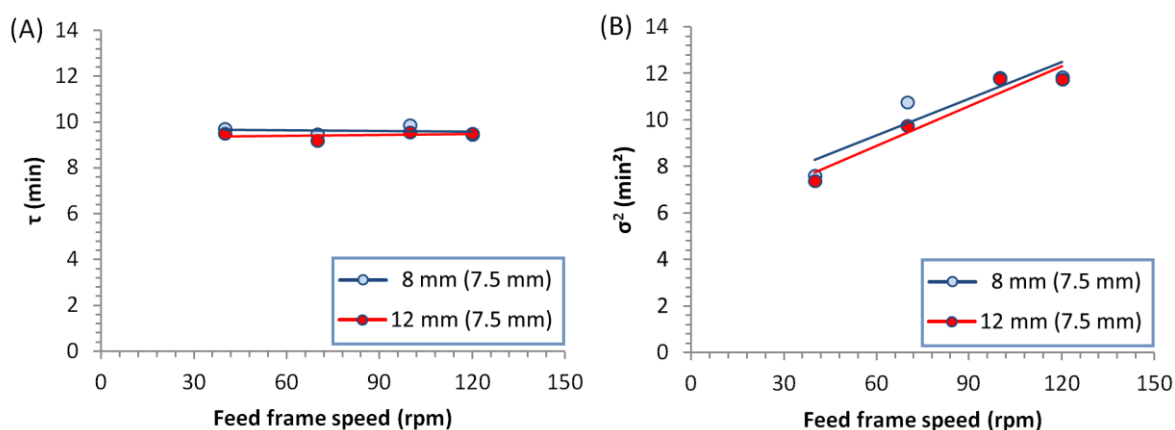
Fig. 27: Influence of the filling cams (8 mm, 12 mm) with the filling depth of 7.5 mm each on (A) τ and (B) σ^2 at the four feed frame speeds.

4.1.3.2. Variation of the filling depth

To clarify the effect of the filling depth on the residence time distribution, an 8 mm filling cam and a 12 mm filling cam were mounted to the tablet press, respectively, and the powder column height was adjusted to the minimum of 0.5 mm. This adjustment results in a die volume of 377 mm³ at a filling depth of 7.5 mm and a die volume of 578 mm³ at a filling depth of 11.5 mm. In comparison to chapter 4.1.3.1, in

which the flow rate was caused by the die disc speed, this subchapter describes the differences in the powder flow rate caused by the filling depth and its change in the die volume.

Hereby it is possible to examine the filling depth without any further influencing factors such as back-dosing and the resulting recirculation from the dosing chamber to the filling chamber. In Fig. 28 the E_t versus time curves at the filling depths of 7.5 mm and 11.5 mm, respectively, as well as a feed frame speed of 100 rpm, representative for all four feed frame speeds, is shown. A low filling depth leads to a decrease of the flow rate because of the resulting lower tablet mass: a high filling depths of 11.5 mm result in a flow rate of 7,200 g/h whereas a low filling depth of 7.5 mm results in a flow rate of 5,400 g/h. Therefore, a low filling depth as well as flow rate lead to an increase of the residence time.
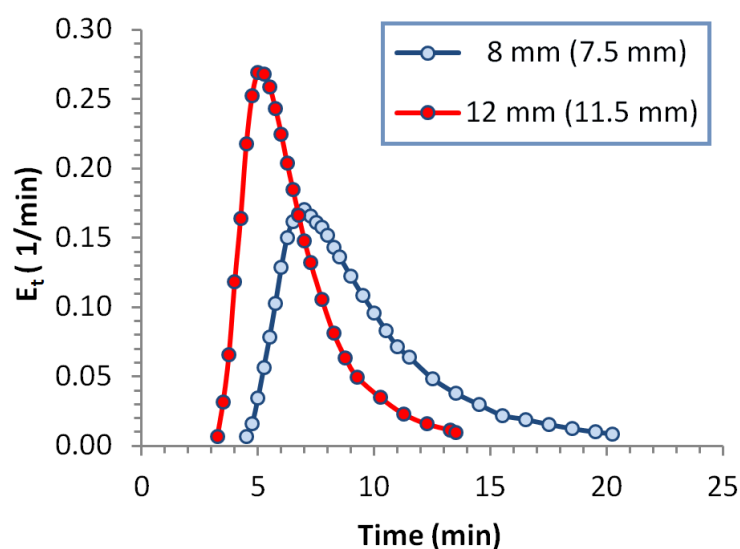

Fig. 28: E_t versus profiles of the two different filling cams (8 mm, 12 mm) and filling depths (7.5 mm, 11.5 mm) at a feed frame speed 100 rpm (representative for all four feed frame speeds).

In Fig. 29A, differences between the two filling depths with regard to τ at the four feed frame speeds are displayed. However, it is interesting to notice that τ is independent of the feed frame speed. This relationship has already been mention in the previous chapters. Remarkably, differences in σ^2 values are affected by an increasing feed frame speed. The high increase of σ^2 at a filling depth of 7.5 mm in comparison to the low increase of σ^2 at a filling depth of 11.5 mm is depicted in Fig. 29B. The differences in σ^2 may be explained by the intermixing effect as well as the variation in the flow rate because of the different filling depths.
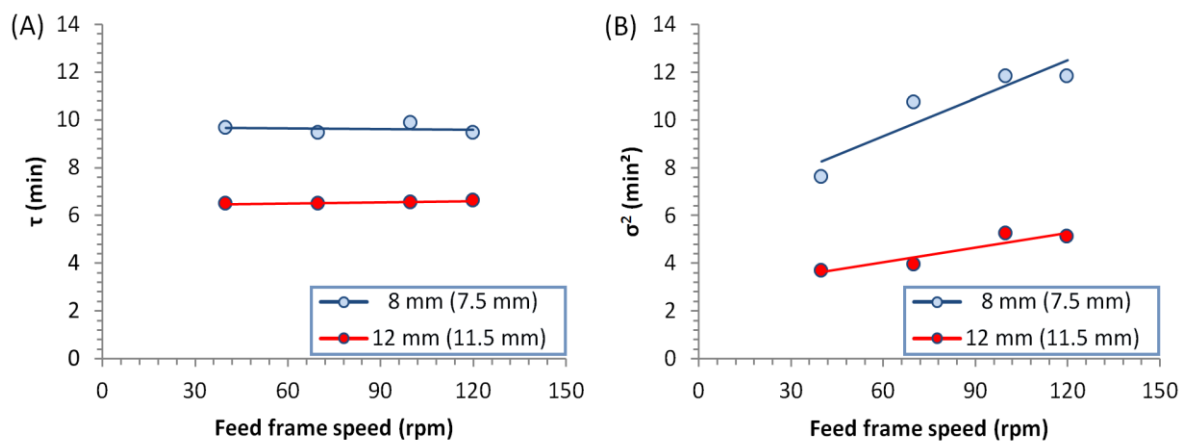

Fig. 29: Influence of the filling cams (8 mm, 12 mm) and filling depths (7.5 mm, 11.5 mm) on (A) τ and (B) σ^2 at the four feed frame speeds.

4.1.4. Conclusion

The aim of this study was to investigate the influence of various geometric and parametric setups of the three-chamber feed frame of a rotary tablet press on the residence time distribution. It was found, that the configurations of the applied scrapers had an effect on E_t of the tracer blend. The inner scraper led to a longer residence time caused by the recirculation and reuse of the powder from the collecting channel. This finding was confirmed by the mean residence time and the

mean centered variance values. However, the effect of recirculation on the residence time diminished at the highest feed frame speed of 120 rpm. The mean residence time was not affected by the feed frame speed, while the mean centered variance and therefore the intermixing of the powder in the feed frame were clearly influenced. The die disc speed was found to be a significant parameter affecting the residence time distribution. Increasing the die disc speed also increased the flow rate of the powder through the feed frame and consequently decreased the mean residence time of the feed frame. That means the flow rate of the powder is the predominant influencing factor of the mean residence time. The results of the investigation of the filling cams with identical filling depth showed that the respective filling cam and the resulting back-dosing effect had no influence on the residence time distribution. The E_t versus time profiles showed that no effect of recirculation was observed because of the pronounced relationship between the dosing and filling wheel of the Fill-O-Matic. However, the filling depths of the dies influenced E_t by altering the tablet mass and consequently the flow rate. Increasing the filling depth increased the flow rate and decreased the mean residence time. Comparing the high increase of the mean centered variance values resulting from the increase of the feed frame speed at a filling depth of 7.5 mm with the low increase of mean centered variance values at a filling depth of 11.5 mm indicated an unsuitable setting of the feed frame speed. For the industrial production of tablets, it is recommended to adjust the feed frame speed accordingly if a smaller filling depth is applied.

4.2. Effect of the powder properties on the powder behaviour in the FOM

4.2.1. Effect of the amount of tracer blend on the residence time distribution

This chapter of the study focuses on the effect of the amount of tracer blend on the residence time distribution in the three-chamber Fill-O-Matic (FOM). The concentration versus time profiles of the respective amount of tracer blend in the tablets are shown in Fig. 30. It is evident that the increase of the profiles from the beginning (t_{Start}) to the maximum concentration value (c_{Max}) have similar profile shapes. Furthermore, the profiles show an exponential approximation to the concentration of 100 %, which means that the FOM was filled completely with tracer blend. After the tracer blend completely entered the FOM, the MCC blend followed and the concentration of the tracer blend in the tablet decreased immediately.
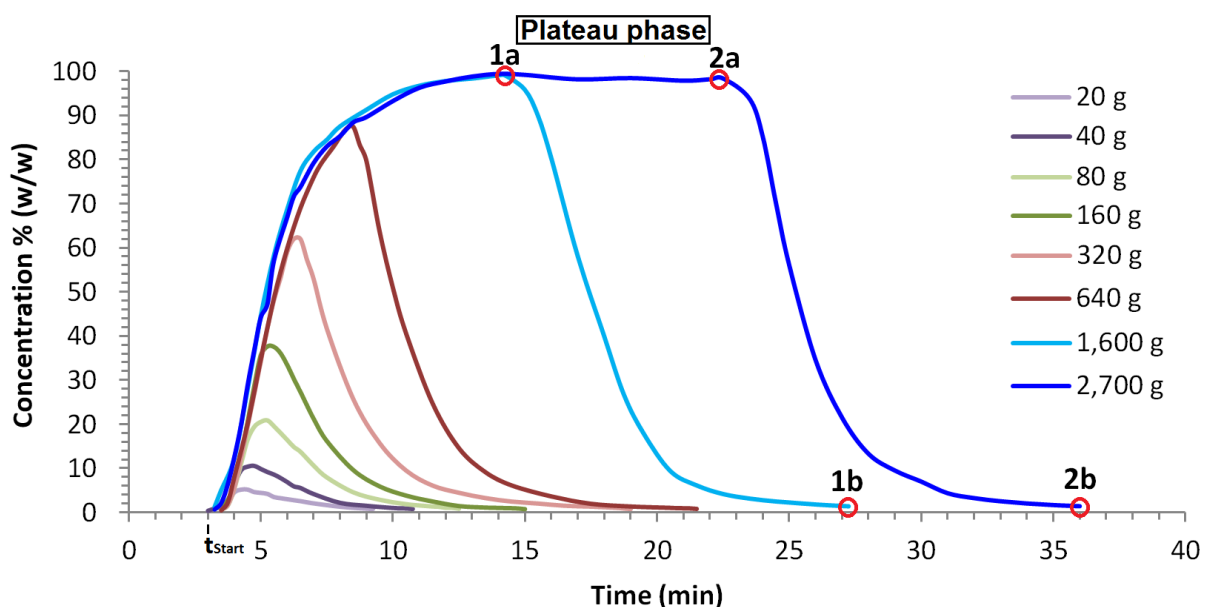

Fig. 30: Tracer blend concentration versus time profiles of the investigated amounts of tracer blend. The time periods from the plateau phase (time point 1a and 2a) to the end of the profiles (time points 1b and 2b) are identical.

Comparing the two profiles of the amount of tracer blend of 1,600 g (light blue) and 2,700 g (dark blue), respectively, the time needed from t_{start} to the plateau phase (Fig. 30; time point 1a) is identical. The time periods between 1a and 1b as well as between 2a to 2b are the same (Fig. 30; 1a to 1b and 2a to 2b). Considering the draining time of the light blue profile (1,600 g of tracer blend) and the dark blue profile (2,700 g of tracer blend), it may be observed that the time periods between the time points 1a and 1b (13.25 min) and those between the points 2a and 2b (13.5 min) are similar. Moreover, the time periods between the time points 1a and 2a (8.50 min) and those between the points 1b and 2b (8.75 min) are also similar. Based on these time periods and the powder flow rate of 7.5 kg/h, the resulting mass differences between time points 1a and 2a as well as between time points 1b and 2b amounted to about 1,063 g and 1,094 g, respectively. This mass difference was similar to the actual weighed mass difference between the two amounts of tracer blends (1,600 g and 2,700 g) which was 1,100 g.

The sudden decrease of the curve profiles from c_{Max} to the end of the respective profile, when the tracer is completely removed from the FOM, is rather interesting. The time differences between c_{Max} and the end of the respective profile were used to calculate the half-life of each profile. The half-life is the time period during which the tracer blend concentration of the tablets and therefore the amount of tracer blend in the FOM decreased by 50 %. The half-lives of the investigated tracer blends were between 1.51 min and 2.00 min, with an arithmetic mean of 1.75 min and a standard deviation of 0.18 min. The results of the half-lives of the different tableting runs showed no obvious trend (Fig. 31). For all tableting runs, the same die disc speed was used. It is evident that the half-life depends on the die disc speed and thus the corresponding flow rate of the powder through the FOM.

The information acquired on the residence time of the powder (MCC blend) in the FOM is particularly interesting for the continuous manufacturing of tablets. If the FOM is completely filled with powder from one blend, it is possible to determine the respective time point of the removal of this blend and the transition between different blends. From the results obtained, a time course of a tableting run may be predicted and a visualization of the transition between the blends is possible.
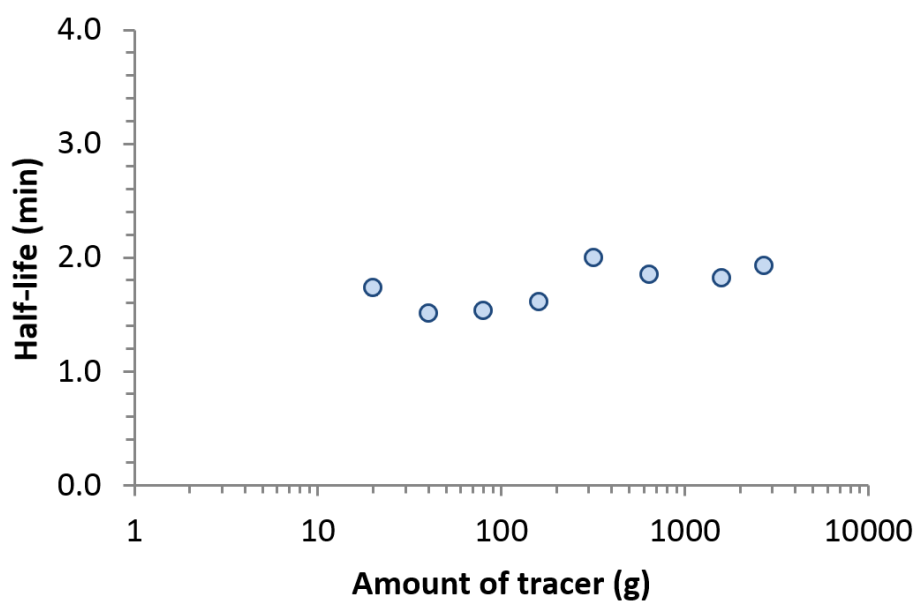

Fig. 31: Half-lives of the removal of the different amounts of tracer blend from the FOM.

In Fig. 32, the transition between the MCC blend (blend # 1) and the tracer blend (blend #2) (Fig. 32, 1-2), the time period during which only blue tablets (blend #2) were produced (Fig. 32, 2-3), and the transition between the tracer blend (batch #2) and the plain MCC blend (blend #3) (Fig. 32, 3-4) is shown. In this experimental setup, the duration of the transitions between the respective blends was approximately 13.5 min.
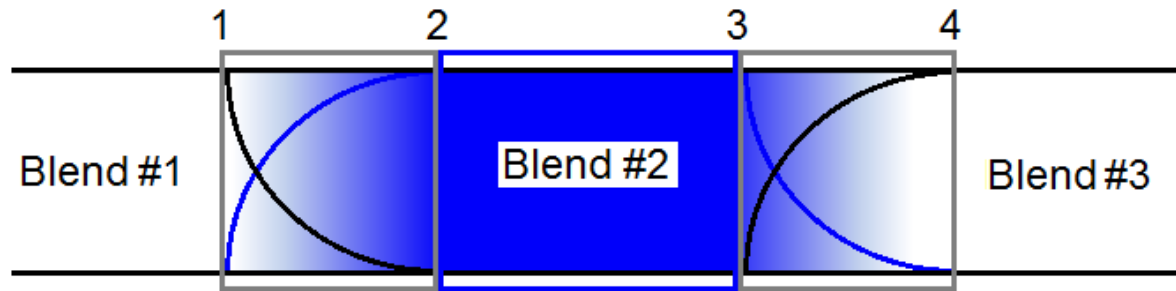
Fig. 32: Schematic illustration of the transition between tracer and MCC blends during continuous manufacturing (grey boxes) without intermixing (blue box).

The results of the concentration versus time profiles were used to calculate the E_t versus time profiles. The effect of the different amounts of tracer blend on the E_t is shown in Fig. 33. It is evident that the increase of the amount of tracer blend lowered the maximum height of the E_t versus time profile and thus the profile shapes broadened.

Furthermore, large amounts of tracer blend led to a generally increased residence time indicated by the τ values (Fig. 34A) and to a greater intermixing of the powder in the FOM indicated by the σ^2 values (Fig. 34B).
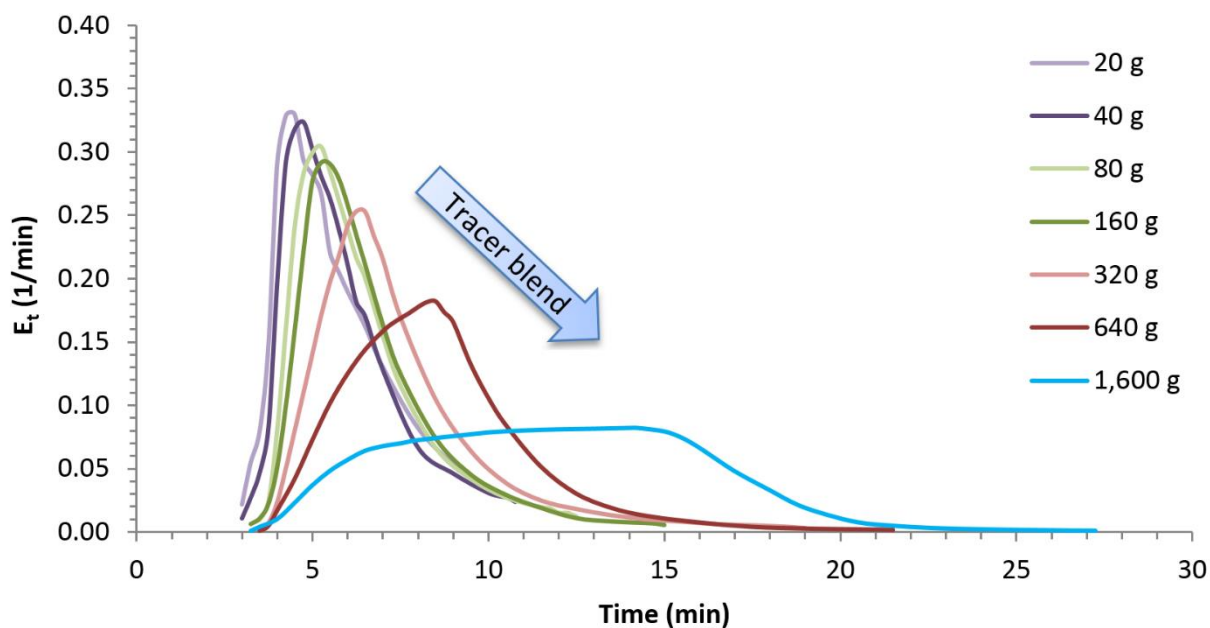
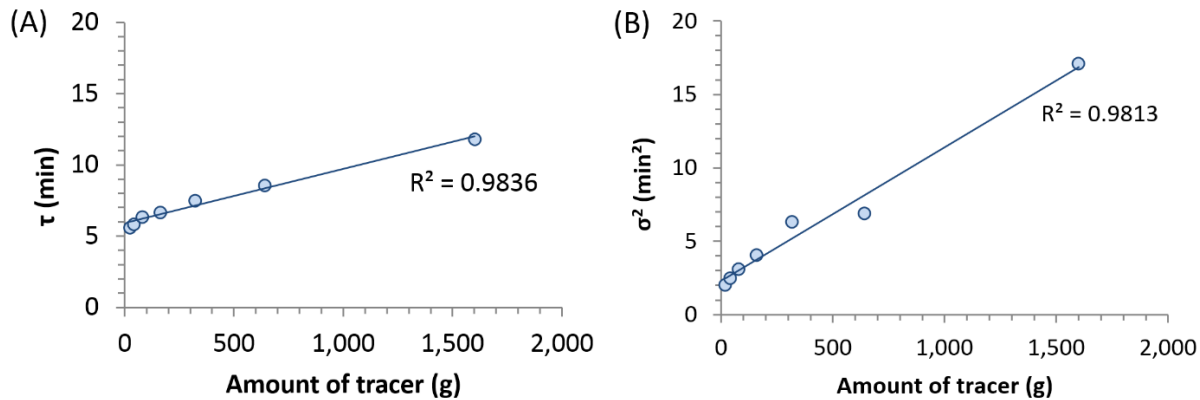Fig. 33: E_t versus time profiles of the different amounts of tracer blend.

Fig. 34: τ (A) and σ^2 (B) values of the E_t versus time profiles of the different amounts of tracer blend.

4.2.2.   Effect of the flow rate on the residence time distribution

In this chapter, the effect of the flow rate of tracer blend on the residence time distribution in the three-chamber Fill-O-Matic was investigated. The tracer concentration versus time profiles of the different powder flow rates through the FOM are shown in Fig. 35. An increase of the flow rate corresponded to a shift of the profiles to lower values on the time axis and led to a narrowing of the profile shapes. Interestingly, the respective maximum concentrations (c_{Max}) of each profile are independent of the flow rate of the powder through the feed frame (table in Fig. 35).
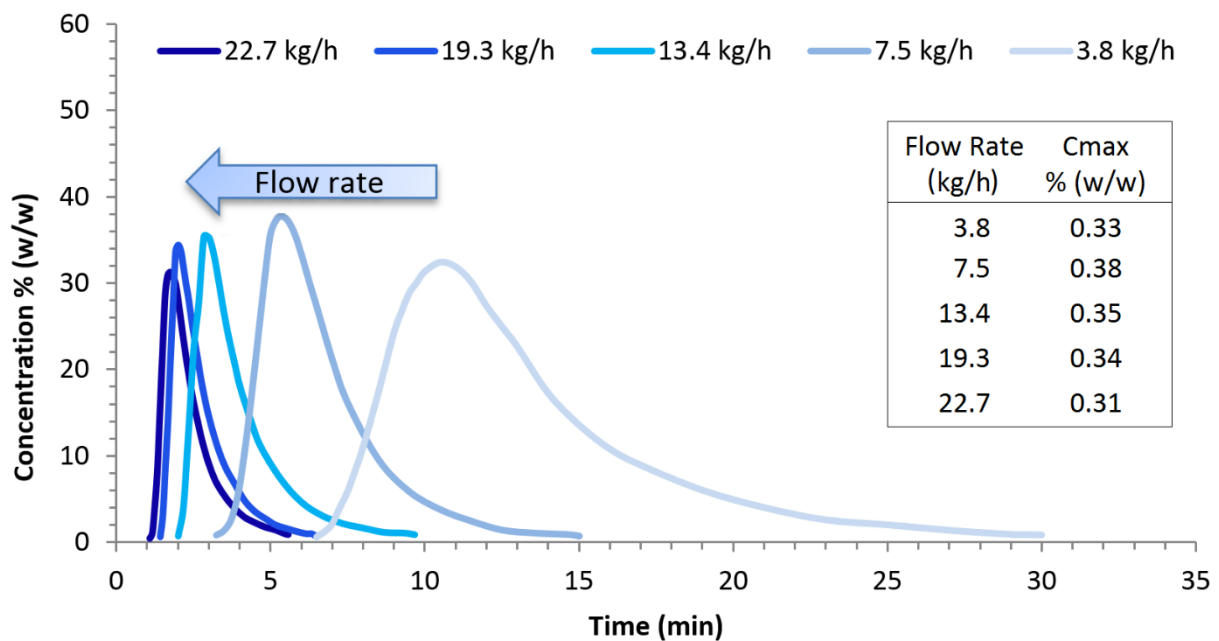

Flow Rate (kg/h)	Cmax % (w/w)
3.8	0.33
7.5	0.38
13.4	0.35
19.3	0.34
22.7	0.31

Fig. 35: Tracer blend concentration versus time profiles of the different powder flow rates through the FOM.

In $Fig.\ 36$ the starting time points of the profiles (t_{Start}), the profile end points (t_{End}), and the time difference between t_{End} and t_{Start} were plotted versus the reciprocal of the powder flow rates. It is obvious, that the reciprocal values of the flow rates and the time points of the respective setting are proportional. These results may be of interest for the continuous manufacturing to predict the time points t_{Start} and t_{End} also for other flow rates.
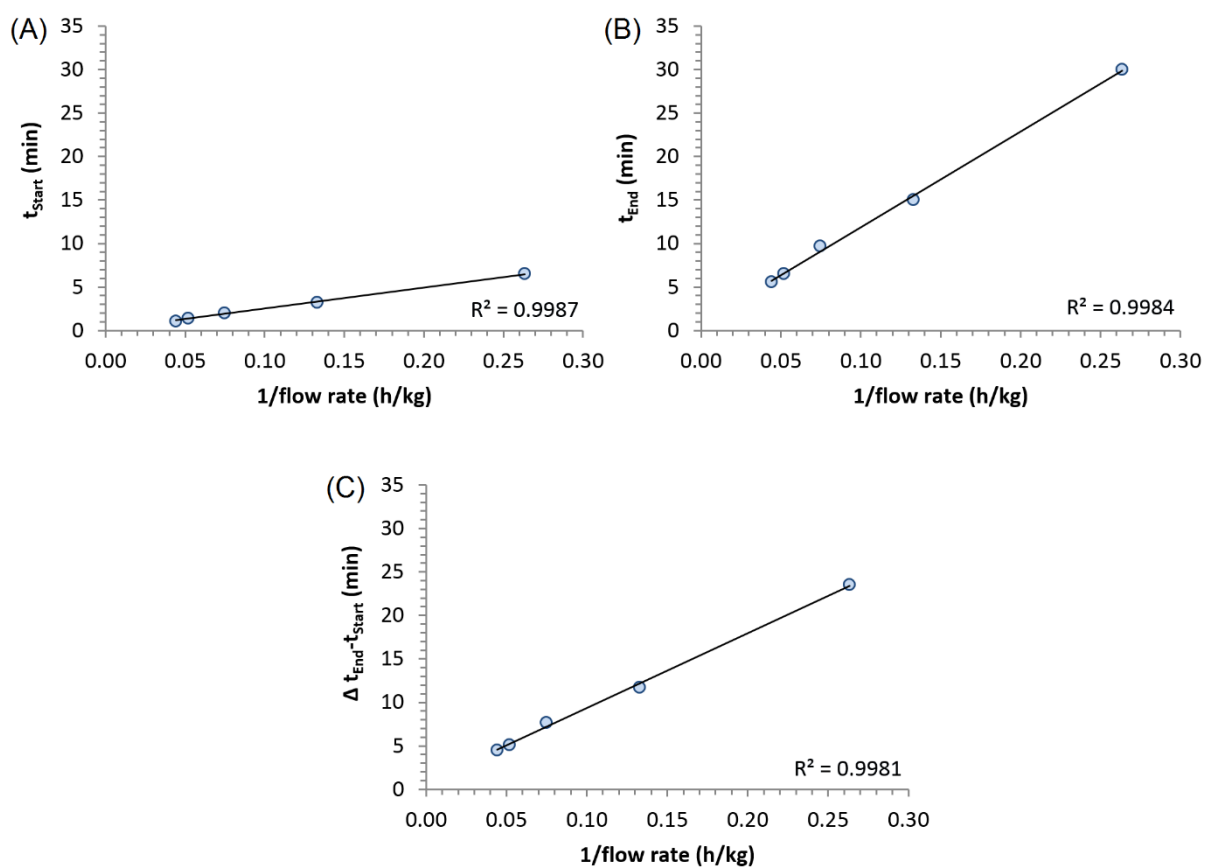

Fig. 36: The time points (A) t_{Start}, (B) t_{End}, as well as (C) the differences between t_{End} and t_{Start} versus the reciprocal flow rates of the respective tableting run.

The E_t versus time profiles are depicted in Fig. 37. It may be observed that an increase of the powder flow rate through the FOM not only leads to a shift of the E_t versus time profiles to lower values on the time axis but also to an increase of the $E_{t\,Max}$ values. Furthermore, it is evident that the width of the profile again became narrower with an increasing powder flow rate.
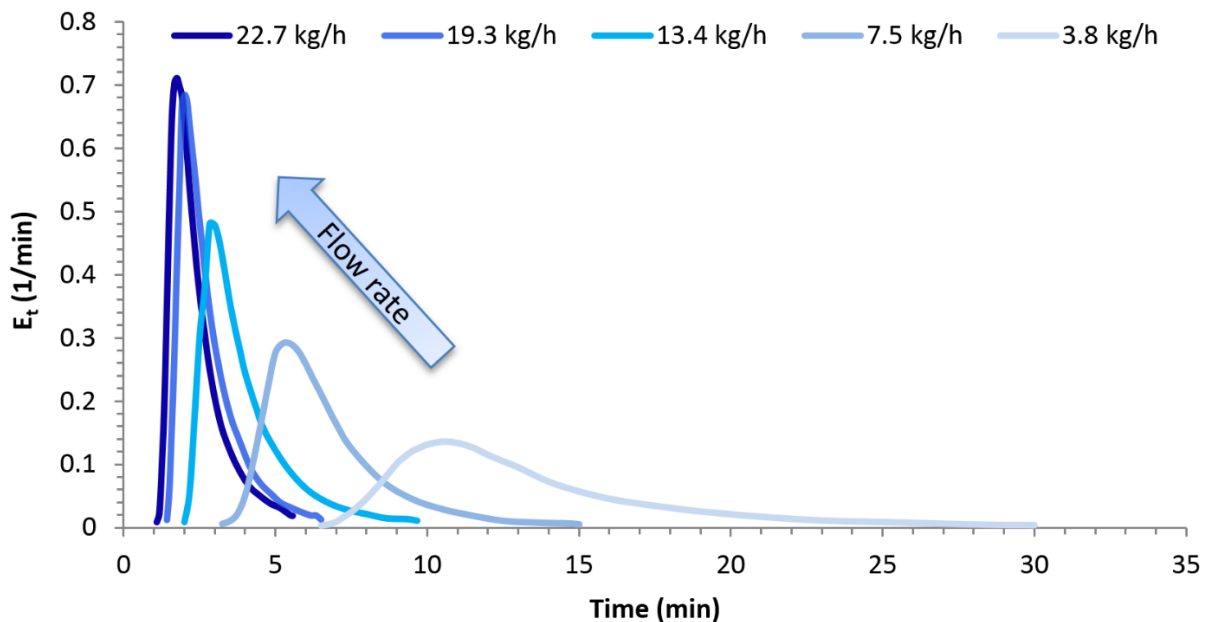

Fig. 37: E_t versus time profiles of the different powder flow rates through the FOM.

These results are confirmed by the т and σ² values in Fig. 38. The increase of the flow rate from 3.8 to 7.5 kg/h led to a decrease of the т value of 12.3 min and a decrease of the σ² value of 9.3 min², whereas the increase of the flow rate from 7.5 kg/h to 13.4 kg/h led to a decrease of the т value of only 2.7 min and a decrease of the σ² value of only 2.0 min². With a doubling of the flow rate corresponded to a 4.5-fold decrease of the т and σ² values. These differences between the individual т and σ² values decrease at higher flow rates. Consequently, low values of σ² indicate a low mechanical powder strain. However, it has to be taken into account that the rotational speed of the feed frame and that of the die disc are identical.
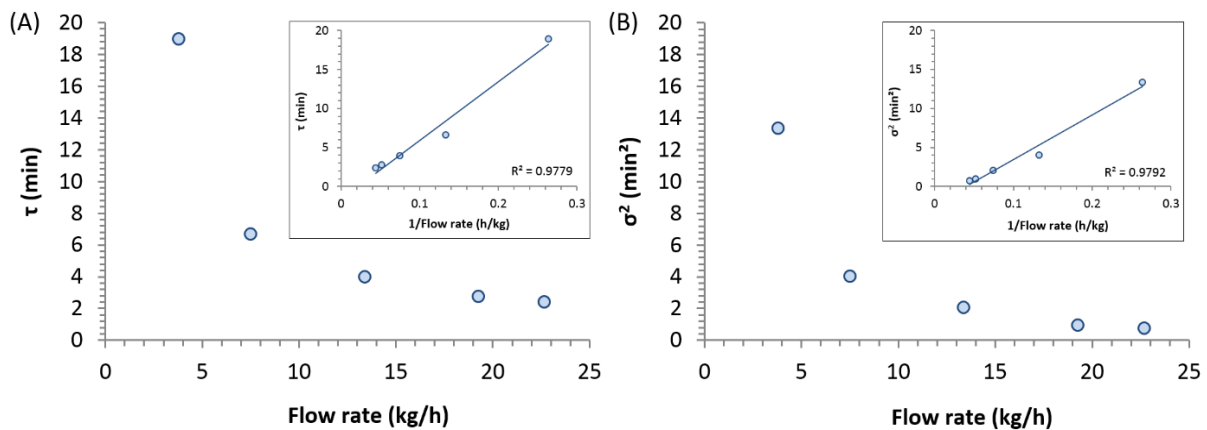
Fig. 38: τ (A) and σ² (B) of the different powder flow rates through the FOM and their linear dependency on the reciprocal of the flow rates (inserts).

For the manufacturing of tablets, it is preferred to have a low strain applied to the powder because a high total shear may affect the properties of the powder particles, such as powder attrition and particle breakage [131]. Mateo et al. reported that the paddle wheel speed and thus the number of paddle passes is the most influential factor on the total strain applied to the powder. Moreover, a high feed frame speed results in a high number of paddle passes (Npp) and thus to a higher mechanical powder strain [84]. The Npp determined in the present study, is illustrated in Fig. 39. These results show that an increase in the powder flow rate by increasing the rotational die disc speed with a simultaneous increase of the rotational feed frame speed does not affect the number of paddle passes. Under consideration of the number of paddle passes (7) and the linearity between the τ values and the reciprocal of the powder flow rates (Fig. 38A, insert), it is obvious, that the Npp values are constant in the given setup. At the lowest flow rate of 3.8 kg/h, the Npp appears to be higher than the constant Npp values at higher flow rates. This result may be explained by a non-uniform powder movement of the particles at this lowest

flow rate. Thus, a uniform powder flow through the FOM could not be achieved and the residence time as well as the Npp were increased.
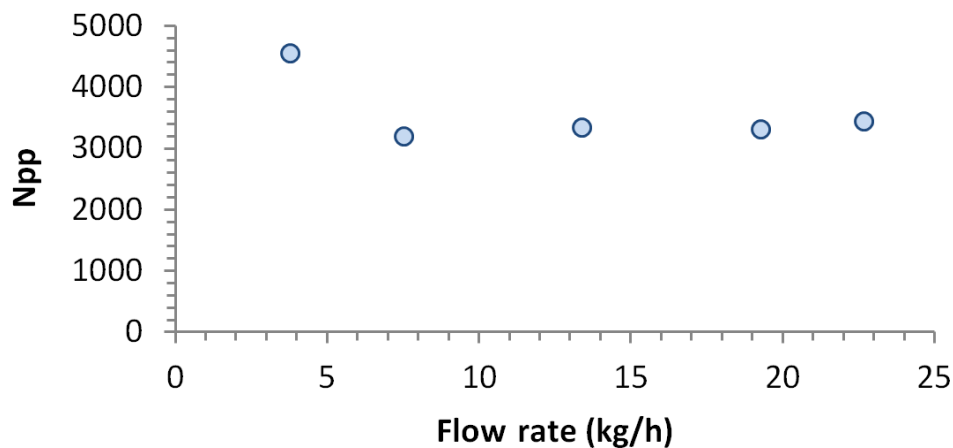

Fig. 39: The numbers of paddle passes (Npp) of the respective powder flow rates through the FOM.

4.2.3. Effect of the residual moisture content on the residence time distribution

The purpose of this chapter of this study was to investigate the effect of different residual moisture contents (RMCs) of the tracer blend on the E_t versus time profile. In Fig. 40A, the E_t profiles of the three different RMCs at a rotational die disc speed of 20 rpm and a rotational feed frame speed of 40 rpm are shown. These E_t profiles do not change even at increased rotational feed frame speeds Fig. 40B: 70 rpm; Fig. 40C: 100 rpm). It is evident that the RMC does not influence the residence time distribution of the tracer blend in the feed frame.
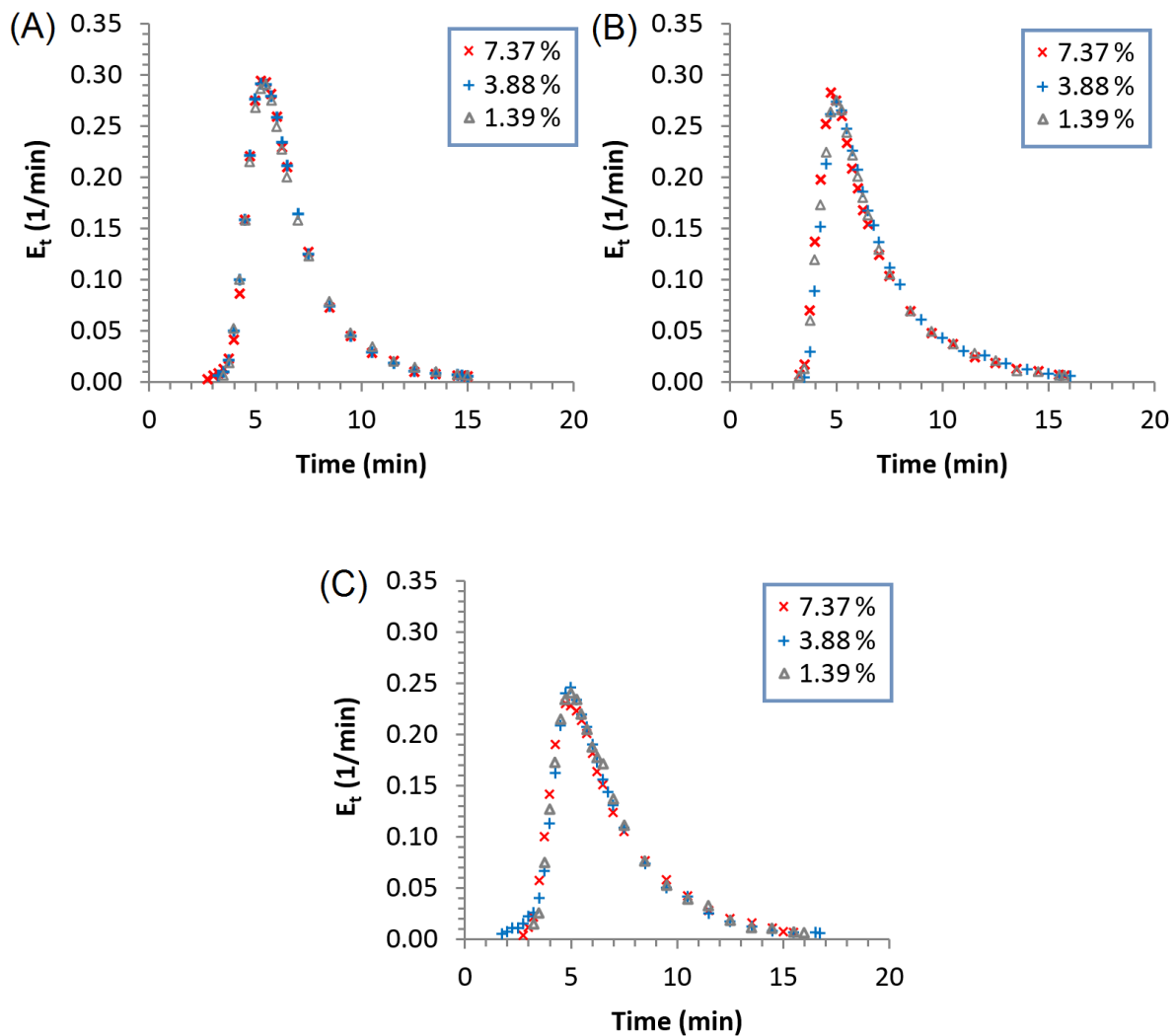
Fig. 40: The effect of the different residual moisture contents (wet (x): 7.37 %, medium (+): 3.88 %, dry (Δ): 1.39 %) on E_t at a rotational die disc speed of 20 rpm with rotational feed frame speeds of (A) 40 rpm, (B) 70 rpm, and (C) 100 rpm.

These results are also confirmed by the τ and σ² values (Fig. 41). It is evident that the τ values are not influenced by the RMCs and the feed frame speeds. Furthermore, the σ² values do not depend significantly on the RMC. Remarkably, there is a dependence of the σ² values on the feed frame speed. An increase in the feed frame speed leads to an increase of the σ² values. These changes in the σ² values may be explained by an increased intermixing of the powder particles in the feed frame.
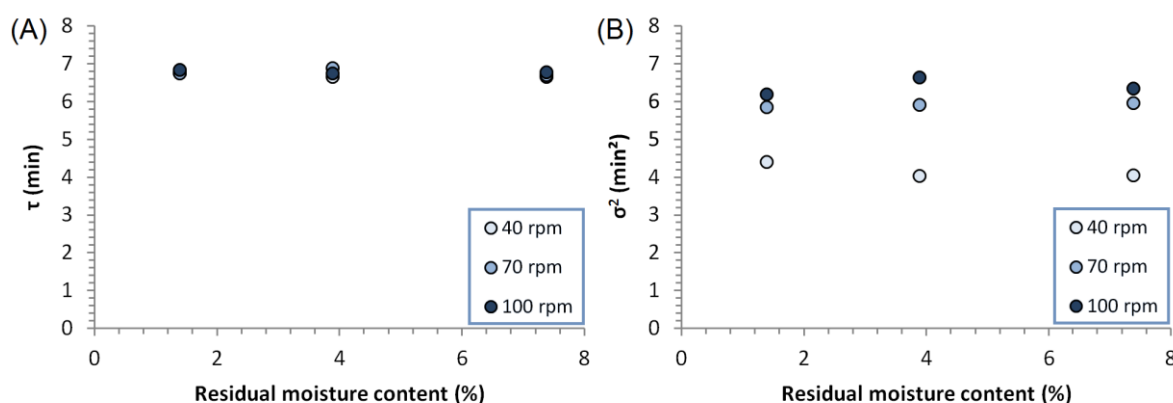
Fig. 41: The effect of the RMCs and the feed frame speeds on (A) τ and (B) σ².

4.2.4.   Effect of particle size segregation on the residence time distribution

The purpose of this chapter was to investigate the effect of different particle sizes of the tracer blend on the E_t versus time profile. In Fig. 42, the distribution of the differently sized particles at the top and bottom of the tablet samples, which were collected 2 min after t_{Start}, in triplicate, is shown. The top of the sampled tablets was marked with a red dot. It is evident that more tracer blend particles of the 400-315 µm fraction are located at the top surface than at the bottom surface (Fig. 42A). The 180-125 µm fraction showed a homogeneous distribution of the tracer blend particles at the top and the bottom surface (Fig. 42B) whereas the <50 µm fraction showed that more tracer blend particles accumulate at the bottom surface of the tablet (Fig. 42C). Comparing these results with the different particle size fractions with the d_{50} value of the certificate of analysis of Vivapur® 102, it may be concluded that a similar particle size of the tracer blend and the MCC blend is important for a homogeneous particle distribution in the feed frame and the produced tablet.

The different particle sizes in the powder and the resulting accumulation in the produced tablet and in the feed frame may lead to a change in E_t. By a deposition of

smaller particles at the bottom of the feed frame, these particles may reach the dies more quickly than larger particles which are deposited at the top [84,124].
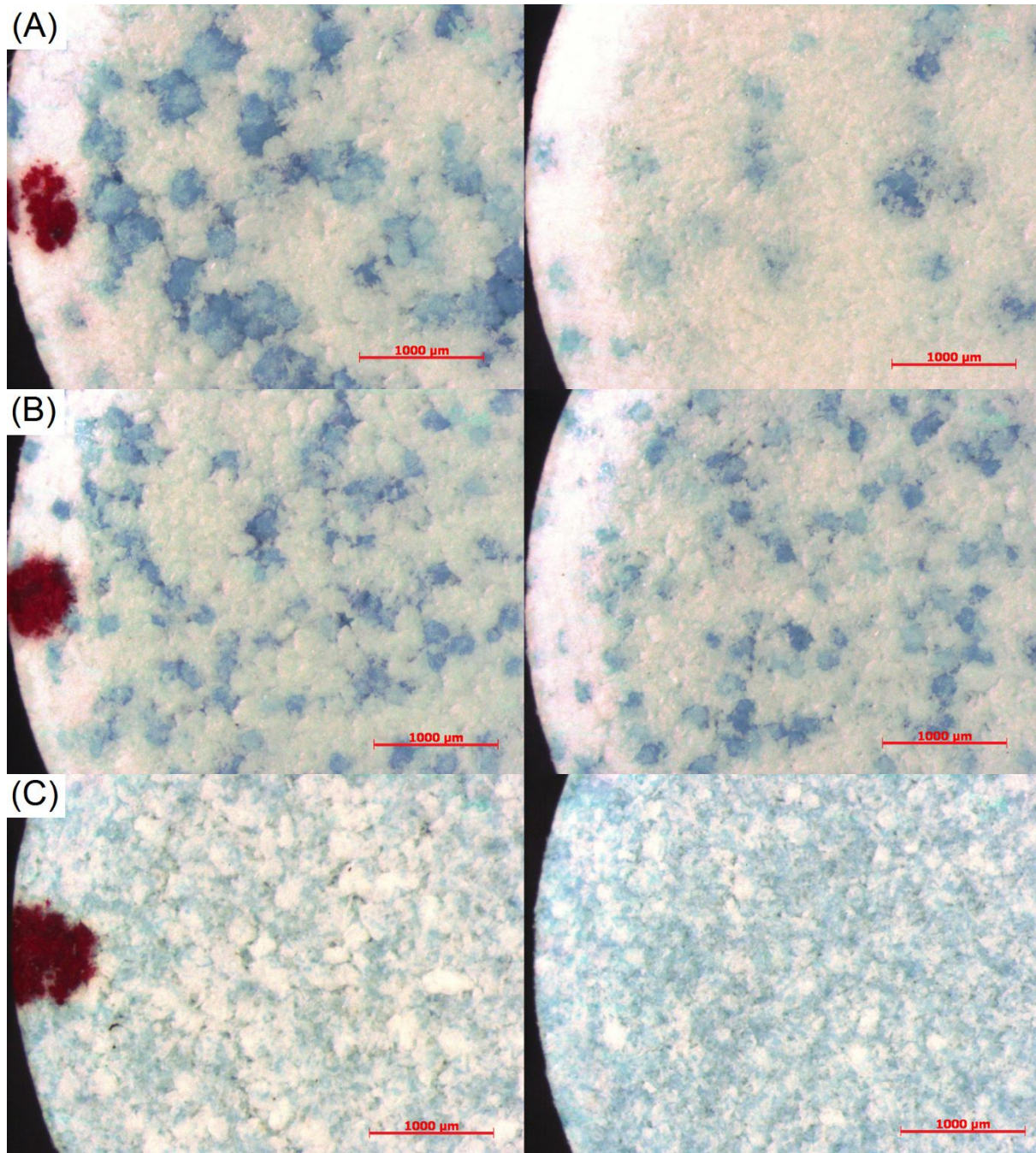

Fig. 42: Effect of the segregation of differently sized particles on the particle size distribution in sample tablets: (A) 400-315 µm, (B) 180-125 µm, and (C) <50 µm. Left column: upper tablet surface; Right column: lower tablet surface.

The E_t versus time profiles of the three particle fractions (blue lines) and, for comparative purposes, the E_t versus time profile of the MCC blend with Vivapur® 200, which contains all particle sizes from 400 µm down to <50 µm (red dashed line), are displayed in Fig. 43. In contrast to the expectations that a small particle size leads to a short residence time and a large particle size leads to a long residence time, the E_t versus time profiles of the different particle size fractions are almost identical. Differences in the profile shapes were recognized at the maximum E_t value ($E_{t\,Max}$). It is evident that a large particle size of the tracer blend leads to a lower $E_{t\,Max}$ of the profiles. Therefore, the probability that a tracer blend particle enters the feed frame at the time point t_{Start} and leaves the feed frame at the time point of $E_{t\,Max}$, decreased. However, the τ and σ^2 values show no clear tendency (table in Fig. 43).

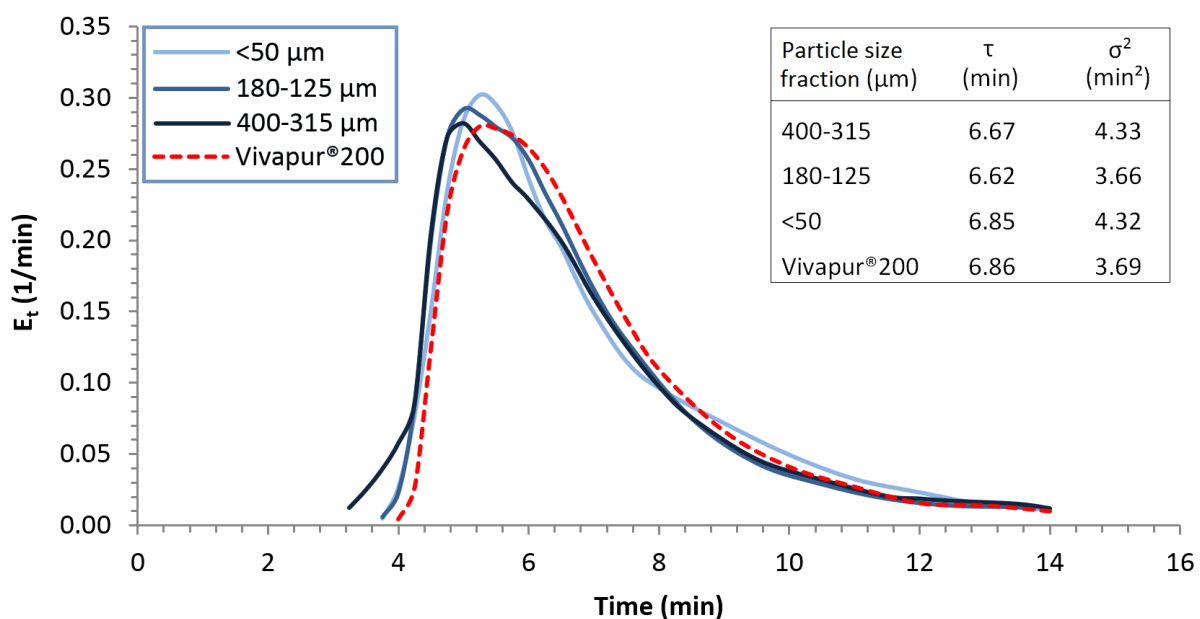| Particle size fraction (µm)	τ (min)	σ^2 (min²)
400-315	6.67	4.33
180-125	6.62	3.66
<50	6.85	4.32
Vivapur®200	6.86	3.69

Fig. 43: E_t versus time profiles of different particle size fractions of the tracer blend (light blue: <50 µm, blue: 180-125 µm, dark blue: 400-315 µm, and red: Vivapur® 200).

4.2.5. Conclusion

In this study it was found that the mean residence time (τ) and the mean centered variance (σ^2) were increased by increasing the amount of tracer blend. Thus, if the content of tracer blend in the feed frame was increased, a longer residence time resulted. With this knowledge of the powder behaviour of different amounts of tracer blend, the interface transition between the MCC blend and the tracer blend of the tableting run could be illustrated.

The E_t turned out to be dependent on the powder flow rate through the Fill-O-Matic. The τ and σ^2 values decreased with increasing flow rate. It is noteworthy that the difference between the τ values at high flow rates was diminished. This effect was also observed with the σ^2 values. Remarkably, at the same rotational speed of the feed frame wheels as well as of the die disc, the change of the flow rate had no significant influence on the mechanically powder strain because of the inverse proportionality of the flow rate and the τ. These results were confirmed by the constant number of paddle passes. Surprisingly, at the lowest powder flow rate of 3.8 kg/h an increase of the Npp was observed. A low powder flow rate may lead to a non-uniform movement of the powder particles through the FOM and to a high strain applied to the particles.

The residual moisture content is an important parameter regarding the quality of the product. It affects e.g. the stability of the excipients and active pharmaceutical ingredients (APIs) and it may influence the compressibility of the powder. Interestingly, the investigation of the E_t at different residual moisture contents of the tracer blend particles showed that it was independent of the residual moisture content.

Furthermore, the particle size of the tracer blend was part of the investigation of this study. Surprisingly, a low influence of the particle size on the E_t was demonstrated in this investigation, but it was shown that the particle size segregation had a high influence on the distribution of the tracer blend particles in the produced tablet. Large particles were deposited at the top of the tablet surface, whereas small particles were deposited at the bottom.

4.3.   Influence of the feed frame components on the powder behaviour

4.3.1.   *Influence of the FOM volume on the residence time distribution E_t*

The E_t versus time profiles of the two dosing chamber configurations at the three rotational feed frame speeds (40 rpm, 70 rpm, and 100 rpm) are displayed in Fig. 44. It is evident, that the use of the perspex disc led to narrower E_t versus time profiles. Both, the later start of the profile of the perspex disc configuration as well as the earlier end of the profile led to a decrease of the residence time of the tracer blend. In addition, the pronounced difference between the $E_{t\ Max}$ values of the two different configurations is an indicator for a narrower distribution of the tracer blend residence time and a decrease of the intermixing of the powder particles in the FOM.
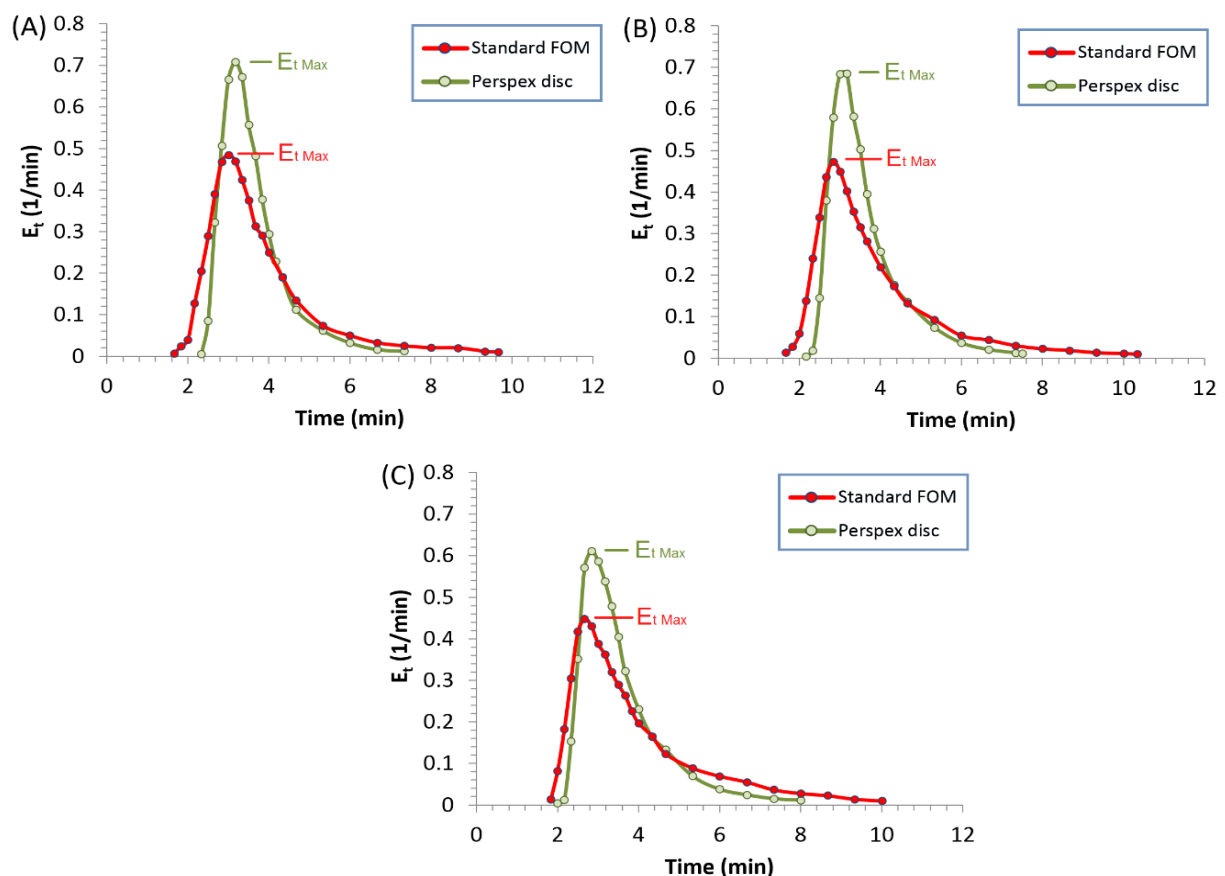

Fig. 44: E_t versus time profiles of the configuration, volume-reduced with a perspex disc, and the standard FOM configuration at three rotational feed frame speeds: (A) 40 rpm; (B) 70 rpm; (C) 100 rpm.

These differences between the E_t versus time profiles of the perspex disc and standard configurations may be confirmed by both the τ values and the σ² values of the two configurations (Fig. 45). In comparison to the standard configuration with the perspex disc configuration, the τ values at the three different rotational feed frame speeds (40 rpm, 70 rpm, and 100 rpm) were lower (Fig. 45A). The σ² data obtained with the dosing chamber configurations increased with increasing rotational feed frame speed (Fig. 45B). If the σ² values of the two configurations are compared, it is noticeable that the corresponding regression lines have similar slopes. The linear regression lines of each configuration were determined using the three τ values as well as the three σ² values, respectively. However, the regression line of the perspex disc configuration is considerably lower than that of the regression line of the standard configuration. Thus, the increase of the rotational feed frame speed in combination with a large filling volume of the FOM may be result in a higher intermixing of the inner powder particles. These results may be explained by the different powder paths through the FOM. With the use of the perspex disc configuration, the function of the dosing chamber was no longer available and thus the powder from the distribution chamber flowed through the filling chamber directly into the dies. Therefore, no intermixing of the powder particles occurred between the dosing chamber and the filling chamber, which was confirmed by the low σ² values (Fig. 45B).
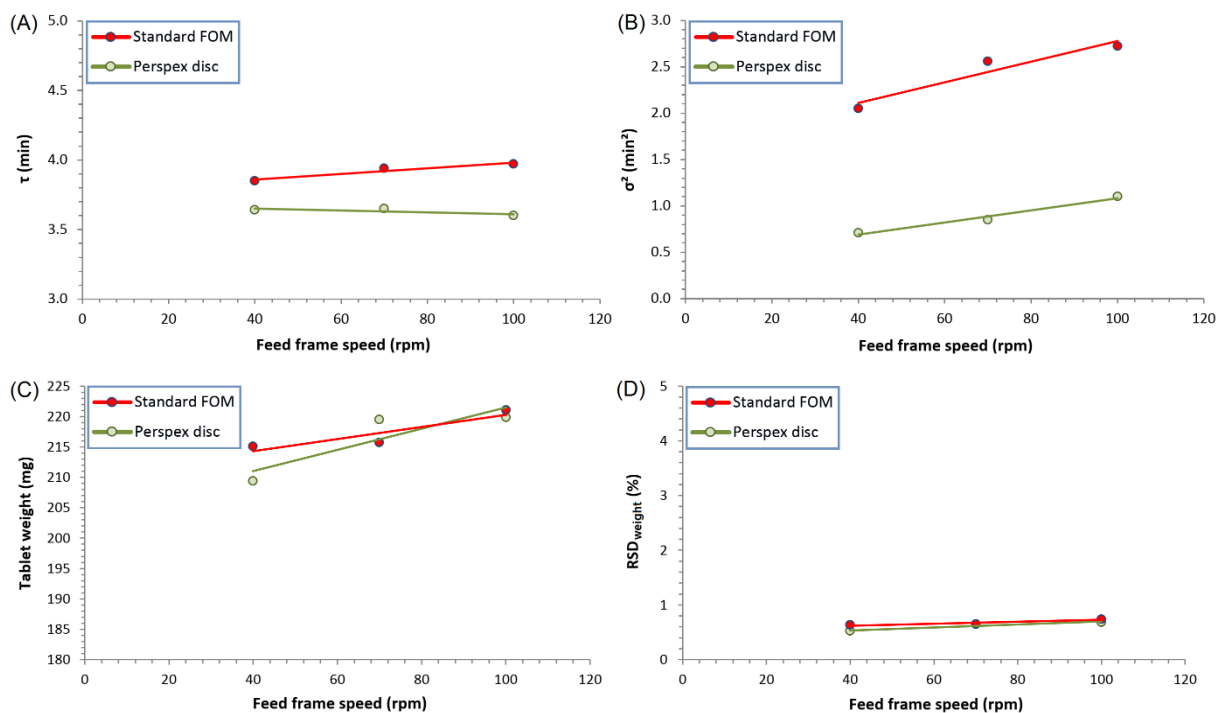
Fig. 45: Effect of the configuration, volume-reduced with a perspex disc, on (A) τ, (B) σ², (C) tablet weight (means, n = 10), and (D) RSD in comparison to the standard FOM configuration.

The tablet weight data and the corresponding relative standard deviation (RSD) values are shown in Fig. 45C and Fig. 45D. Comparing the tablet weights resulting from both, the standard configuration and the perspex disc configuration, no significant differences were recognized and the results of the "Uniformity of dosage units" met the requirements of the Ph. Eur. monograph 2.9.40. Furthermore, the RSDs of the tablet weights were identical with both configurations. In summary, the determined residence time distributions showed that a reduction of the FOM volume had a remarkable effect on the E_t versus time profiles as well as a high influence on the τ and σ² values.

4.3.2.   Influence of the filling wheel design on the powder behaviour in the FOM

The E_t versus time profiles of the flat rod filling wheel and the round rod filling wheel at three rotational feed frame speeds (40, 70, and 100 rpm) and at a rotational die disc speed of 36 rpm (64,800 tablets/h) are shown in Fig. 46. The ascending and the descending sections of the respective profile shapes are similar. However, slight differences are recognizable. It is obvious, that the flat rod filling wheel at the rotational feed frame speeds of 40 and 70 rpm led to differences in the maximum of the E_t versus time profiles ($E_{t\ Max}$). These differences decreased at the rotational feed frame speed of 100 rpm. Furthermore, it is obvious that the last section of the profile of the flat rod filling wheel ends (t_{End}) earlier than that of the profile of the round rod filling wheel. t_{end} was determined as the time point at which the adsorption of a sample solution exceeds the validation range (absorption 0.05-1.00). These time periods between t_{Max} and t_{End} of the respective configuration decreased by increasing the rotational feed frame speed. Thus, the higher $E_{t\ Max}$ and the lower t_{End} values indicated a narrower distribution of the powder residence time.
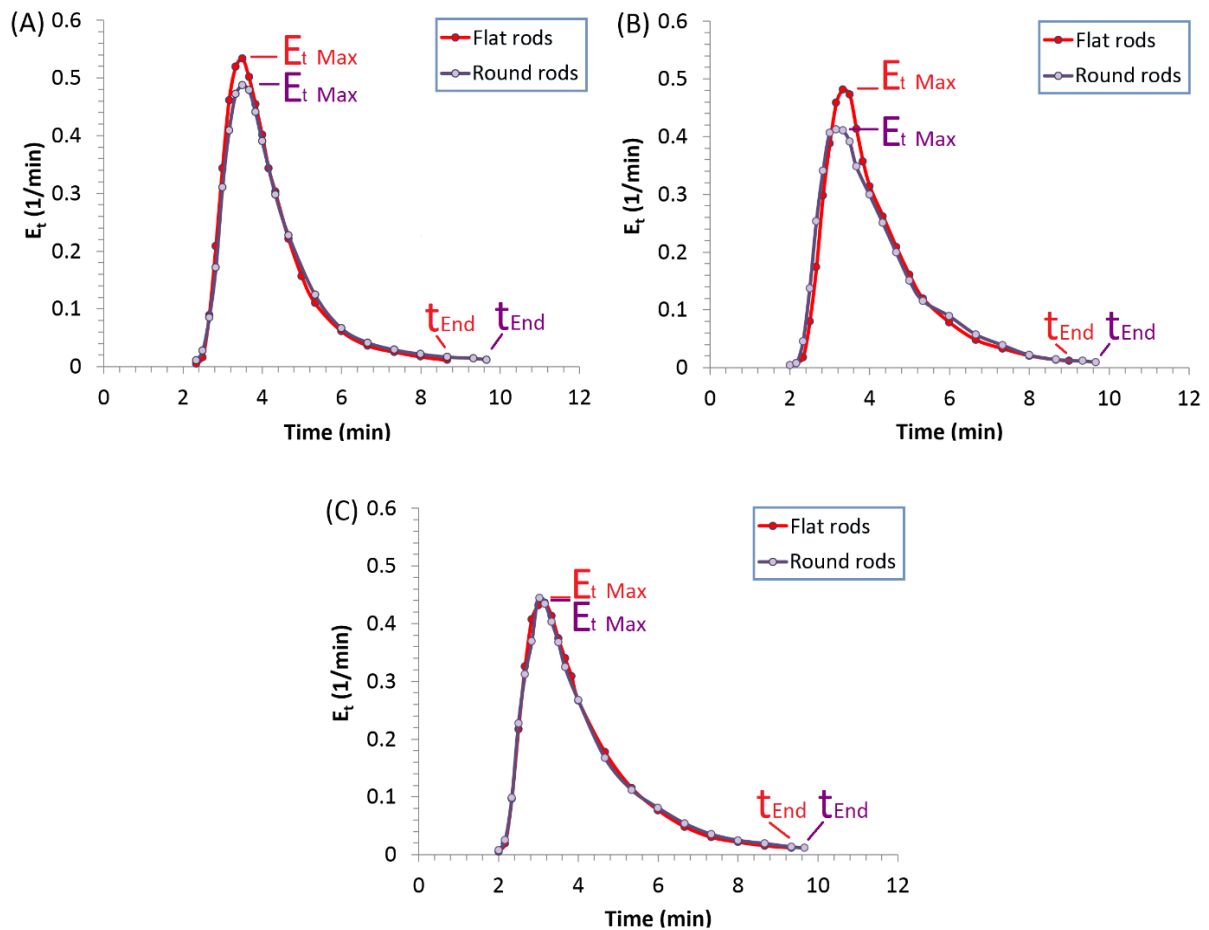
Fig. 46: E_t versus time profiles of the flat rods and the round rods of the filling wheels at three rotational feed frame speeds: (A) 40 rpm; (B) 70 rpm; (C) 100 rpm with a rotational die disc speed of 36 rpm, respectively.

The results of the E_t versus time profiles of the two differently designed filling wheels were confirmed by the τ and the σ^2 values. The τ values determined from the E_t profiles of the flat rod filling wheel (40 rpm: 4.15 min; 70 rpm: 4.19 min; 100 rpm: 4.09 min) and the round rod filling wheel (40 rpm: 4.30 min; 70 rpm: 4.24 min; 100 rpm: 4.15 min) were almost independent on the three different rotational feed frame speeds. According to the broader E_t versus time profiles and their σ^2 values of the round rod filling wheel (40 rpm: 1.68 min²; 70 rpm: 1.97 min²; 100 rpm: 2.17 min²), the σ^2 values were higher than those of the flat rod filling wheel (40 rpm: 1.22 min²;

70 rpm: 1.59 min²; 100 rpm: 1.90 min²). This result may be explained by the different geometric shape of the rods and their different intermixing effect of the powder particles. The rod of the round rod filling wheel is thinner than the rod of the flat rod filling wheel. Therefore, the round rods glide through the powder particles in the chamber, causing a high intermixing effect of the particles. In contrast, the flat rods led to a separation of the powder particles within the feed frame chambers. As part of an additional experimental test, the effect of the different geometric shape of the round rods and flat rods on the intermixing of the powder particles in the filling chamber is shown in Fig. 47. Already after the first five revolutions, a homogeneous distribution of the tracer blend and the MCC blend was achieved with the round rod filling wheel (Fig. 47, top row). In contrast, the flat rod filling wheel with its larger rods led to a separation of the tracer blend and the MCC blend (Fig. 47, bottom row). Only a slight exchange between the powder blends in the spaces between the flat rods was noted after five revolutions. Further revolutions led to an intermixing of the powder blends primarily at the edge of the filling chamber. An intermixing of the powder blends close to the hub was not observed.
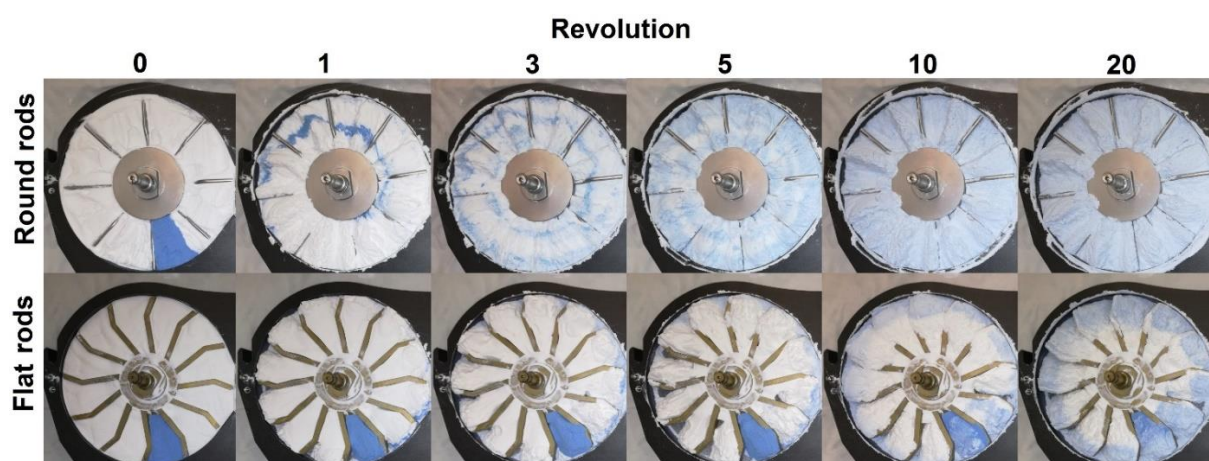

Fig. 47: Intermixing effect of the round rods (top row) and flat rods (bottom row) after 1, 3, 5, 10, and 20 revolutions.

The tablet weights obtained with the two filling wheel designs turned out to be identical (Fig. 48A). The tablet weights increased with increasing rotational feed frame speed. Grymonpré et al. found a similar effect by increasing the rotational feed frame speed of a two-chamber feed frame system [132]. Regarding the RSD values of the tablet weights, an increase of the rotational feed frame speed of the round rod filling wheel led to an increase of the RSD values (Fig. 48B). In contrast, increasing the rotational feed frame speed of the flat rod filling wheel led to a decrease in the RSD values. However, the effect of the different filling wheel designs on the tablet weights and their RSDs was non-significant and therefore practically irrelevant. Furthermore, the obtained results still met the requirements of the Ph. Eur. monograph 2.9.40. "Uniformity of dosage units".
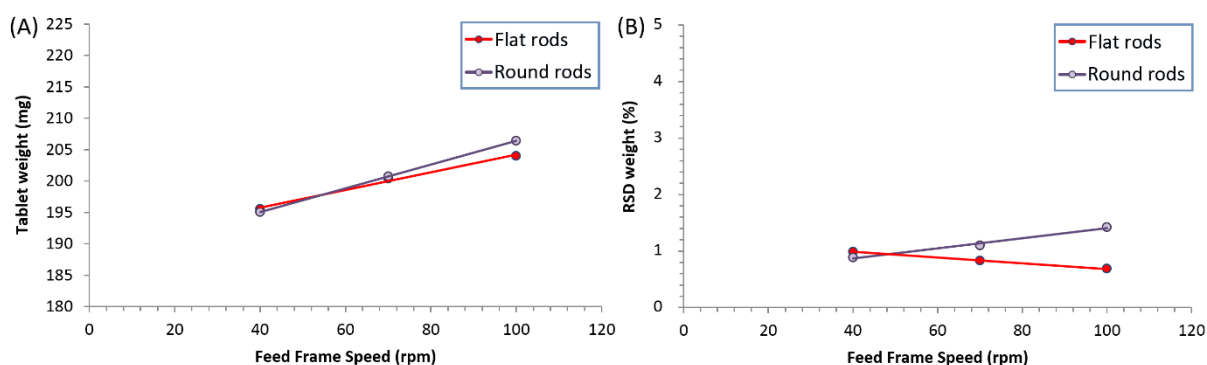

Fig. 48: Effect of the filling wheel with round rods on (A) the tablet weight and (B) the RSD in comparison to the filling wheel with flat rods.

4.3.3. Influence of the gap size between FOM and die disc on the powder behaviour

The E_t profiles of the two gap size configurations at a rotational feed frame speed of 40 rpm, 70 rpm, and 100 rpm and a rotational die disc speed of 36 rpm (64,800 tablets/h), respectively, are shown in Fig. 49. The two E_t versus time profiles of the respective gap size configurations have similar shapes. However, considering the last section of the profiles, differences were identified. The E_t profiles of the 25 mm gap size configuration (Fig. 49, red lines) end earlier than those of the 11 mm gap size configuration (Fig. 49, blue lines).
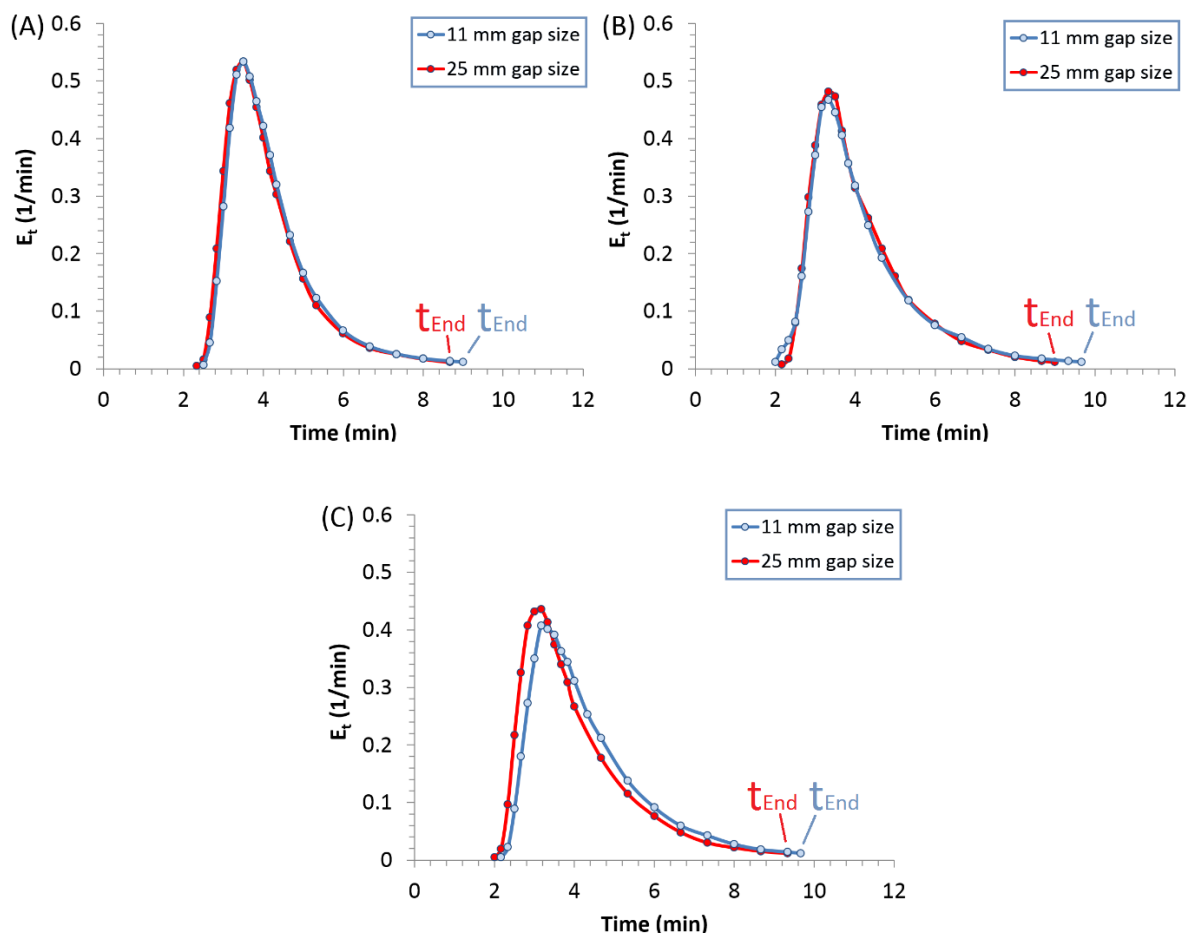

Fig. 49: E_t versus time profiles of the 25 mm gap size and the 11 mm gap size configuration at three rotational feed frame speeds: (A) 40rpm; (B) 70 rpm; (C) 100 rpm.

The τ values confirmed the observations from the E_t versus time profiles (Fig. 50A). The 11 mm gap size slightly increased the residence time of the powder particles in the FOM, which was confirmed by an increased τ. With regard to the σ^2 values, it is obvious that the 11 mm gap size configuration led to slightly higher σ^2 values in comparison to the 25 mm gap size configuration (Fig. 50B). Furthermore, the σ^2 values increased with increasing rotational feed frame speed. Thus, an increase in σ^2 corresponds to a higher intermixing of the powder whitin the FOM as well as to a higher mechanical strain and particle attrition [25]. These differences in τ and σ^2 may be explained by the differences in the flow rate of the powder through the FOM. The flow rate was influenced by the tablet production output and by the tablet weight, respectively. If the tracer blend flows faster through the FOM because of a higher flow rate, then the τ value is decrease. The tablet weights and their standard deviation (SD) are shown in Fig. 50C. The tablet weights obtained with the 11 mm gap size configuration were significantly lower and the SDs was increased by application of the 11 mm gap size than those obtained with the 25 mm gap size. Nevertheless, under consideration of the standard deviation, the examined tablets met the requirements of the Ph. Eur. monograph 2.9.40 "Uniformity of dosage units". Furthermore, the tablet weights increased with increasing rotational feed frame speed. These results are similar to those by Mendez et al. [26]. So far, it might be assumed that the filling of the dies was not uniform because of the selection of a too small gap size for a die with a diameter of 8 mm. In case of problems with the standard deviation of the tablet weights, an increase of the gap size may improve the uniformity of the tablet weights.
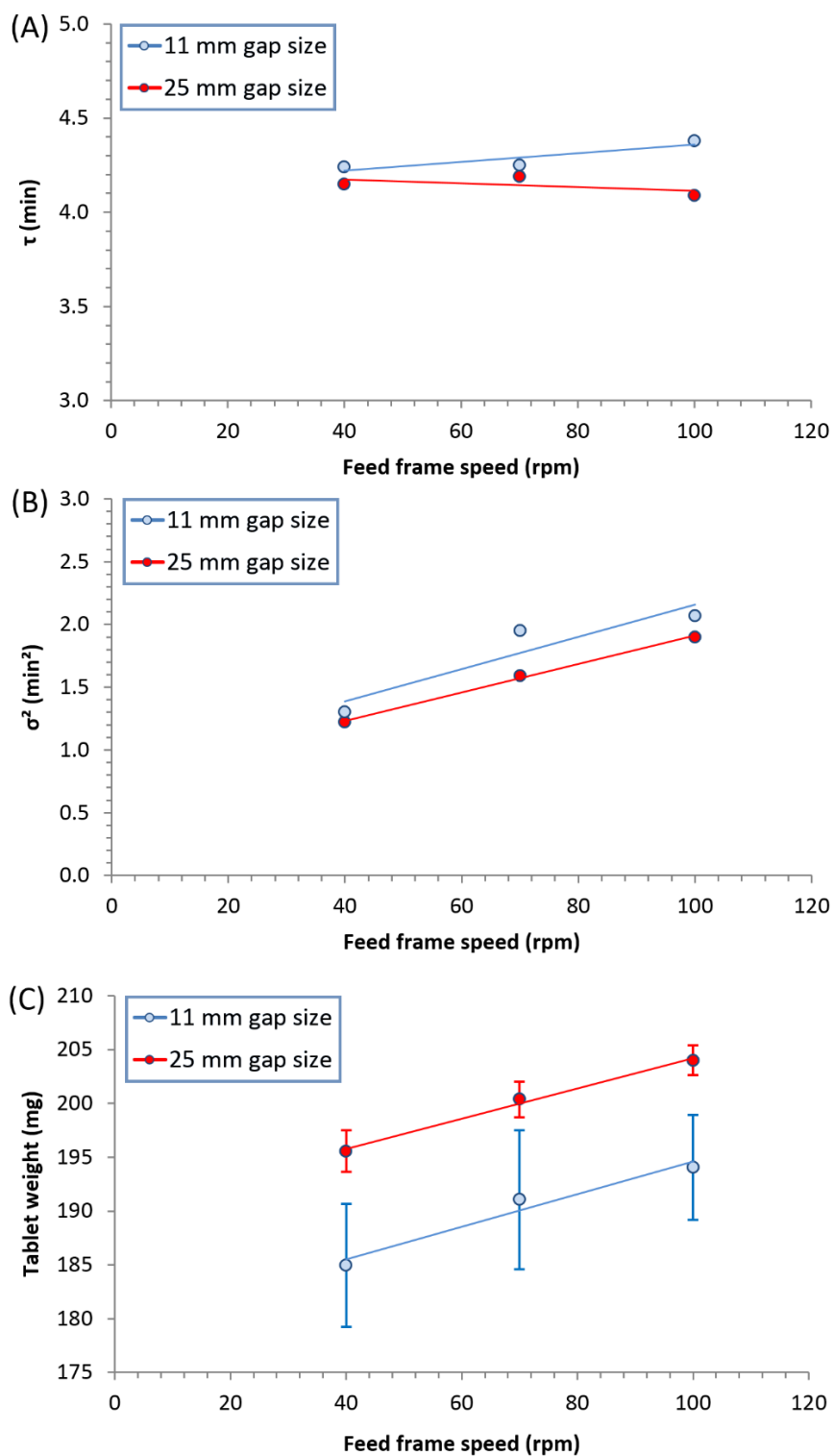
Fig. 50: Effect of the 11 mm gap size configuration on (A) τ, (B) σ², and (C) tablet weight (means, n = 10) with its SD in comparison to the 25 mm gap size configuration.

4.3.4. Conclusion

The aim of this study was to investigate the influence of various Fill-O-Matic (FOM) components on the powder behaviour and E_t. The effect of the volume reduction with a perspex disc, the rod shape of the filling wheel, and the gap size between the FOM and the die disc on the E_t in the FOM were investigated.

An interesting effect of the volume reduction with a perspex disc on the E_t was found. The data from the E_t versus time profile as well as the mean residence time and the mean centered variance showed that the volume reduction has a high influence on the powder residence time. A reduction of the FOM volume with a perspex disc resulted in a shorter residence time as well as in less intermixing of the powder particles in the FOM. It has to be mentioned that the FOM configuration with the perspex disc was only investigated for scientific purposes because the dosing chamber with its dosing wheel is an essential component of the FOM and is of particular importance for the manufacturing of tablets.

The influence on the E_t of the two filling wheel shapes showed that the round rod filling wheel led to similar E_t versus time profile shapes and a slight increase of the mean residence time of the tracer blend particles in the Fill-O-Matic. Interestingly, the round rods of the filling wheel led to a pronounced increase of the mean centered variance. This observation may be explained by the high intermixing of the powder particles caused by the round rod filling wheel. With regard to continuous manufacturing, a low intermixing of the powder particles in the feed frame is preferred. Remarkably, the two different filling wheel designs had no influence on the tablet weights and their relative standard deviation.

It was found that the 11 mm gap size between the FOM and the die disc had an only minor effect on the residence time distribution. Moreover, it was found that the 11 mm

gap size in combination with a die diameter of 8 mm led to a significant decrease of the tablet weights. Nevertheless, the results from the "uniformity of mass" met the requirements of the Ph. Eur. monograph 2.9.40. "Uniformity of dosage units". In view of the manufacturing of tablets, an increase of the gap size between the FOM and the die disc may improve the uniformity of the tablet weights.

4.4.   Influence of the feed frame designs on the FE55

4.4.1.   *Comparison of feed frame systems with different filling volume and the same feed frame design*

The effect of the filling volume of the three-chamber Fill-O-Matic (FOM) on the residence time distribution E_t, the mean residence time τ, and the mean centered variance σ^2 were investigated in this subchapter. The E_t versus time profiles of the standard FOM (Std FOM) configuration as well as of the modified FOM configuration with the reduced volume (Mod FOM) at a tablet output of 65,000 tablets/h and at a rotational feed frame speed of 70 rpm, representative for all three rotational feed frame speeds, is shown in Fig. 51A. It is evident, that the Mod FOM with its large hub wheels led to a narrower E_t versus time profile than the Std FOM. Both, the later start of the E_t versus time profile of the Mod FOM configuration as well as the earlier end of the profile led to a decrease of the residence time of the tracer blend. However, the τ values of both configurations at the three different rotational feed frame speeds (40 rpm, 70 rpm, and 100 rpm) were similar (Fig. 51B). Under these tableting conditions, the powder flow in the feed frame was about 13 kg/h, resulting from the tablet weight of 200 mg multiplied by the tablet output/h of 65,000. In a previous chapter, it was shown that τ depends on the powder flow rate through the FOM and that τ is independent of the feed frame speed. From these results, it may be concluded that the FOMs with identical feed frame design but different filling volume have no influence on τ, because the powder path through the feed frame of the Std FOM and Mod FOM is identical.
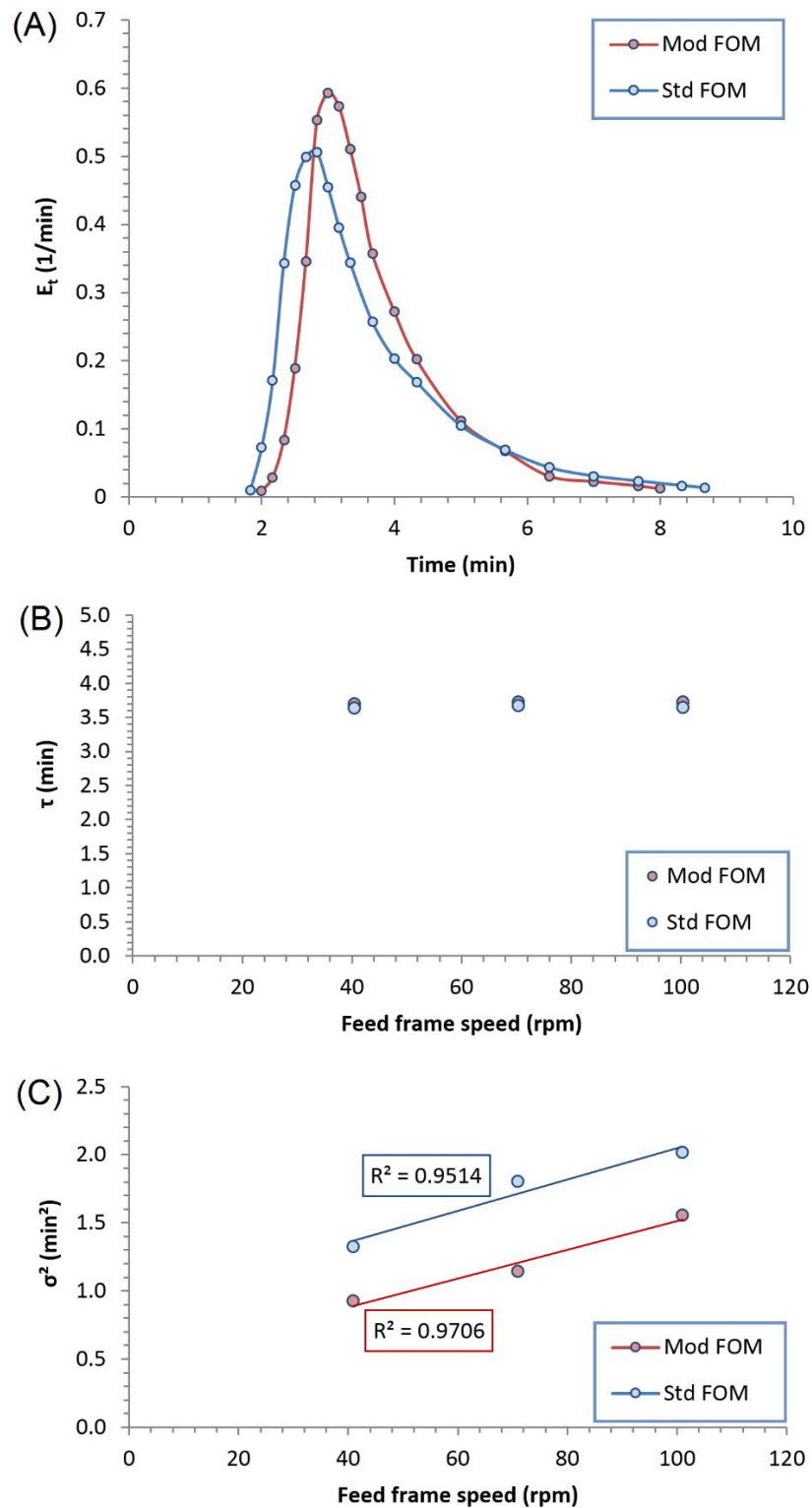
Fig. 51: Effect of the two different FOM configurations on the E_t characteristics. (A) E_t versus time profiles of the Mod FOM and the Std FOM at a rotational feed frame speed of 70 rpm. (B) τ values and (C) σ^2 values of the E_t versus time profiles of all three selected feed frame speeds.

Furthermore, this result might be explained by the intermixing of the MCC blend and the tracer blend in the feed frame chambers. At the beginning of the tableting runs, the Mod FOM contained a lower amount of MCC blend in the feed frame chambers than the Std FOM. During the tableting process, the tracer blend following the MCC blend flowed from the feed pipe into the Mod FOM and thus the tracer blend particles were mixed with a lower amount of MCC blend. The different intermixing behaviour of the powder blends within the two FOM configurations was confirmed by the σ^2 values (Fig. 51C). It is obvious, that the lower filling volume of the Mod FOM led to a decreased intermixing of the powder blends, which is indicated by the lower σ^2 values. Interestingly, if the σ^2 values of the two configurations are compared, it is noticeable, that the corresponding regression lines of the respective σ^2 values have a similar slope.

The E_t versus time profiles of all three tablet outputs/h (65,000, 95,000, and 125,000 tablets/h) are shown in Fig. 52. The narrowest E_t versus time profile was observed at 125,000 tablets/h followed by 95,000 tablets/h and 65,000 tablets/h. Furthermore, the use of the Mod FOM led to an increase of the maximum of the E_t versus time profile.
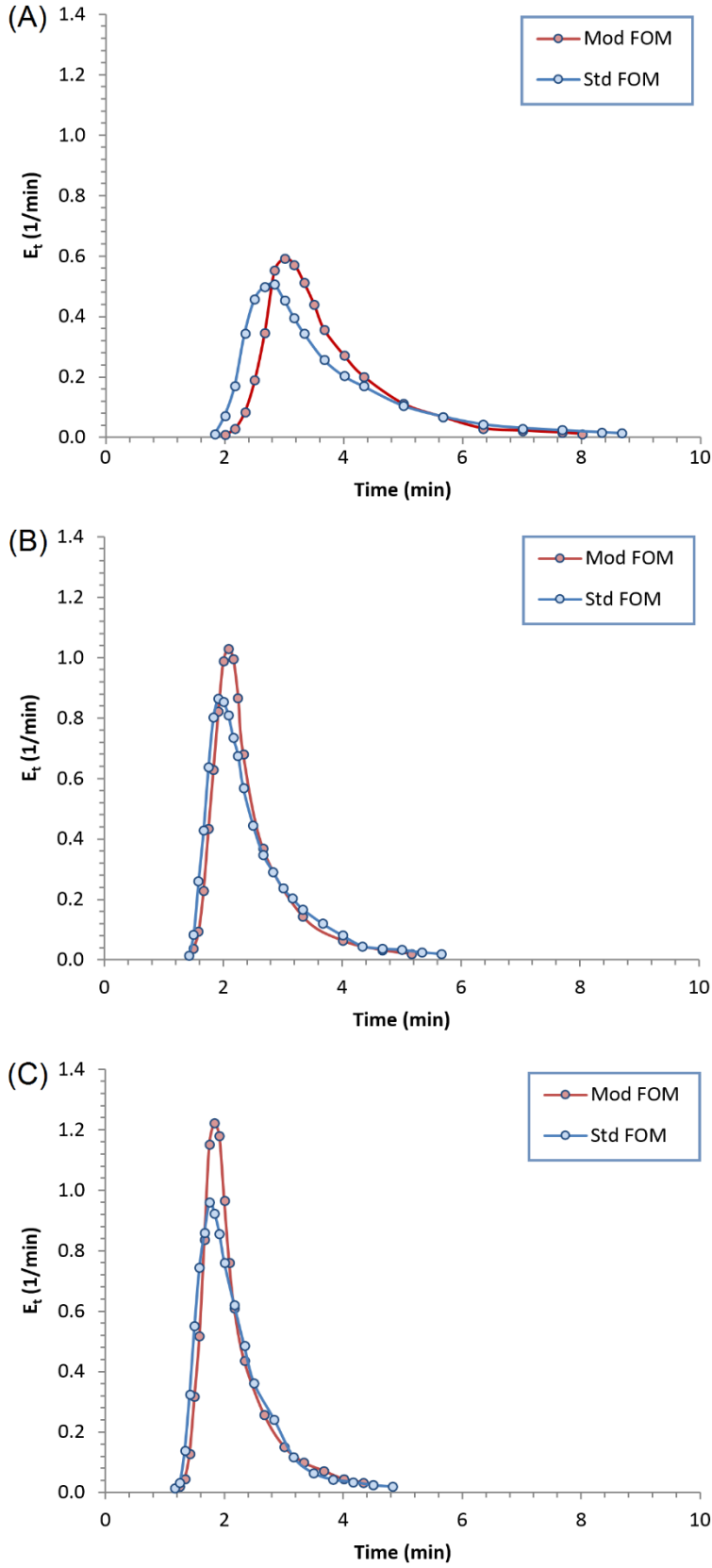
Fig. 52: E_t versus time profiles of the two different FOM configurations at different tablet outputs/h: (A) 65,000 tablets/h, (B) 95,000 tablets/h, and (C) 125,000 tablets/h.

To understand these E_t versus time profiles, the τ values and the σ² values were plotted versus the tablet output/h in Fig. 53. It is obvious, that the τ values decreased with increasing the tablet output/h (Fig. 53A). As a result, the residence time of the powder particles of the respective blend in the feed frame decreased with increasing tablet output/h. However, there was no difference between the τ values of the two FOM configurations at the respective tablet output/h because the Mod FOM with its high maximum and narrow width of the E_t versus time profile and the Std FOM with its low maximum and broad width of the E_t versus time profile led to similar τ values.
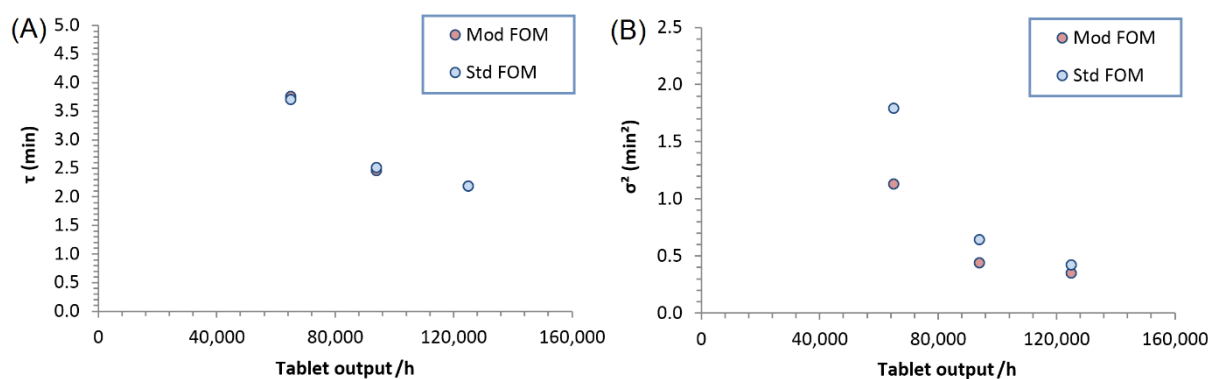

Fig. 53: Influence of the two different FOM configurations at different tablet outputs/h on (A) τ and (B) σ².

The intermixing of the powder blends within the Std FOM and the Mod FOM, respectively, is described by the σ² values, which are shown in Fig. 53B. It is evident, that the Mod FOM led to lower σ² values. This result might be explained by the different amount of powder in the FOM. Remarkably, with increasing tablet output, the difference between the σ² values was diminished, because the particles of the powder blend flowed quickly through the FOM and therefore the intermixing of these particles was decreased.

The effect of the two different FOM configurations on E_t with regard to the amount of tracer blend was also investigated. The E_t versus time profiles of the three different amounts of tracer blend at a tablet output/h of 65,000 are shown in Fig. 54. It is evident, that with increasing amount of tracer blend the maximum of the E_t versus time profiles decreases. Furthermore, the E_t versus time profiles broadened with higher amounts of tracer blend. With the Mod FOM configuration, the later start and the earlier end of the E_t versus time profile as well as the higher maximum in comparison to the Std FOM configuration, indicated a decrease of the powder residence time within the Mod FOM. However, with increasing the amount of tracer blend, the difference between the maxima of the E_t versus time profiles decreased (Fig. 54). Increasing amounts of tracer blend led to an increased residence time with increased τ values (Fig. 55A). From the results of the σ^2 values at different amounts of tracer blends, it was observed that they were lower with the Mod FOM configuration (Fig. 55B). Remarkably, the decrease of the FOM volume led to a similar slope of the respective σ^2 values. This investigation of different feed frame volumes was intended to provide a more comprehensive process understanding of the influence of the feed frame volume on the E_t versus time profiles. It is obvious, that the different feed frame volumes had a pronounced effect on the intermixing of the powder particles, indicated by the respective σ^2 values. During continuous manufacturing of tablets, it is preferred to have a low shear stress applied to the powder particles, because a high shear stress may affect the properties of the powder, such as powder attrition and particle breakage. With this knowledge of the powder behaviour within the Std FOM and Mod FOM, it is possible to reduce the powder intermixing as well as to minimize the powder shear stress in the feed frame and thus to improve the quality of the resulting tablets.
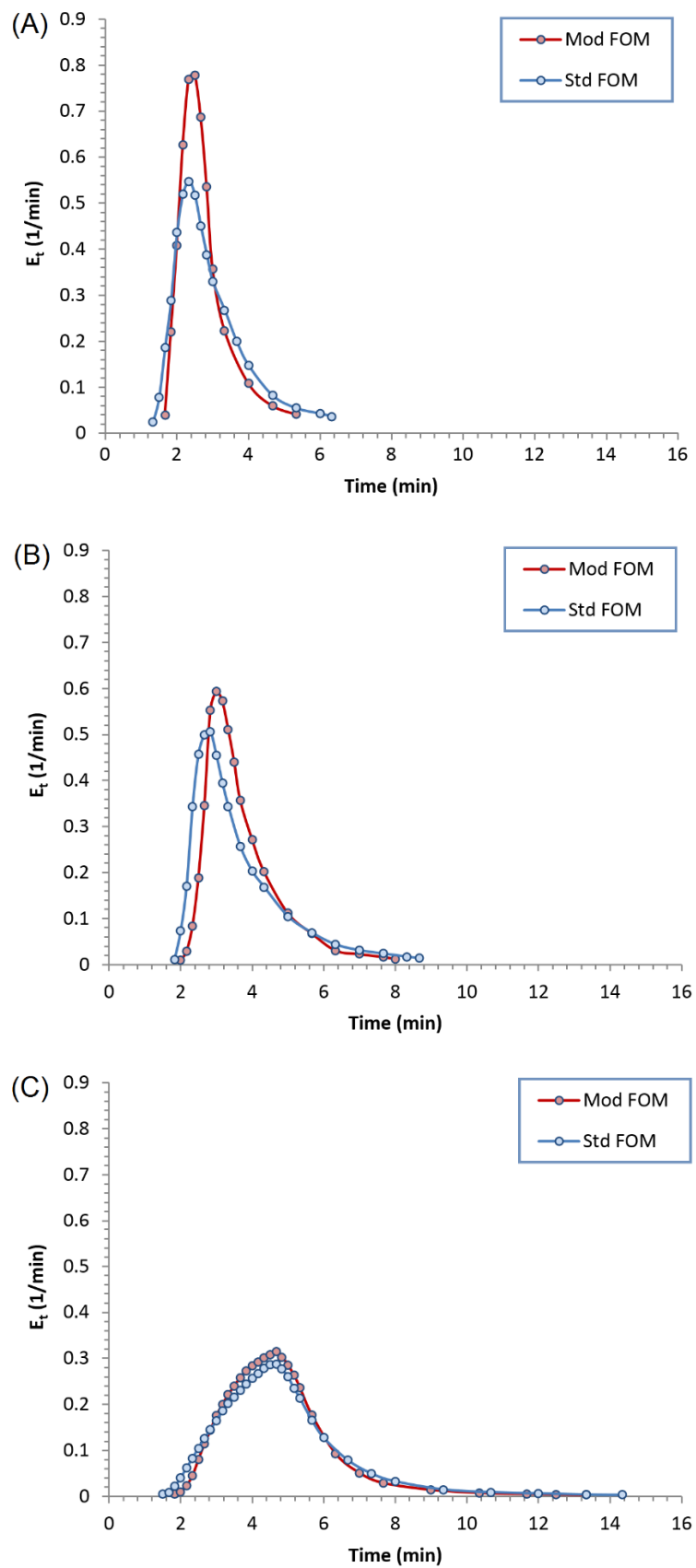
Fig. 54: E_t versus time profiles depending on the amount of tracer blend of (A) 40 g, (B) 160 g, and (C) 640 g at a tablet output/h of 65,000.
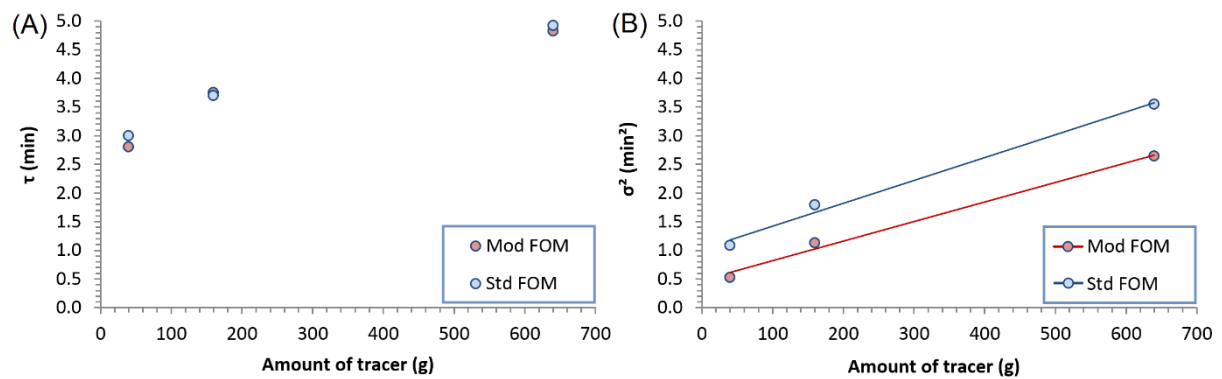
Fig. 55: Influence of the feed frame volume at different amounts of tracer blend on (A) τ and (B) σ².

4.4.2. Comparison of feed frame systems with the same filling volume and different feed frame designs

The effect of the single-chamber filling cone and the three-chamber FOM on E_t, τ, and σ² was investigated in this subchapter. In Fig. 56A, the E_t versus time profiles of the two feed frame designs at three different feed frame speeds are shown. It is obvious, that the filling cone with its single chamber led to a narrower E_t versus time profile than the Std FOM. The profiles of the Std FOM start earlier and end later than the profiles of the filling cone. Furthermore, the maxima of the E_t versus time profiles of the filling cone were almost twice as high as the maxima of the Std FOM profiles. The higher the maximum of the E_t versus time profile the more particles of the powder blend leave the feed frame at this time point. According to these results, the filling cone led to a decrease of the powder residence time in the feed frame system. Furthermore, the narrow E_t versus time profiles of the filling cone indicated a lower intermixing of the powder blends in the feed frame system.
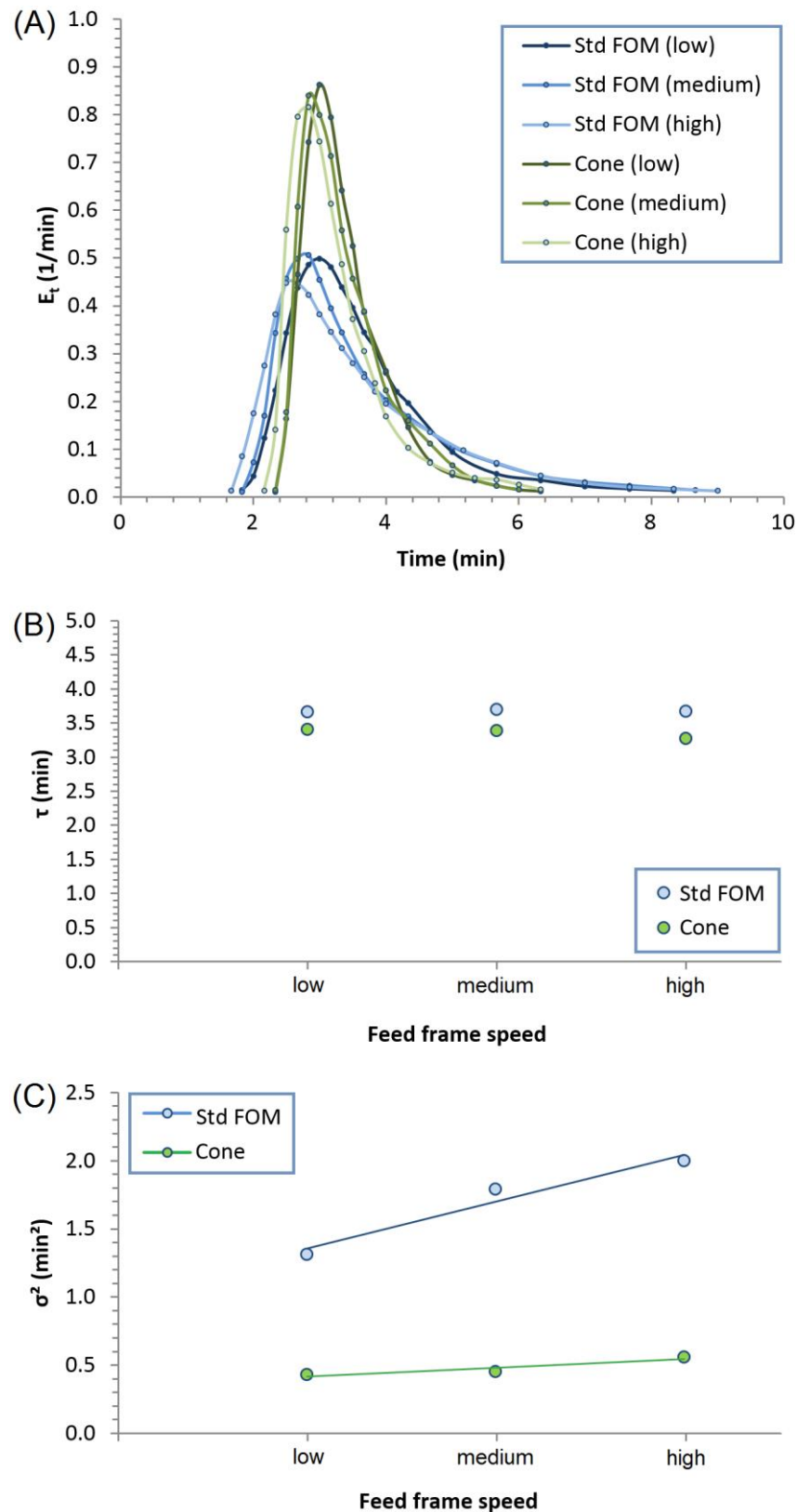
Fig. 56: Effect of the two feed frame designs on the E_t characteristics. (A) E_t versus time profiles of the filling cone and the Std FOM at different rotational feed frame speeds with (B) τ and (C) σ².

In Fig. 56B, the τ values of the two feed frame systems at three feed frame speeds and a tablet output/h of 65,000 are shown. It is evident, that the filling cone led to a decrease in τ, because of the direct powder flow through the single chamber into the dies. The difference in degree of intermixing of the powder blends in the two feed frame designs was indicated by the σ² values (Fig. 56C). The pronounced increase of the σ² values of the Std FOM in comparison to the low increase of the σ² values of the filling cone can be explained by the different powder paths through the feed frame systems. Two theoretically ideal models of chemical reactors with different intermixing and different residence time distributions of the tracer particles were described by [78]. The model of the plug flow reactor (PFR) based on the assumption that all tracer particles move in axial direction without any intermixing. Thus, all particles which enter the PFR at the time point t = 0, will leave the operation unit at a time point t > 0. In contrast, the model of the continuous flow stirred tank reactor (CSTR) describes a homogeneous intermixing of all tracer particles in the reactor because the continuously added particles are mixed with the particles already present in the CSTR. Based on the assumption, that the volume of the PFR and the CSTR are similar, the powder flow through the respective models leads to similar τ values. In contrast, the different intermixing of the particles in the models leads to different σ² values. If comparing the powder flow through the different feed frame systems with the two ideal models, similarities are obvious. The tracer particles in the filling cone with its single chamber were subject to low intermixing, because of its direct powder flow through the filling cone is comparable to that of the PFR. In contrast, the tracer particles in the Std FOM were subject to high intermixing, because of its three chambers and feed frame wheels.
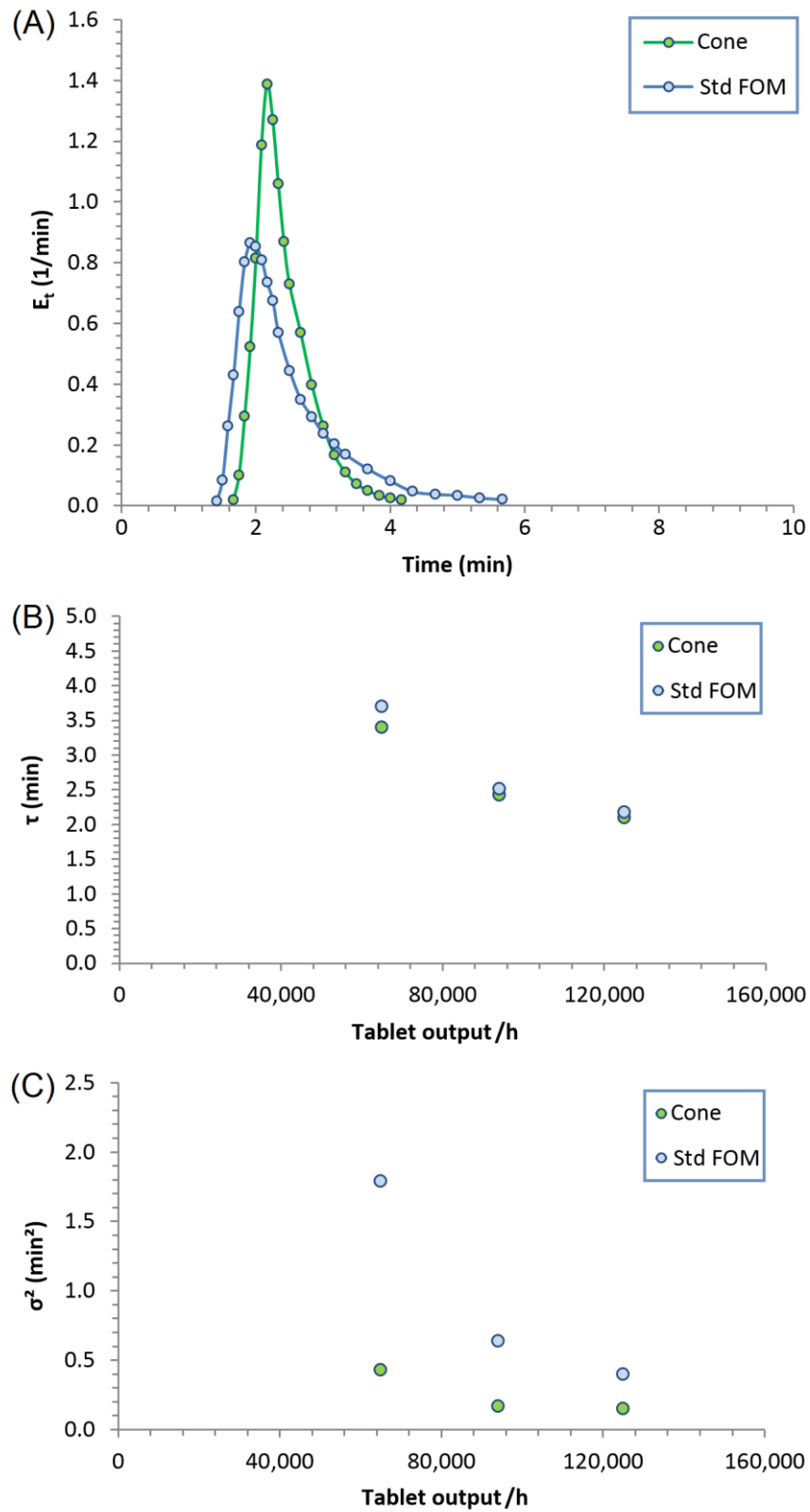
Fig. 57: Effect of the two feed frame designs on the E_t characteristics. (A) E_t versus time profiles of the filling cone and the Std FOM at different tablet outputs with (B) τ and (C) σ^2.

The influence of the two different feed frame designs at a tablet output of 95,000 tablets/h, representative for all three tablet outputs/h, on E_t is shown in Fig. 57A. It is obvious, that the E_t versus time profile of the filling cone was narrower and showed a higher maximum than the profile of the Std FOM. As a result, the powder residence time within the filling cone was reduced, also indicated by the low т and the σ^2 values (Fig. 57B and C). However, the differences between the т and the σ^2 values of the two feed frame designs at higher tablet outputs/h decreased, because the fast powder flow through the feed frame designs at higher tablet outputs/h reduced the intermixing of the powder particles within the feed frame designs and thus the powder particles were more quickly processed. To investigate the effect of the two feed frame designs on powder behaviour, the three amounts of tracer blend were used again. The concentration versus time profiles of the three amounts of tracer blend are displayed in Fig. 58. It is obvious, that the filling cone led to a narrower distribution of the tracer blend residence time. Interestingly, the maximum of the concentration versus time profile of the filling cone at an amount of tracer blend of 640 g almost reach 100 %, which means that the filling cone was almost filled completely with the tracer blend (Fig. 58A). In contrast, the maximum of the concentration versus time profile of the Std FOM at the same amount of tracer blend only reached about 85 % (Fig. 58B).
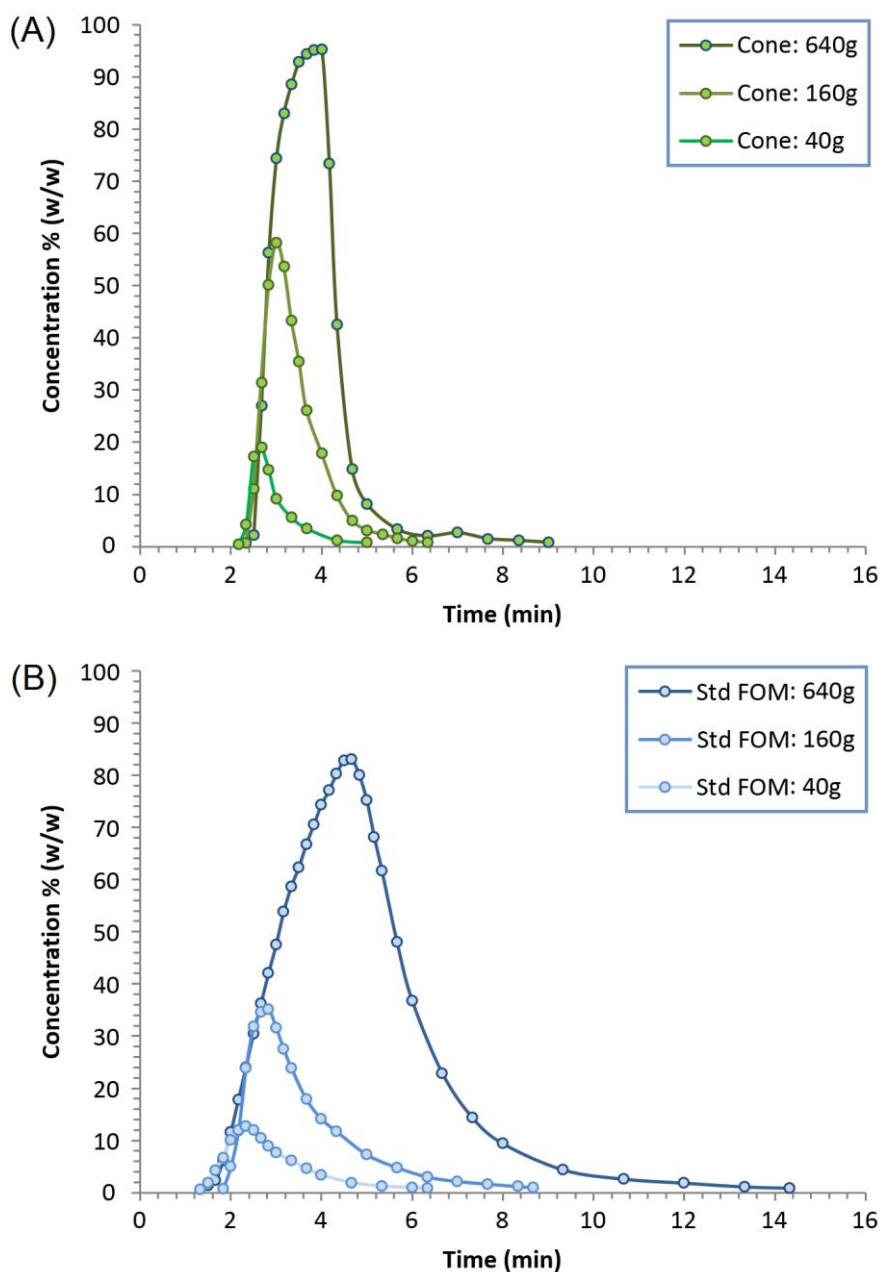
Fig. 58: Concentration versus time profiles depending on the amount of tracer blend at a tablet output/h of 65,000.

To fill the Std FOM completely with the tracer blend to 100 %, an amount of about 1,600 g is necessary, as shown in a previous chapter (see chapter 4.2.1). These results can be explained by an improved powder removal out of the filling cone, because of its single-chamber design. This powder flow through the filling cone is

similar to that of the ideal PFR model. During the tableting run, the powder particles within the filling cone were pushed out of the feed frame by the powder particles from the feed pipe. In contrast, the powder particles within the Std FOM were subject to a high intermixing because of the three chambers and feed frame wheels. The τ values and the σ² values confirmed the excellent powder removal out of the filling cone (Fig. 59).
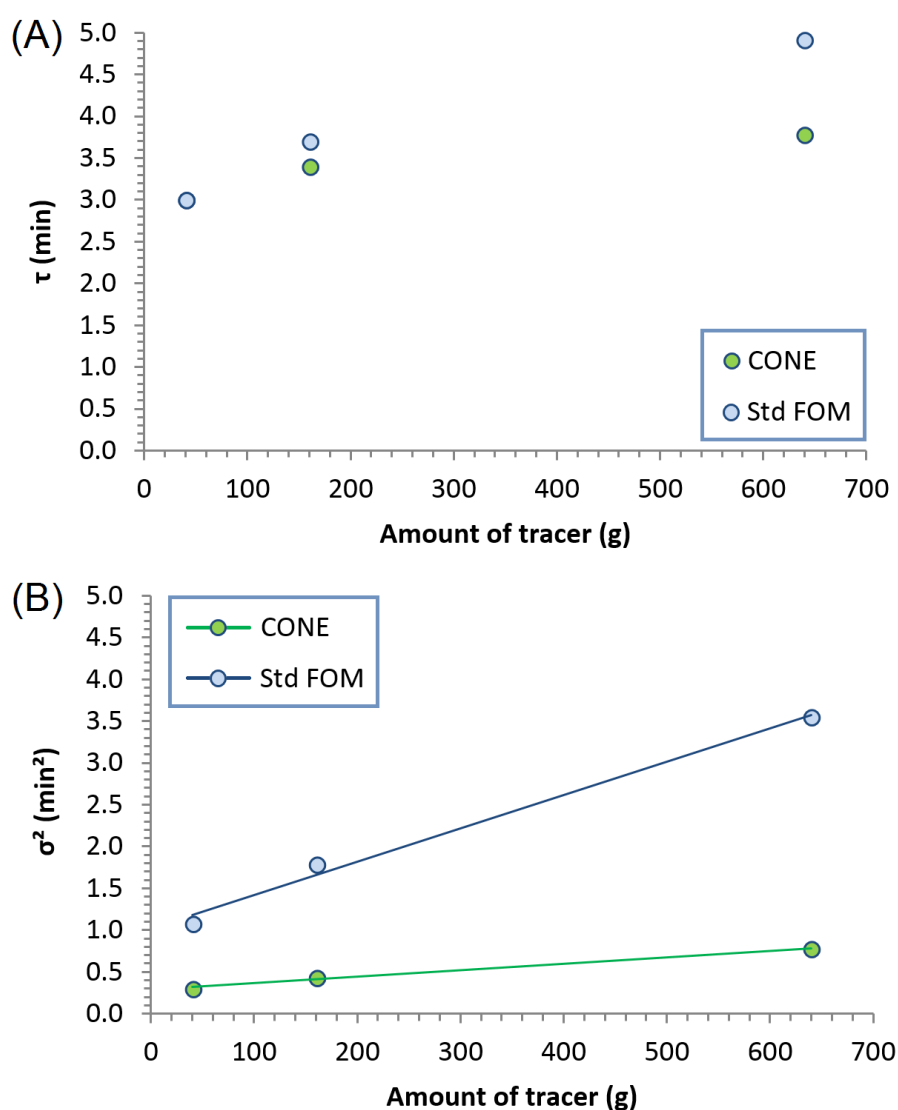

Fig. 59: Influence of the feed frame designs at different amounts of tracer blend on (A) τ and (B) σ².

4.4.3. Conclusion

In this study the effect of the filling volume of the Fill-O-Matic (FOM) as well as the influence of two different feed frame designs of a production-scale rotary tablet press on E_t was investigated. It was found, that a reduction of the FOM volume had a pronounced effect on the powder behaviour and the powder residence time within the FOM, indicated by a narrow E_t versus time profile. The mean residence time τ was not affected by a change of the FOM volume, while the mean centered variance $σ^2$ and therefore the intermixing of the powder blends in the feed frame were clearly affected. Interestingly, if the $σ^2$ values of the two FOM volumes, investigated at different feed frame speeds and amounts of tracer blend, were compared, it was noticeable that the corresponding regression lines had the same slope. These results on the residence time distribution in the feed frames are particularly interesting for the continuous manufacturing of tablets, where the operation units are arranged one after the other and a narrow E_t versus time profile is preferable in which all powder particles remain in the operation unit approximately for about the same time. This information on the residence time distribution is of interest in continuous manufacturing for material traceability, development of predictive models, and the influence of different feed frame designs on the powder flow rate through the respective feed frame. Therefore, the exchange of the standard wheels by the modified large hub wheels is a simple measure to reduce the residence time distribution and intermixing of the powder particles within the FOM, because a long residences time may lead to a higher shear stress in the powder, which possibly leading to a decline in tablet quality.

From the results obtained with the different feed frame designs, the filling cone with its single chamber had a more pronounced effect on the residence time of the

powder blends within the feed frame. The data showed that the filling cone led to a decrease of the residence time of the powder blends as well as of the τ and the σ^2 values. Remarkably, comparing the two concentration versus time profiles of the filling cone and the Std FOM at different amounts of tracer blend, an improved powder removal out of the filling cone was observed. This result might be explained by the direct powder flow through the single chamber to the die disc, whereas the powder particles within the three chambers of the Std FOM were subject to a high intermixing between the three chambers. The results indicated that both the filling volume of the feed frame as well as the feed frame design had an influence on the powder residence time.

With regard to the continuous manufacturing, a narrow residence time distribution as well as a low intermixing of the powder particles in the feed frame is preferred, because the run time of the operation units in the continuous manufacturing of tablets is much longer than the run time during batch manufacturing. For this reason, the selection of the feed frame system is of particular importance for the continuous manufacturing of tablets to decrease the residence time as well as the intermixing of the powder particles in the feed frame and to improve the quality of the tablets

5. References

[1] W. Brockedon, Shaping pills, lozenges, and black lead by pressure in dies, 1843.

[2] M. Çelik, The past, present, and future of tableting technology, Drug Dev. Ind.
     Pharm. 22 (2008) 1–10.

[3] M. Jivraj, L.G. Martini, C.M. Thomson, An overview of the different excipients
     useful for the direct compression of tablets, Pharm. Sci. Technol. To. 3 (2000)
     58–63.

[4] S.V. Sastry, J.R. Nyshadham, J.A. Fix, Recent technological advances in oral
     drug delivery – a review, Pharm. Sci. Technol. To. 3 (2000) 138–145.

[5] J. Swarbrick, J.C. Boylan, Encyclopaedia of pharmaceutical technology, Org.
     Process Res. Dev. 7 (2003) 609–610.

[6] W.A. Ritschel, A. Bauer-Brandl, Die Tablette: Handbuch der Entwicklung,
     Herstellung und Qualitätssicherung, 2nd ed., ECV - Editio-Cantor-Verl.,
     Aulendorf, 2002.

[7] N. Ahmat, H. Ugail, G.G. Castro, Method of modelling the compaction behaviour
     of cylindrical pharmaceutical tablets, Int. J. Pharm. 405 (2011) 113–121.

[8] S.S. Bharate, S.B. Bharate, A.N. Bajaj, Incompatibilies of pharmaceutical
     excipients with active pharmaceutical ingredients: a comprehensive review, J.
     Excip. Food Chem. 5 (2014) 152–160.

[9] C. Ferrero, N. Muñoz, M.V. Velasco, A. Muñoz-Ruiz, R. Jiménez-Castellanos,
     Disintegrating efficiency of croscarmellose sodium in a direct compression
     formulation, Int. J. Pharm. 147 (1997) 11–21.

[10] A.C. Shah, A.R. Mlodozeniec, Mechanism of surface lubrication: Influence of duration of lubricant-excipient mixing on processing characteristics of powders properties of compressed tablets, J. Pharm. Pharmaceut. Sci. 66 (1977) 1377–1382.

[11] S. Patel, A.K. Bansal, Prediction of mechanical properties of compacted binary mixtures containing high-dose poorly compressible drug, Int. J. Pharm. 403 (2011) 109–114.

[12] R.C. Rowe, Handbook of pharmaceutical excipients, 6th ed., Pharmaceutical Press, London, 2009.

[13] M. Šantl, I. Ilić, F. Vrečer, S. Baumgartner, A compressibility and compactibility study of real tableting mixtures: the impact of wet and dry granulation versus a direct tableting mixture, Int. J. Pharm. 414 (2011) 131–139.

[14] N.A. Armstrong, Direct compression characteristics of granulated Lactitol, Pharm. Technol. Eur. 9 (1997) 24–30.

[15] M.E. Aulton (Ed.), Pharmaceutics: the science of dosage form design, 1st ed., Livingstone, New York, 1988.

[16] M.G. Herting, P. Kleinebudde, Roll compaction/dry granulation: Effect of raw material particle size on granule and tablet properties, Int. J. Pharm. 338 (2007) 110–118.

[17] S. Inghelbrecht, J.P. Remon, Reducing dust and improving granule and tablet quality in the roller compaction process, Int. J. Pharm. 171 (1998) 195–206.

[18]   D. McCormick, Evolutions in direct compression, Pharm. Technol. 29 (2005) 52–62.

[19]   Y. Fujimoto, N. Hirai, T. Takatani-Nakase, K. Takahashi, Novel tablet formulation of amorphous indomethacin using wet granulation with a high-speed mixer granulator combined with porous calcium silicate, J. Drug. Deliv. Sci. Technol. 33 (2016) 51–57.

[20]   P. Kleinebudde, Roll compaction/dry granulation: pharmaceutical applications, Eur. J. Pharm. Biopharm. 58 (2004) 317–326.

[21]   M.C. Gohel, A review of co-processed directly compressible excipients, J. Pharm. Pharmaceut. Sci. 8 (2005) 76–93.

[22]   P.R. Watt, N.A. Armstrong, Tablet and capsule machine instrumentation, Pharmaceutical Press, London, 2008.

[23]   E.D. Liss, S.L. Conway, J.A. Zega, B.J. Glasser, Segregation of powders during gravity flow through vertical pipes, Pharm. Technol. 445 (2004) 78–96.

[24]   Prescott, James K., R.A. Barnum, On powder flowability, Pharm. Technol. 24 (2000) 60-86.

[25]   W.R. Ketterhagen, Simulation of powder flow in a lab-scale tablet press feed frame: effects of design and operating parameters on measures of tablet quality, Powder Technol. 275 (2015) 361–374.

[26]   R. Mendez, F. Muzzio, C. Velazquez, Study of the effects of feed frames on powder blend properties during the filling of tablet press dies, Powder Technol. 200 (2010) 105–116.

[27]   S. Jackson, I.C. Sinka, A.C.F. Cocks, The effect of suction during die fill on a
        rotary tablet press, Eur. J. Pharm. Biopharm. 65 (2007) 253–256.

[28]   C.-Y. Wu, L. Dihoru, A.C.F. Cocks, The flow of powder into simple and
        stepped dies, Powder Technol. 134 (2003) 24–39.

[29]   C.-Y. Wu, A.C.F. Cocks, Flow behavior of powders during die filling, Powder
        Metall. 47 (2013) 127–136.

[30]   M. Levin, Pharmaceutical process scale-up, 1st ed., Informa Healthcare,
        Hoboken, 2001.

[31]   C.K. Tye, C.C. Sun, G.E. Amidon, Evaluation of the effects of tableting speed
        on the relationships between compaction pressure, tablet tensile strength, and
        tablet solid fraction, J. Pharm. Sci. 94 (2005) 465–472.

[32]   H. Leuenberger, The compressibility and compactibility of powder systems,
        Int. J. Pharm. 12 (1982) 41–55.

[33]   J.M. Sonnergaard, Quantification of the compactibility of pharmaceutical
        powders, Eur. J. Pharm. Biopharm. 63 (2006) 270–277.

[34]   Fette Compacting, FE75: The new standard for the production of large
        batches, 2019. http://www.fette-compacting-america.com/tablet-press-fe75/.
        Accessed 11 January 2019.

[35]   M.C. Monedero, M.R. Jiménez-Castellanos, M.V. Velasco, A. Muñoz-Ruiz,
        Effect of compression speed and pressure on the physical characteristics of
        maltodextrin tablets, Drug Dev. Ind. Pharm. 24 (1998) 613–621.

[36]   I.C. Sinka, F. Motazedian, A.C.F. Cocks, K.G. Pitt, The effect of processing

       parameters on pharmaceutical tablet properties, Powder Technol. 189 (2009)

       276–284.

[37]   M. Celik, Pharmaceutical powder compaction technology, 2nd ed., Informa

       Healthcare, London, New York, 2011.

[38]   W.R. Vezin, H.M. Pang, K.A. Khan, S. Malkowska, The effect of

       precompression in a rotary machine on tablet strength, Drug Dev. Ind. Pharm.

       9 (2008) 1465–1474.

[39]   A.V. Potapov, C.S. Campbell, Computer simulation of shear-induced particle

       attrition, Powder Technol. 94 (1997) 109–122.

[40]   L.A. Mills, I.C. Sinka, Effect of particle size and density on the die fill of

       powders, Eur. J. Pharm. Biopharm. 84 (2013) 642–652.

[41]   P.R. Watt, Tablet machine instrumentation in pharmaceutics: Principles and

       practice, Ellis Horwood, Chichester, 1988.

[42]   W. Engisch, F. Muzzio, Using residence time distributions (RTDs) to address

       the traceability of raw materials in continuous pharmaceutical manufacturing,

       J. Pharm. Innov. 11 (2016) 64–81.

[43]   S.L. Lee, T.F. O'Connor, X. Yang, C.N. Cruz, S. Chatterjee, R.D. Madurawe,

       C.M.V. Moore, L.X. Yu, J. Woodcock, Modernizing pharmaceutical

       manufacturing: from batch to continuous production, J. Pharm. Innov. 10

       (2015) 191–199.

[44]   R. Singh, F. Boukouvala, E. Jayjock, R. Ramachandran, M. Ierapetritou, Flexible multipurpose continuous processing of pharmaceutical tablet manufacturing process, Pharm. Process. Mag. 27 (2012) 22–30.

[45]   T. Wright, Solid dosage manufacturing trends, 2015. http://www.contractpharma.com/issues/2015-03-01/view_features/solid-dosage-manufacturing-trends--724749. Accessed 27 October 2017.

[46]   M. Ierapetritou, F. Muzzio, G. Reklaitis, Perspectives on the continuous manufacturing of powder-based pharmaceutical processes, AIChE J. 62 (2016) 1846–1862.

[47]   M.A. Järvinen, J. Paaso, M. Paavola, K. Leiviskä, Continuous direct tablet compression: Effects of impeller rotation rate, total feed rate and drug content on the tablet properties and drug release, Drug Dev. Ind. Pharm. 39 (2013) 1802–1808.

[48]   S. Mascia, P.L. Heider, H. Zhang, R. Lakerveld, B. Benyahia, P.I. Barton, R.D. Braatz, C.L. Cooney, J.M.B. Evans, T.F. Jamison, K.F. Jensen, A.S. Myerson, B.L. Trout, End-to-end continuous manufacturing of pharmaceuticals: integrated synthesis, purification, and final dosage formation, Angew. Chem. Int. Ed. Engl. 52 (2013) 12359–12363.

[49]   S.D. Schaber, D.I. Gerogiorgis, R. Ramachandran, J.M.B. Evans, P.I. Barton, B.L. Trout, Economic analysis of integrated continuous and batch pharmaceutical manufacturing: a case study, Ind. Eng. Chem. Res. 50 (2011) 10083–10092.

[50] F. Boukouvala, V. Niotis, R. Ramachandran, F.J. Muzzio, M.G. Ierapetritou, An integrated approach for dynamic flowsheet modeling and sensitivity analysis of a continuous tablet manufacturing process, Comput. Chem. Eng. 42 (2012) 30–47.

[51] A.E. Cervera-Padrell, T. Skovby, S. Kiil, R. Gani, K.V. Gernaey, Active pharmaceutical ingredient (API) production involving continuous processes - a process system engineering (PSE)-assisted design framework, Eur. J. Pharm. Biopharm. 82 (2012) 437–456.

[52] W.E. Engisch, F.J. Muzzio, Feedrate deviations caused by hopper refill of loss-in-weight feeders, Powder Technol. 283 (2015) 389–400.

[53] G. Tian, S.L. Lee, X. Yang, M.S. Hong, Z. Gu, S. Li, R. Fisher, T.F. O'Connor, A dimensionless analysis of residence time distributions for continuous powder mixing, Powder Technol. 315 (2017) 332–338.

[54] T. Ervasti, S.-P. Simonaho, J. Ketolainen, P. Forsberg, Continuous manufacturing of extended release tablets via powder mixing and direct compression, Int. J. Pharm. 495 (2015) 290–301.

[55] G. Allison, Y.T. Cain, C. Cooney, T. Garcia, T.G. Bizjak, O. Holte, N. Jagota, B. Komas, E. Korakianiti, D. Kourti, R. Madurawe, E. Morefield, F. Montgomery, M. Nasr, W. Randolph, J.-L. Robert, D. Rudd, D. Zezza, Regulatory and quality considerations for continuous manufacturing, J. Pharm. Sci. 104 (2015) 803–812.

[56]   J. Vercruysse, U. Delaet, I. van Assche, P. Cappuyns, F. Arata, G. Caporicci, T. de Beer, J.P. Remon, C. Vervaet, Stability and repeatability of a continuous twin screw granulation and drying system, Eur. J. Pharm. Biopharm. 85 (2013) 1031–1038.

[57]   J.S. Srai, C. Badman, M. Krumme, M. Futran, C. Johnston, Future supply chains enabled by continuous processing, J. Pharm. Sci. 104 (2015) 840–849.

[58]   H. Leuenberger, New trends in the production of pharmaceutical granules: batch versus continuous processing, Eur. J. Pharm. Biopharm. 52 (2001) 289–296.

[59]   S.-P. Simonaho, J. Ketolainen, T. Ervasti, M. Toiviainen, O. Korhonen, Continuous manufacturing of tablets with PROMIS-line - Introduction and case studies from continuous feeding, blending and tableting, Eur. J. Pharm. Sci. 90 (2016) 38–46.

[60]   L.X. Yu, G. Amidon, M.A. Khan, S.W. Hoag, J. Polli, G.K. Raju, J. Woodcock, Understanding pharmaceutical quality by design, AAPS j. 16 (2014) 771–783.

[61]   S. Byrn, M. Futran, H. Thomas, E. Jayjock, N. Maron, R.F. Meyer, A.S. Myerson, M.P. Thien, B.L. Trout, Achieving continuous manufacturing for final dosage formation: challenges and how to meet them, J. Pharm. Sci. 104 (2015) 792–802.

[62]   O.S. Sudah, A.W. Chester, J.A. Kowalski, J.W. Beeckman, F.J. Muzzio, Quantitative characterization of mixing processes in rotary calciners, Powder Technol. 126 (2002) 166–173.

[63] D.N. Whittles, S. Kingman, I.S. Lowndes, R. Griffiths, An investigation into the parameters affecting mass flow rate of ore material through a microwave continuous feed system, Adv. Powder Technol. 16 (2005) 585–609.

[64] H.S. Ramaswamy, K.A. Abdelrahim, B.K. Simpson, J.P. Smith, Residence time distribution (RTD) in aseptic processing of particulate foods: a review, Food Res. Int. 28 (1995) 291–310.

[65] A.P. Torres, F.A.R. Oliveira, Residence time distribution studies in continuous thermal processing of liquid foods: a review, J. Food Eng. 36 (1998) 1–30.

[66] A.U. Vanarase, F.J. Muzzio, Effect of operating conditions and design parameters in a continuous powder mixer, Powder Technol. 208 (2011) 26–36.

[67] V. Patravale, J.I. Disouza, M.T. Rustomjee, Pharmaceutical product development: insights into pharmaceutical processes, management, and regulatory affairs, CRC Press, Florida, 2016.

[68] S. Laske, A. Witschnigg, R.K. Selvasankar, C. Holzer, Measuring the residence time distribution in a twin screw extruder with the use of NIR-spectroscopy, J. Appl. Polym. Sci. 131 (2014).

[69] H.W. Ward, D.O. Blackwood, M. Polizzi, H. Clarke, Monitoring blend potency in a tablet press feed frame using near infrared spectroscopy, J. Pharm. Biomed. Anal. 80 (2013) 18–23.

[70] M. Fonteyne, J. Vercruysse, F. de Leersnyder, B. van Snick, C. Vervaet, J.P. Remon, T. de Beer, Process analytical technology for continuous manufacturing of solid-dosage forms, Trends Anal. Chem. 67 (2015) 159–166.

[71] K. Plumb, Continuous processing in the pharmaceutical industry, Chem. Eng. Res. Des. 83 (2005) 730–738.

[72] J. Kruisz, J. Rehrl, S. Sacher, I. Aigner, M. Horn, J.G. Khinast, RTD modeling of a continuous dry granulation process for process control and materials diversion, Int. J. Pharm. 528 (2017) 334–344.

[73] M.C. Martinetz, J. Rehrl, I. Aigner, S. Sacher, J. Khinast, A continuous operation concept for a rotary tablet press using mass flow operating points, Chem. Ing. Tech. 89 (2017) 1006–1016.

[74] C. Vervaet, J.P. Remon, Continuous granulation in the pharmaceutical industry, Chem. Eng. Sci. 60 (2005) 3949–3957.

[75] FDA, Guidance for industry: PAT - a framework for innovative pharmaceutical development, manufacturing, and quality assurance, Biotechnol. Law. Rep. 23 (2004) 68–86.

[76] FDA, Guidance for Industry: Q8 (R2) Pharmaceutical development (2009).

[77] FDA, Guidance for Industry: Q10 Pharmaceutical quality system (2009).

[78] O. Levenspiel, Chemical reaction engineering, 3rd ed., Wiley, New York, 1999.

[79] M.T. Sisay, S.A. Emire, H.S. Ramaswamy, T.S. Workneh, Residence time distribution and flow pattern of reduced-gluten wheat-based formulations in a twin–screw extruder, Food Sci. Technol. 79 (2017) 213–222.

[80] Y. Gao, A. Vanarase, F. Muzzio, M. Ierapetritou, Characterizing continuous powder mixing using residence time distribution, Chem. Eng. Sci. 66 (2011) 417–425.

[81] A. Kumar, J. Vercruysse, V. Vanhoorne, M. Toiviainen, P.-E. Panouillot, M. Juuti, C. Vervaet, J.P. Remon, K.V. Gernaey, T. de Beer, I. Nopens, Conceptual framework for model-based analysis of residence time distribution in twin-screw granulation, Eur. J. Pharm. Sci. 71 (2015) 25–34.

[82] D.L. Penry, P.A. Jumars, Chemical reactor analysis and optimal digestion, BioScience 36 (1986) 310–315.

[83] D. Wolf, W. Resnick, Residence time distribution in real systems, Ind. Eng. Chem. Fund. 2 (1963) 287–293.

[84] D. Mateo-Ortiz, R. Méndez, Relationship between residence time distribution and forces applied by paddles on powder attrition during the die filling process, Powder Technol. 278 (2015) 111–117.

[85] M.S. Escotet-Espinoza, S. Moghtadernejad, S. Oka, Y. Wang, A. Roman-Ospino, E. Schäfer, Effect of tracer material properties on the residence time distribution (RTD) of continuous powder blending operations, Powder Technol. 342 (2019) 744–763.

[86] J. Hanson, Control of a system of loss-in-weight feeders for drug product continuous manufacturing, Powder Technol. 331 (2018) 236–243.

[87] Y. Wang, T. Li, F.J. Muzzio, B.J. Glasser, Predicting feeder performance based on material flow properties, Powder Technol. 308 (2017) 135–148.

[88]   K. Marikh, H. Berthiaux, V. Mizonov, E. Barantseva, D. Ponomarev, Flow

         analysis and markov chain modelling to quantify the agitation effect in a

         continuous powder mixer, Chem. Eng. Res. Des. 84 (2006) 1059–1074.

[89]   R.E. Altomare, P. Ghossi, An analysis of residence time distribution patterns in

         a twin screw cooking extruder, Biotechnol. Prog. 2 (1986) 157–163.

[90]   C. Bi, B. Jiang, Study of residence time distribution in a reciprocating single-

         screw pin-barrel extruder, J. Mater. Process. Tech. 209 (2009) 4147–4153.

[91]   G.R. Ziegler, C.A. Aguilar, Residence time distribution in a co-rotating, twin-

         screw continuous mixer by the step change method, J. Food Eng. 59 (2003)

         161–167.

[92]   W. Han, B. Mai, T. Gu, Residence time distribution and drying characteristics

         of a continous vibro fluidized bed, Drying Technol. 9 (1991) 159–181.

[93]   A.T. Harris, R.B. Thorpe, J.F. Davidson, Stochastic modelling of the particle

         residence time distribution in circulating fluidised bed risers, Chem. Eng. Sci.

         57 (2002) 4779–4796.

[94]   A. Dubey, A. Sarkar, M. Ierapetritou, C.R. Wassgren, F.J. Muzzio,

         Computational approaches for studying the granular dynamics of continuous

         blending processes, Macromol. Mater. Eng. 296 (2011) 290–307.

[95]   A. Rogers, M.G. Ierapetritou, Discrete element reduced-order modeling of

         dynamic particulate systems, AIChE J. 60 (2014) 3184–3194.

[96] N.-H. Duong, P. Arratia, F. Muzzio, A. Lange, J. Timmermans, S. Reynolds, A homogeneity study using NIR spectroscopy: Tracking magnesium stearate in Bohle bin-blender, Drug Dev. Ind. Pharm. 29 (2003) 679–687.

[97] J. Kushner, F. Moore, Scale-up model describing the impact of lubrication on tablet tensile strength, Int. J. Pharm. 399 (2010) 19–30.

[98] K. Pingali, R. Mendez, D. Lewis, B. Michniak-Kohn, A. Cuitiño, F. Muzzio, Evaluation of strain-induced hydrophobicity of pharmaceutical blends and its effect on drug release rate under multiple compression conditions, Drug Dev. Ind. Pharm. 37 (2011) 428–435.

[99] J. Wang, H. Wen, D. Desai, Lubrication in tablet formulations, Eur. J. Pharm. Biopharm. 75 (2010) 1–15.

[100] B.L. Diffey, Sources and measurement of ultraviolet radiation, Methods 28 (2002) 4–13.

[101] G.K. Pal, P. Pal, Textbook of practical physiology, Orient Longman, Calcutta, [Great Britain], 2001.

[102] W. Reusch, Visible and ultraviolet spectroscopy. https://www2.chemistry.msu.edu/faculty/reusch/virttxtjml/spectrpy/uv-vis/spectrum.htm. Accessed 26 June 2018.

[103] H.-H. Perkampus, UV-Vis spectroscopy and its applications, Springer Berlin Heidelberg, Berlin, Heidelberg, 1992.

[104] S.M. Gaonkar, P.R. Kulkarni, Microcrystalline cellulose from coconut shells, Acta Polym. 40 (1989) 292–293.

[105] Y. Padmadisastra, I. Gonda, Preliminary studies of the development of a direct compression cellulose excipient from bagasse, J. Pharm. Sci. 78 (1989) 508–514.

[106] L.-G. Tang, D.N.-S. Hon, S.-H. Pan, Y.-Q. Zhu, Z. Wang, Z.-Z. Wang, Evaluation of microcrystalline cellulose: changes in ultrastructural characteristics during preliminary acid hydrolysis, J. Appl. Polym. Sci. 59 (1996) 483–488.

[107] J. Chen, S. Yan, J. Ruan, A study on the preparation, structure, and properties of microcrystalline cellulose, J. Macromol. Sci., Pure Appl. Chem. 33 (1996) 1851–1862.

[108] A.M. Bochek, I.L. Shevchuk, V.N. Lavrent'ev, Fabrication of microcrystalline and powdered cellulose from short flax fiber and flax straw, Russ. J. Appl. Chem. 76 (2003) 1679–1682.

[109] O.A. Battista, P.A. Smith, Microcrystalline cellulose: The oldest polymer finds new industrial uses, Ind. Eng. Chem. 54 (1962) 20–29.

[110] M. El-Sakhawy, M.L. Hassan, Physical and mechanical properties of microcrystalline cellulose prepared from agricultural residues, Carbohydr. Polym. 67 (2007) 1–10.

[111] S.F. Serwanis, P. Szabo-Revesz, K. Pintye-Hodi, P. Kasa, I. Erös, Study of the flowability and compactibility of some types of Vivapur 53 (1998) 881–882.

[112] C.C. Sun, Setting the bar for powder flow properties in successful high speed tableting, Powder Technol. 201 (2010) 106–108.

[113] R.F. Shangraw, D.A. Demarest, A survey of current industrial practices in the formulation and manufacture of tablets and capsules, Pharm. Technol. 17 (1993) 32–38.

[114] C. Nyström, G. Alderborn, M. Duberg, P.-G. Karehill, Bonding surface area and bonding mechanism - two important factors fir the understanding of powder comparability, Drug Dev. Ind. Pharm. 19 (2008) 2143–2196.

[115] G. Alderborn, C. Nyström, Pharmaceutical powder compaction technology, Marcel Dekker, New York, 1996.

[116] Evonik Industries, AEROSIL® colloidal silicon dioxide regulatory information, 2018. http://www.aerosil.com/product/aerosil/en/industries/pharmaceuticals/regulatory-information/. Accessed 2 June 2018.

[117] J. Mathias, G. Wannemacher, Basic characteristics and applications of aerosil, J. Colloid Interface Sci. 125 (1988) 61–68.

[118] N. Stasiak, W. Kukuła-Koch, K. Głowniak, Modern industrial and pharmacological applications of indigo dye and its derivatives - a review, Acta. Pol. Pharm. 71 (2014) 215–221.

[119] J. König, 2 - Food colour additives of synthetic origin, in: M.J. Scotter (Ed.) Colour Additives for Foods and Beverages, Woodhead Publishing, Oxford, 2015, pp. 35-60

[120] FDA, Summary of color additives for use in the united states in foods, drugs,

cosmetics, and medical devices, 2017.

https://www.fda.gov/forindustry/coloradditives/coloradditiveinventories/ucm115

641.htm. Accessed 3 August 2018.

[121] F.J. Green, The Sigma-Aldrich handbook of stains, dyes, and indicators, 2nd

ed., Aldrich Chemical Co., Milwaukee, 1991.

[122] M.J. O'Neil (Ed.), The Merck index: An encyclopedia of chemicals, drugs, and

biologicals, 15th ed., RSC Publ. Royal Soc. of Chemistry, Cambridge, 2013.

[123] C.F. Harwood, Powder segregation due to vibration, Powder Technol. 16

(1977) 51–57.

[124] D. Mateo-Ortiz, F.J. Muzzio, R. Méndez, Particle size segregation promoted

by powder flow in confined space: the die filling process case, Powder

Technol. 262 (2014) 215–222.

[125] H. Kalman, Attrition of powders and granules at various bends during

pneumatic conveying, Powder Technol. 112 (2000) 244–250.

[126] P.A. Langston, U. Tüzün, D.M. Heyes, Discrete element simulation of internal

stress and flow fields in funnel flow hoppers, Powder Technol. 85 (1995) 153–

169.

[127] Fette Compacting, The FE series: High production potential and compact,

2019. https://www.fette-compacting.com/en/products/tablet-presses/fe-series/.

Accessed 11 January 2019.

[128] L. Babout, K. Grudzien, E. Maire, P.J. Withers, Influence of wall roughness and packing density on stagnant zone formation during funnel flow discharge from a silo, Chem. Eng. Sci. 97 (2013) 210–224.

[129] E.B. Nauman, Residence time theory, Ind. Eng. Chem. Res. 47 (2008) 3752–3766.

[130] B. van Snick, J. Holman, C. Cunningham, A. Kumar, J. Vercruysse, T. de Beer, J.P. Remon, C. Vervaet, Continuous direct compression as manufacturing platform for sustained release tablets, Int. J. Pharm. 519 (2017) 390–407.

[131] R. Mendez, C. Velazquez, F.J. Muzzio, Effect of feed frame design and operating parameters on powder attrition, particle breakage, and powder properties, Powder Technol. 229 (2012) 253–260.

[132] W. Grymonpré, V. Vanhoorne, B. van Snick, B. Blahova Prudilova, F. Detobel, J.P. Remon, T. de Beer, C. Vervaet, Optimizing feed frame design and tableting process parameters to increase die-filling uniformity on a high-speed rotary tablet press, Int. J. Pharm. 548 (2018) 54–61.

Appendix

A   Hazardous materials

Substance	Supplier	Danger symbol	Hazard statements	Precautionary statements
Indigo carmine	Carl Roth, Germany		H302	P264, P270, P301+P312, P330, P501

B   Curriculum vitae

The CV is not published for reasons of data protection.

C   Acknowledgments

Declaration on oath (affirmation in lieu of oath) / Eidesstattliche Versicherung

Hiermit versichere ich an Eides statt, die vorliegende Dissertation selbst verfasst und keine anderen als die angegebenen Hilfsmittel benutzt zu haben. Die eingereichte schriftliche Fassung entspricht der auf dem elektronischen Speichermedium. Ich versichere, dass diese Dissertation nicht in einem früheren Promotionsverfahren eingereicht wurde.

Hamburg, den

_____

Matthias Dülle

Declaration on oath (affirmation in lieu of oath) / Eidesstattliche Versicherung